MASTER IN BIOCHEMISTRY AND MOLECULAR AND CELLULAR BIOLOGY

Study of the senescence-associated secretory phenotype and cell signaling of keratinocytes in uvb-stress induced premature senescence

Hellin, Sébastien

Award date:
2017

Awarding institution:
University of Namur

Faculté des Sciences

STUDY OF THE SENESCENCE-ASSOCIATED SECRETORY PHENOTYPE AND CELL SIGNALING OF KERATINOCYTES IN UVB-STRESS INDUCED PREMATURE SENESCENCE

Mémoire présenté pour l'obtention

du grade académique de master 120 en biochimie et biologie moléculaire et cellulaire

Sébastien HELLIN

Août 2017

Université de Namur
FACULTE DES SCIENCES
Secrétariat du Département de Biologie
Rue de Bruxelles 61 - 5000 NAMUR
Téléphone: + 32(0)81.72.44.18 - Téléfax: + 32(0)81.72.44.20
E-mail: joelle.jonet@ unamur.be - http://www.unamur.be

Study of the senescence-associated secretory phenotype and cell signaling of keratinocytes in UVB-stress induced premature senescence

HELLIN Sébastien

Abstract

The social and economic impact of an ageing population is a worrying concern our developed countries are facing, as well as less developed countries. Therefore, there is a real necessity to develop novel approaches to better understand the ageing process and to prevent age-related diseases. Cellular senescence, a predominant hallmark of ageing of mitotic tissues, can be related to proliferative potential exhaustion, oncogene activation or stress exposure. Moreover, emerging evidence indicates that cellular senescence is involved in the promotion of tissue repair and tumor suppression.

In our study, we studied normal human keratinocytes (NHKs) in replicative senescence or in UVB-stress induced premature senescence (UVB-SIPS). First, we compared different biomarkers of senescence in both senescent models including morphological changes and senescence-associated β-galactosidase activity (SA-βgal). Then we analysed the expression and secretion of three major SASP (Senescence Associated Secretory Phenotype) factors. We showed an increased secretion of IL(Interleukin)-6 and -8, and a decreased secretion of VEGF (Vascular endothelial growth factor).

We then investigated different molecular pathways. First, we studied the DNA Damage Response (DDR) pathway, and our results showed an activation of the ATM-Chk2-p53 pathway. Then we looked for the oxidative stress and we demonstrated an increased generation of reactive oxygen species (ROS) including superoxide anions after UVB exposures.. We finally studied Nrf2 activation and the expression of Nrf2-dependent antioxidant genes.

Our data allow us to clarify the active pathways following UVB stresses that are potentially involved in the appearance of the senescent phenotype.

Mémoire de master 120 en biochimie et biologie moléculaire et cellulaire

Août 2017

Promoteur: F. Debacq-Chainiaux

Université de Namur
FACULTE DES SCIENCES
Secrétariat du Département de Biologie
Rue de Bruxelles 61 - 5000 NAMUR
Téléphone: + 32(0)81.72.44.18 - Téléfax: + 32(0)81.72.44.20
E-mail: joelle.jonet@ unamur.be - http://www.unamur.be

Etude du phénotype sécrétoire associé à la sénescence et de la signalisation cellulaire dans des kératinocytes en sénescence induite prématurément par les stress UVB (SIPS-UVB)

HELLIN Sébastien

Résumé

L'impact social et économique du vieillissement de la population représente une préoccupation importante pour nos pays développés, ainsi que pour les pays moins développés. Par conséquent, il existe une réelle nécessité à développer de nouvelles approches pour mieux comprendre le processus de vieillissement et prévenir les maladies liées à l'âge. La sénescence cellulaire, caractéristique prédominante du vieillissement des tissus mitotiques, peut être liée à l'épuisement du potentiel prolifératif, à l'activation des oncogènes ou à l'exposition au stress. De plus, des preuves émergentes indiquent que la sénescence cellulaire est impliquée dans la réparation tissulaire et la suppression des tumeurs.

Dans ce travail, nous avons étudié les kératinocytes humains en sénescence réplicative (SR) ou en sénescence induite prématurément par des expositions répétées à des doses subcytotoxiques d'UVB (SIPS-UVB).

La première partie de ces recherches consistait à comparer les différents biomarqueurs de sénescence dans les deux modèles de sénescence, dont les changements morphologiques et l'activité β-galactosidase associée à la sénescence (SA-βgal) Ensuite, nous avons analysé l'expression et la sécrétion de trois facteurs du phénotype sécrétoire associé à la sénescence (SASP). Nous avons montré une augmentation de la sécrétion des interleukines(IL)-6 et -8, et une diminution de la sécrétion du facteur de croissance de l'endothélium vasculaire (VEGF).

Secondement, nous avons investigué différents mécanismes moléculaires. Nous avons étudié la voie de réparation des dommages à l'ADN (DDR) et nos résultats ont montré une activation de la voie ATM-Chk2-p53. Nous nous sommes intéressés au stress oxydatif et nous avons démontré une augmentation de la production des radicaux libres dérivés de l'oxygène (ROS), incluant les anions superoxydes après exposition aux UVB. Nous avons finalement analysé l'activation de Nrf2 et l'expression de gènes antioxydants dépendants de Nrf2. Nos données ont permis de clarifier des voies activées après exposition aux UVB et qui pourraient potentiellement être impliquées dans l'apparition du phénotype sénescent.

Mémoire de master 120 en biochimie et biologie moléculaire et cellulaire

Août 2017

Promoteur: F. Debacq-Chainiaux

REMERCIEMENTS

Après ces 10 mois de recherches (+ 2 mois de prolongation ces vacances d'été), il est enfin temps pour moi de remercier toutes les personnes qui m'ont épaulé durant ce mémoire.

Premièrement, je tiens à remercier Florence Chainiaux pour son dévouement, son expérience et ses conseils dans la rédaction qui m'ont énormément aidé. Souvent disponible et patiente, tu as été là pour me soutenir dans mon travail. Très à l'écoute, tu as toujours eu les mots justes pour m'aider.

Je tiens aussi à te remercier Emilie de m'avoir appris la rigueur au labo avec par exemple la préparation des protocoles avant les expériences qui m'a parfois joué des tours durant les manipulations (en stage, j'ai bien suivi cette démarche et je n'ai heureusement pas eu de problèmes à ce niveau ☺ , d'ailleurs je pense que je vérifiais tellement les flasques de culture, que ça en devenait une obsession après). Tu m'impressionnais à jongler entre les TP, les corrections des rapports, les expériences et ta vie de famille, ça ne devait pas être facile mais j'espère que tu as trouvé ton équilibre.

Un grand merci à l'équipe des SAGE aussi pour leurs conseils avisés durant les réunions et pour les expériences.

Merci aux autres membres du labo, notamment les HIFs qui ont été souvent là pour égayer mes temps d'incubations. Spéciale attention aussi à Guy avec qui je discutais pas mal de sport, à Maudette, Antoine (j'adore tes montages haha), Noëlle et à Martine.

Bien entendu, merci à mes 3 acolytes de bureau, Alexis (Chouchou), Sophie (Kitty) et Patricia (Pastel), sur qui je pouvais compter pour décompresser un peu après une journée intense au labo. Je te souhaite bonne chance Alexis pour la suite avec les SAGE avec, je l'espère, le FRIA à la clé!

C'est un sentiment étrange de quitter Namur après ces belles années. Malgré parfois les désillusions, j'ai vraiment passé un cursus enrichissant. Merci à toutes mes amis qui m'ont soutenu depuis le début, toujours disponibles et à l'écoute. Je pense notamment à Pierre, Denis, Hugo, Morgane et j'en passe!

Il est également important pour moi de remercier mes parents. Papa, j'espère et je sais que tu es fier de moi là-haut. Maman, tu es la personne qui m'a le plus soutenu durant mes études, tout le temps préoccupée, tu as su me motive quand ça n'allait pas. Merci à mes frères et soeurs également pour leur soutien.

Sébastien,

Abbreviations list

(6-4)pp	6-4 photoproducts
8-MOP	8-methoxypsoralen
8-oxodG	8-oxo-7,8-dihydro-2'-deoxyguanosine
AA	Antimycin A
AMP	Adenosine monophosphate
AMPK	AMP-activated protein kinase
AP	Activator protein
Apo J	Apolipoprotein J
ARE	Antioxidant response element
ARF	Alternate-reading-frame protein
ATF6	Activating transcription factor 6
ATM	Ataxia telangiectasia mutated
ATP	Adenosine triphosphate
ATR	Ataxia telangiectasia Rad3 related
BER	Base excision repair
BPE	Bovine pituitary extract
BRCA1	Breast cancer type-1 susceptibility
CDC25	Cell division cycle 25
CDK	Cyclin-dependent kinase
CDKI	Cyclin-dependent kinase inhibitor
CHK	Checkpoint kinase
CNV	Copy number variations
CPD	Cumulative population doubling
Ct	Threshold cycle
CUL3	Cullin 3 E3 ligase complex
DCF	2',7'-dichlorofluorescein
DCFH-DA	2',7'-dichlorofluorescein diacetate
DDR	DNA damage response
DMEM	Dulbecco's modified Eagle's medium
DNA	Deoxyribonucleic acid
DSB	Double-strand DNA break
ECM	Extracellular matrix
EDTA	Ethylenediaminetetraacetic acid
EGFR	Epidermal growth factor receptor
ELISA	Enzyme-linked immunosorbent assay
ER	Endoplasmic reticulum
FACS	Fluorescence-activated cell sorting
FCCP	Carbonyl cyanide-4-(trifluoromethoxy)phenylhydrazone
FOXO3α	Forkhead box O3α
GAPDH	Glyceraldehyde 3-phosphate dehydrogenase
GH	Growth hormone
GLB1	Galactosidase beta 1
GLC	Glutamate cysteine ligase
GG-NER	Global genome NER
GGR	Global genome repair
GSH	Glutathione
GnRH	Gonadotropin-releasing hormone
HB	Hypotonic buffer
HBSS	Hanks' balanced salt solution
HDM2	E3 ubiquitin-protein ligase
HR	Homologous recombination
HSC	Hepatic activated stellate cells

H_2O_2	Hydrogen peroxide
HGPS	Hutchinson-Gilford progeria syndrome
HMOX1	Heme-oxygenase 1
HP1α	Heterochromatin protein 1α
HRP	Horseradish peroxidase
hTERT	Human telomerase catalytic subunit
IDCR	Ionic detergent compatibility reagent
IGF-1	Insulin-like growth factor 1
IL	Interleukin
K-SFM	Keratinocyte serum-free medium
Keap1	Kelch-like ECH- associated protein 1
LAMP2A	Lysosome-associated membrane protein 2A
Maf	Masculoaponeurotic fibrosarcoma
MAPK	Mitogen-activated protein kinase
MIP	Macrophage inflammatory protein
MnSOD	Manganese superoxide dismutase
MMP	Matrix metalloproteinase
MMR	DNA mismatch repair
MRN	MRE11/RAD50/NBS1
MSRA	Peptide methionine sulfoxide reducate A
mtDNA	Mitochondrial DNA
mTOR	Mammalian target of rapamycin
NAD^+	Nicotinamide adenine dinucleotide oxidized
NER	Nucleotide excision repair
NF	Neurofibromin
NF-kB	Nuclear factor kappa-light-chain-enhancer of activated B cells
NHEJ	Non-homologous end joining
NHEK	Normal human epidermal keratinocytes
NLRP3	Nod-like receptor
NQO1	NAD(P)H:quinone dehydrogenase
Nrf2	NF-E2-related factor 2
O_2	Oxygen
O_2^-	Superoxide anion
OD	Optical density
$^{\bullet}OH$	Hydroxyl radical
OIS	Oncogene-induced senescence
PARP-1	Poly(ADP-ribose) polymerase 1
PBS	Phosphate buffered saline
PCNA	Proliferating cell nuclear antigen
PCR	Polymerase chain reaction
PFA	Paraformaldehyde
PIGs	P53-induced genes
POT-1	Protection of telomeres protein-1
POX	Proline oxidase
PUVA	Psoralen and ultraviolet A
PVDF	Polyvinylidene fluoride
qPCR	quantitative Polymerase Chain Reaction
Rb	Retinoblastoma protein
rEGF	recombinant Epidermal Growth Factor
ROS	Reactive oxygen species
RT	Room temperature
RPA	Replication protein A
RS	Replicative senescence
SA-βgal	Senescence-associated β-galactosidase
SAHF	Senescence-associated heterochromatic foci

SASP	Senescence-associated secretory phenotype
SDS	Sodium dodecyl sulfate
SIN-1	3-Morpholinosydnonimine hydrochloride
Sir2	Sirtuin 2
SIPS	Stress-induced premature senescence
SSB	Single-strand break
TC-NER	Transcription-coupled NER
TRF1/2	Telomeric repeat-binding factor 1/2
PSNE	Post-senescence neoplastic emergence
PTEN	Phosphatase and tensin homolog
t-BHP	*Tert*-butylhydroperoxyde
TGF	Transforming growth factor
TNF	Tumor necrosis factor
UPR	Unfolded protein response
UV	Ultraviolet
UVA	Ultraviolet A
UVB	Ultraviolet B
UVC	Ultraviolet C
VEGF	Vascular endothelial growth factor
VHL	Von Hippel-Lindau tumor suppressor
WB	Western blot
XP	Xeroderma pigmentosum

Table of contents

INTRODUCTION

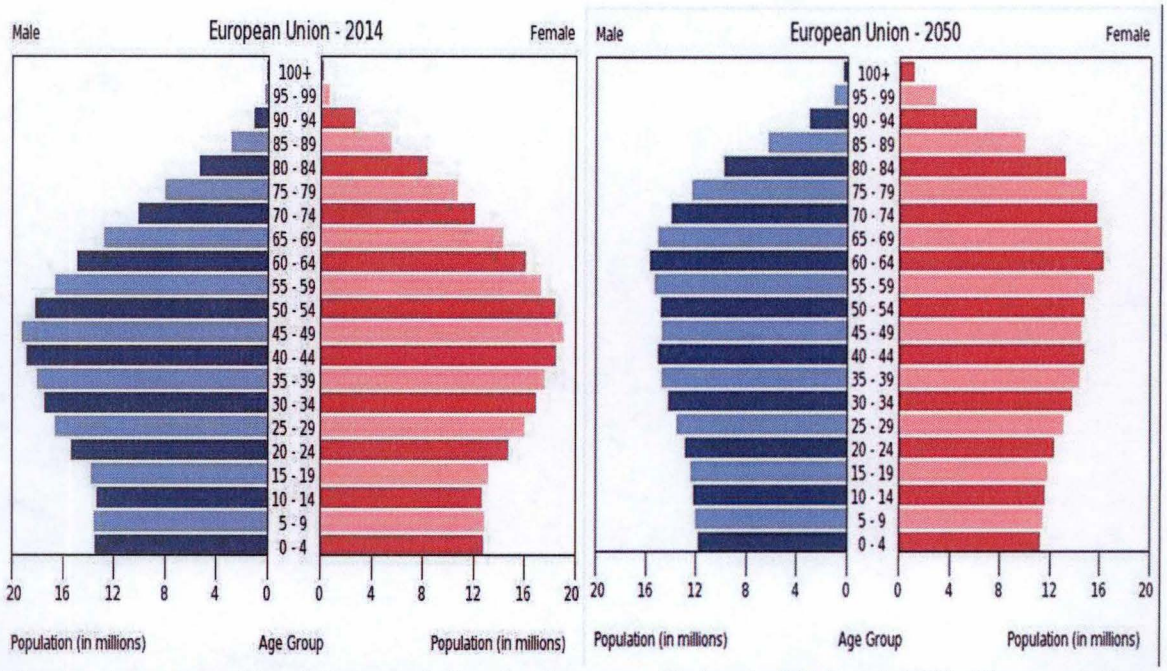

Fig. 1 – Age pyramids of the population in European Union in 2014 and 2050. The population is distributed along the horizontal axis, with males shown on the left (blue) and females on the right (red). The female and male populations are divided into 5 years age groups configured as horizontal bars, with the youngest age groups at the bottom and the oldest at the top. The shape of the pyramid depends on fertility, mortality and also, international migration trends (WHO, 2014).

Fig. 2 – The nine hallmarks of ageing (López-Otín, 2013).

1. Ageing of the population

Population is ageing worldwide. If it is particularly marked in economically developed countries, an increase in life expectancy is also reported in less developed ones. Ageing of the population is probably one of the most significant social challenges of the 21st century, involving all sectors of society such as financial markets and labour (Poterba and National Bureau of Economic Research. 2004). In Belgium, life expectancy at birth increased from 67.3 years for men and 73.7 years for women in 1970, to 78.6 years and 83.5 years respectively in 2015 (economie.fgov.be). Survival rates started to rise in the 1950s because of improvements in public health including clean water, vaccines and antibiotics as well as better condition in lifestyle and housing. This increase in life expectancy combined with decreased birth rates will lead to an increased proportion of elderly people in the population leading to a transformation of the age pyramid in developed countries (mostly in North America and Europe) (fig. 1).
The ageing of the population may have a negative impact on health. In particular, it is expected in the coming years to observe an increase in the number of patients suffering from age-related diseases such as osteoarthritis, osteoporosis, diabetes, cardiovascular and neurodegenerative diseases. Moreover, an increase in the proportion of the people reporting frailty is also feared. Frailty is recognised as a decline in multiple physiological systems leading to the exhaustion of functional reserves and to increased vulnerability and morbidity (Fedarko 2011).
Therefore, there is a real necessity to develop novel approaches to better understand the ageing process and to prevent frailty and age-related diseases. Ageing is then now considered as a public health challenge for researchers and clinicians. Longitudinal and large-scale studies on humans are costly and time-consuming and are probably not sufficient to understand all mechanisms of human ageing and longevity (Dolan et al. 2010). Besides, use of *in vivo, ex vivo* and *in vitro* models is essential to extend knowledge about conserved pathways that regulate human ageing.

2. What is ageing?

2.1. Definition

Ageing is considered as a time-dependent functional decline affecting all living organisms (López-otín et al. 2013). This induces a loss of homeostasis and a decreased ability to adapt to stresses yielding an increased vulnerability to disease and mortality. The maintenance of specific molecular pathways and homeodynamics is also less efficient in the normal process of ageing (Holliday 1995).
Another important finding is that cancer and ageing are linked in different ways. Indeed, the accumulation of cellular damage is known to be responsible for the ageing process. But cellular damage may also induce uncontrolled proliferation of cells leading to cancer. In 2000, a major review combined six hallmarks of cancer (Hanahan et al. 2000), later expanded to ten (Hanahan et al. 2011). In parallel, nine hallmarks have been proposed to contribute to the ageing process (López-otín et al. 2013) (fig. 2). Each hallmark has been related to the ageing process following several criteria: it must appear during normal ageing, its induction should accelerate ageing and if prevented or blocked, it retards the normal ageing process, resulting in increased healthy lifespan.

These hallmarks are not independent and can be categorised into three groups. Firstly, primary hallmarks cause cellular damage and include genomic instability, telomere attrition, epigenetic alterations and loss of proteostasis. Secondly, response or compensatory hallmarks, are the result of the primary hallmarks, such as deregulated nutrient sensing, mitochondrial dysfunction and cellular senescence. Thirdly, integrative hallmarks that integrate the first two classes and induce a functional decline in ageing, including stem cell exhaustion and altered intercellular communication (López-Otín et al. 2013). We will describe some of them hereafter.

2.2. Hallmarks of ageing

2.2.1. Genomic instability

Genomic instability and accumulation of DNA damage can contribute to ageing. First, different types of DNA damage including copy number variations (CNVs) and chromosomal aneuploidies have been associated with ageing(Faggioli et al. 2012). CNVs are DNA segments larger than 1 kb in size that vary in copy number between individuals caused by insertion, duplication or deletion. Indeed, two common CNV regions on chromosomes 11p15.5 and 14q21.3 have been identified and associated with higher mortality at old age (Kuningas et al. 2011). In addition to CNVs, another study demonstrates that aneuploid fibroblasts increase with age (Mukherjee et al. 1997). This acquisition of an abnormal number of chromosomes is usually a common hallmark of many diseases, including cancer.
Secondly, many progeroid syndromes, that are rare genetic disorders associated with a premature ageing, are characterised by increased DNA damage accumulation (Burtner et al. 2010). For example, Hutchinson-Gilford progeria syndrome (HGPS) is caused by a mutation in the *LMNA* gene triggering an abnormal alternative splicing of lamins A and C, two major components of the nuclear lamina, leading to alterations in the nuclear envelope. The nuclear lamina is a dense fibrillar network inside the nucleus providing mechanical support and regulating DNA replication and cell division. HGPS patients appear to be normal at birth but develop after few years characteristics of premature ageing such as musculoskeletal degeneration, kidney failure, loss of eyesight and hair, and cardiovascular diseases(Gonzalez et al. 2011). Moreover, a murine model for HGPS showed increased DNA damage, chromosome aberrations and higher sensitivity to DNA-damaging agents (Liu et al. 2005).
Accumulation of mitochondrial DNA mutations and deletions also contribute to the ageing process. The mtDNA is considered as a major target of DNA mutagenesis due to the lack of protective histones, limited DNA repair mechanisms and oxidative environment of the mitochondria (Gredilla et al. 2010). Moreover, most somatic mtDNA mutations do not result from damage accumulation but rather as replication errors during development (Ameur et al. 2011).

2.2.2. Epigenetic alterations

Chromatin is classified into two forms: heterochromatin and euchromatin. Heterochromatin remains condensed during interphase and is mostly transcriptionally silenced, while euchromatin is decondensed during interphase and is permissive for transcription.
Recently, the epigenetic variation has been recognised as a significant contributor to the ageing phenotype. Indeed, many epigenetic alterations affect cells and tissues throughout life. Among these epigenetic changes are alterations in methylation patterns, post-translational modifications of histones and chromatin remodelling. If ageing is associated with a global

hypomethylation, several analyses also showed a hypermethylation with age in several loci such as various tumour suppressor genes and Polycomb target genes (Maegawa et al. 2010). Histone methylation is also considered as a hallmark of ageing in invertebrates because deletion of histone complexes such as H3K4 and H3K27 can extend lifespan in flies and nematodes (Maures et al. 2011). Indeed, these methylations appear to be associated with transcriptional repression and may represent a key intermediary step between extending lifespan and the expression of specific genes involved in longevity (Han al. 2012). Furthermore, it has been found that abundance of H4K20 methylation increases with age in rat tissue (Sarg et al. 2002). Moreover, accelerated ageing is also associated with an increase of H4K20 methylation in cells derived from HGPS patients (McCord et al. 2013).
Other epigenetic actors can affect cells and tissues throughout life such as an overexpression of Sir2 (a NAD-dependent histone deacetylase) or heterochromatin protein 1α (HP1α) (Whitaker et al. 2013). Nevertheless, how epigenetics alterations can influence ageing is still unknown.

2.2.3. Loss of proteostasis

Damaged and misfolded proteins accumulate during ageing due to impairment in protein homeostasis, what is called proteostasis (Morimoto 2008). Proteostasis involves mechanisms linked to the stabilization of folded proteins and mechanisms for the degradation of proteins by the lysosome/autophagy or by the proteasome (Hartl et al. 2011).
Protein folding is mediated by a family of proteins named chaperones (Hartl et al. 2011). Studies demonstrate that chaperones are significantly altered in ageing. This suggests the hypothesis that ageing in tissues may involve time-dependent loss of protein quality control, an alteration which can lead to aggregation and formation of inclusion body (Calderwood et al. 2009). Results showed that the regulatory role of chaperones declines with age in animal models, whereas mouse strains with overexpressed chaperones are long-lived (Calamini et al. 2010). Therapeutics molecules have been synthesized for maintaining proteostasis and assuring the refolding of damaged proteins in model organisms (Calamini et al. 2010).
Both autophagy-lysosomal and ubiquitin-proteasome systems have dysfunctions in different severe human pathologies and in ageing (Dice 2007). Indeed, the concentration of ubiquitinated proteins appears to be increased in aged cells and tissue, suggesting that the function of 26S proteasome, involved in the regulated degradation of ubiquitinated protein, could be affected by ageing (Dahlmann 2007). In addition, the levels of lysosome-associated membrane protein 2A (LAMP2A), a receptor for chaperone-mediated autophagy, start to decline in a gradual manner by middle age due to an impaired stability (Hartl, Bracher, and Hayer-Hartl 2011). These increasing evidence confirm the idea that proteostasis constitutes a hallmark of ageing.

2.2.4. Deregulated nutrient sensing

The intracellular pathway of insulin and insulin-like growth factor 1 (IGF-1) has been shown to affect ageing and longevity processes (Fontana, Partridge, and Longo 2010). This pathway can sense the availability of adequate glucose and amino acid levels, thereby promoting growth in response to high concentrations of glucose and amino acids. IGF-1 and growth hormone (GH) levels decrease during both normal ageing process and premature ageing in mouse models (Garinis et al. 2008). Indeed, organisms with lower IGF-1 levels have a higher lifespan probably because their metabolism and growth decelerate, as well as the rate of cellular damage declines (Fontana, et al. 2010). In parallel, the caloric restriction, a dietary regimen reducing total energy intake, can potentially increase lifespan in most species and reduces the activity of the GH/IGF-1 axis. However, the biologic effects are still debated

because chronic dietary restriction may turn out deleterious and aggravate ageing (Fontana et al. 2010).
In addition to glucose sensing, three other interconnected nutrient systems are being investigated in ageing: mTOR (sensing of amino acids), sirtuin (sensor of low-energy states through high NAD^+ levels) and AMPK (detection shifts in the AMP:ATP ratio) (Houtkooper et al. 2010).

2.2.5. Stem cell exhaustion

Aged tissues show a progressive decline in the regenerative and in the homeostatic potential of stem cells. This feature has been attributed to the loss of self-renewal capacity due to apoptosis or senescence induced by cellular stresses in tissue-specific stem cells and stem cell niches (Oh et al. 2014). For example, age-dependent reduction in stem cell number has been reported in mouse forebrain, bone, muscular fibers and also in germline stem cell niches (Molofsky et al. 2006). With increasing age, a dramatic decline in the production of naïve T cells led to increased autoimmunity and decreased immune defence (Shaw et al. 2010). Moreover, elevated levels of damaged DNA in aged stem cells could result from a deficient repair in response to DNA or from an accumulation of damage over time. Indeed, studies on mice revealed that the decline of hematopoietic activity is correlated with DNA damage, $p16^{INK4A}$ overexpression and telomeres shortening (Janzen et al. 2006). In contrariwise, an excessive proliferation of progenitor cells and stem cells can be deleterious as it is shown to lead to exhaustion and premature ageing (Rera et al. 2011). It seems that the imbalance between stem cell quiescence and proliferation could be deleterious in aged tissue, although it is not exactly clear which mechanisms are involved.

2.2.6. Altered intercellular communication

One of the characteristics of aged tissues is a chronic inflammation, termed as "inflammageing". It is a low grade, systemic and chronic inflammation in ageing, resulting in inflammatory tissue damage, defective autophagy response and dysfunctional immune system (Salminen et al. 2012). These alterations contribute to the activation of the Nod-like receptor (NLRP3) inflammasome resulting in the production of TNF-β (tumor necrosis factor-beta) and precursors of two inflammatory cytokines including IL-1β and IL-18 (Salminen et al. 2012).
Ageing is also characterized by changes at the level of intercellular communication (endocrine, neuroendocrine, or neuronal). Recent studies explain that stress response combined to inflammation activates NF-kB (nuclear factor kappa-light-chain-enhancer of activated B cells) in the hypothalamus. Once the pathway is activated, the production of gonadotropin-releasing hormone (GnRH) is reduced by neurons and may promote age-related alterations such as muscle weakness, skin atrophy and bone fragility (Zhang et al. 2013). These results suggest that the hypothalamus may regulate the inflammatory response through NF-kB and by extension, the systemic ageing (Zhang et al. 2013).

2.2.7. Telomere attrition and mitochondrial dysfunction

The telomere theory in this review suggests that telomere shortening is the main trigger of ageing (López-Otín et al. 2013). However, a recent review describes telomeres shortening as a promising marker of cellular senescence (Bernadotte et al. 2016). Indeed, telomere length is different in various tissues of the same organism (Bischoff et al. 2006). They consider that this parameter can barely tell us anything about the lifespan. Moreover, telomere lengths

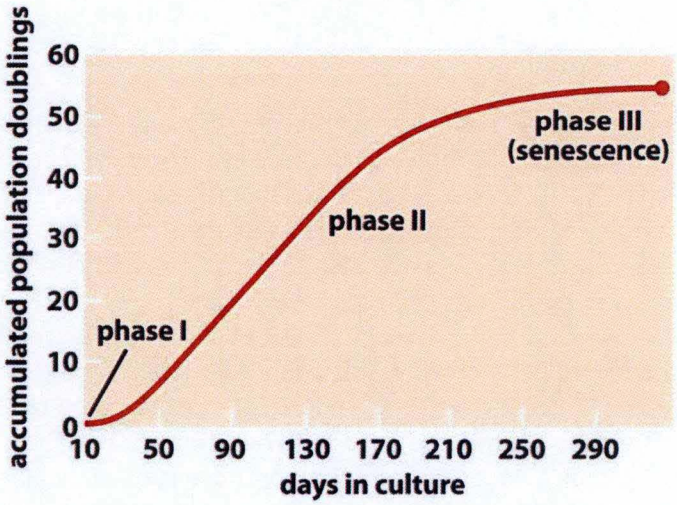

Fig. 3 – The "Hayflick limit" of fibroblasts in culture. Culture could be devided into three phases. Phase I is the primary culture characterised by a slow proliferation. The phase II is characterized by an exponential phase of proliferation. Phase III is called the senescence plateau as it is a period of irreversible growth arrest. Senescent fibroblasts can remain viable and metabolicaly active during almost 1 year (J W Shay and Wright 2000).

between individuals at the same age can significantly change while telomeres lengths are shorter in senescent cells compared to young cells (Kaul et al. 2011).
The controversy is identical for mitochondrial dysfunction because mounting evidence suggests a dynamic relationship between aberrant mitochondria and cellular senescence (Gallage et al. 2016). Consequently, both hallmarks will be described as hallmarks of senescence.

3. What is cellular senescence?

3.1. Replicative senescence

Finally, the last hallmark of ageing is cellular senescence. Indeed, one of the major observations on normal somatic cells cultivated *in vitro* was that these cells could not divide indefinitely, but they are "mortal". In 1961, Leonard Hayflick and Paul Moorhead first described the limited lifespan of cells cultivated *in vitro* while observing cultures of human fibroblasts derived from embryonic tissues (Hayflick and Moorhead 1961). They noticed that fibroblasts stopped dividing after about 50 cumulative population doublings (CPDs). Later, it was shown that senescent cells have an active metabolism and interact with their environment (Goldstein 1990). They also defined that the culture is divided into three critical phases (fig. 3). Phase I is a period of slow proliferation and corresponds to the primary culture when cells derived from biopsies have to adapt to *in vitro* culture and to cover the culture flask. Phase II is characterised by a rapid and exponential proliferation of the cells. Phase III is the period when cell replication declines and irreversibly stops and is also called "the Hayflick limit" (Hayflick 1965). This has been associated with the "ageing" of the cells linked to the exhaustion of their proliferative potential and was therefore called replicative senescence (RS). Replicative senescence will later be associated with the critical shortening of telomeres.

Since these experiments, the fibroblast stays the main cell type used to understand the biological processes underlying cellular senescence. However, it is likely that all other somatic cell types can also enter senescence such as epithelial cells, keratinocytes, etc., and exhibit a cell-type-specific senescence phenotype (Toutfaire et al 2017). The specific phenotype of keratinocytes' senescence will be described later. Besides, replicative senescence is detected after serial cultures of healthy cells isolated from embryonic tissues, from tissues of human donors at different ages and from tissues of many animals such as chicken, mouse, etc (Venkatesan et al. 1998). It was also shown that cells from patients with progeroid syndromes such as Werner syndrome reached senescence after fewer CPDs than normal cells (Faragher et al. 1993). Studies also showed that senescent cells accumulate *in vivo* in aged tissues in humans and in progeroid mice model (Dimri et al. 1995; Baker et al. 2004).
Many studies have shown that senescence may also be induced by other ways such as excessive mitogenic signals (including those produced by oncogenes) and exposure to stresses.

3.2. Oncogene-induced senescence (OIS)

Oncogene activation in human and murine normal fibroblasts has been shown to induce senescence, and this was called "Oncogene-Induced Senescence" or OIS (Serrano et al. 1997). Oncogenes are the mutant version of proto-oncogenes, which are normal genes involved in cellular growth pathways such as RAS, ERK or MYC. Oncogenes have the potential to transform cells, in combination with additional mutations, leading to an uncontrolled proliferation. Several genetic mechanisms explain the conversion of proto-

oncogenes into oncogenes. Indeed, point mutations, chromosomal translocation, insertions or deletions lead to an overexpression of the genes. Contrariwise, tumour suppressor genes encode for proteins inhibiting cell proliferation. Loss of one or more of them contributes to the development of many cancers.
OIS was first demonstrated by the expression of oncogenic *ras* (*H-Ras*^{GV12}) in normal primary rodent and human fibroblasts (Serrano et al. 1997). Ras is known as a small GTPase able to activate several pathways including mitogen-activated protein kinases (MAPK). The oncogenic form of *ras* has been shown to activate an inappropriate proliferation through *c-Myc* overexpression and to inhibit *p53* and *p16*$^{INK-4A}$ expression in rodent cells (Lodish et al. 2000). However, when expressed in normal cells, the oncogenic H-*ras*V12 causes an increase in the abundance of p53 and p16^{INK-4A} and consequently, cell cycle arrest, independently of telomere shortening. In addition, OIS is not triggered by H-*ras*V12 in normal human fibroblasts expressing the hTERT subunit of telomerase (Wei et al. 1999). Furthermore, Ras-induced senescence can be bypassed by inactivation of the p53 and Rb pathways, suggesting that this evolved as a mechanism of tumour suppression (Courtois-Cox et al. 2008).
Senescence can also be induced by the expression of mutated form of tumour suppressor genes like *PTEN*, *VHL*, *RB1* and *NF-1* leading to their inactivation (Nardella et al. 2011)

3.3. Stress-induced premature senescence (SIPS)

Senescence can also be induced by exposure of cells to stress from physical or chemical agents causing oxidative stress and/or DNA damage. This was defined as the "Stress-Induced Premature Senescence" or SIPS (Toussaint et al. 2000). SIPS can be induced by several stress models such as a prolonged exposure to hypoxia (von Zglinicki et al. 2005), repeated exposures to *tert*-butylhydroperoxyde (*t*-BHP) (Dumont et al. 2002), hydrogen peroxide (H_2O_2) (Q M Chen et al. 2001) or UVB radiation (Chainiaux et al. 2002). This type of senescence is also independent of the shortening of telomeres and can be induced in normal cells but also in immortalised or transformed cells (Debacq-Chainiaux et al. 2016).

The three types of senescence induce a senescent phenotype characterised by an irreversible growth arrest but also by the appearance of several senescence-associated biomarkers.

3.4. Biomarkers of senescence

3.4.1. Morphological changes

Senescent cells are subjected to morphological changes. They enlarged, often doubling in volume, and if adherent adopted a flattened morphology. They also display organelle alterations including mitochondria and peroxisomes (Cho et al. 2004). These morphological changes have been reported in RS, in OIS (Serrano et al. 1997) and in SIPS (Dumont et al. 2000; Q M Chen et al. 2001). A study from Chen's group revealed that the presence of underphosphorylated retinoblastoma protein (Rb) in fibroblasts may be essential but not sufficient for senescent morphogenesis induced by hydrogen peroxide (Qin M Chen et al. 2000). Recently, it was also demonstrated that ATF6α (Activating transcription factor 6), a protein involved in the unfolded protein response (UPR), is necessary for the establishment of the senescence-associated cell shape modifications in normal human primary fibroblasts (Druelle et al. 2016).

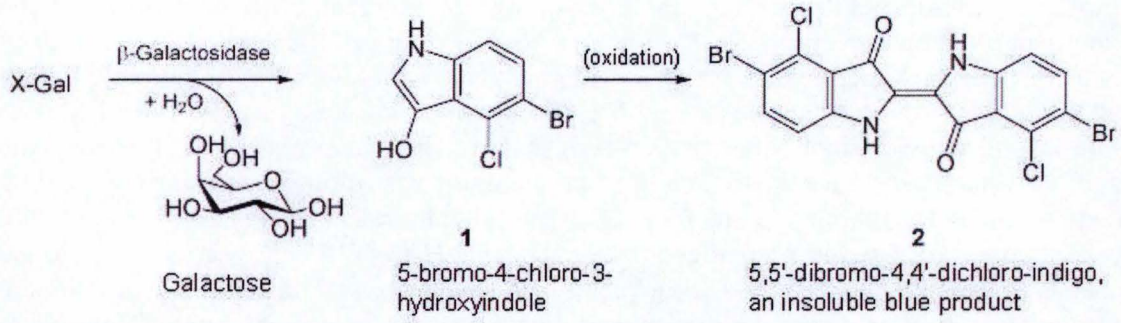

Fig. 4 – X-gal (5-bromo-4-chloro-3-indolyl-β-D-galactopyranoside) is used to measure the abundance of β-galactosidase. X-gal is hydrolyzed by the β-galactosidase enzyme thereby yielding 5-bromo-4-chloro-3-hydroxyindole (1). After spontaneous dimerization and oxidation, 5,5'-dibromo-4,4'-dichloro-indigo (2), an insoluble blue product is formed (http://partsregistry.org/Part:BBa_K173004).

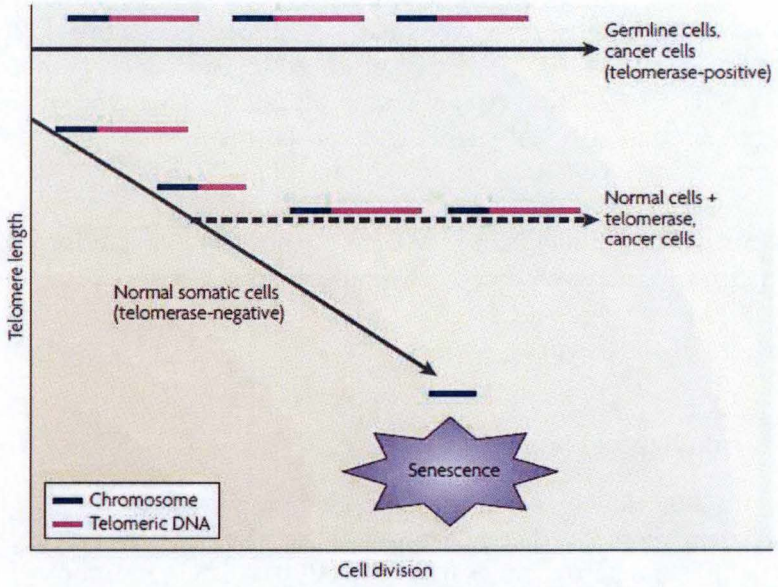

Fig. 5 - The impact of telomeres shortening in human diploid fibroblasts (HDFs). Expression of exogenous telomerase reverse transcriptase (TERT) is expressed in germline cells and allows the formation of cancer cells. In normal somatic cells, telomerase is not expressed inducing a decline in telomere length. Dysfunctional telomeres can trigger a DDR, to which cells respond by undergoing senescence (Campisi, 2007).

3.4.2. Senescence-associated β-galactosidase

Senescence-associated β-galactosidase (SA-βgal) is probably the most widely used marker of cellular senescence allowing a rapid and easy identification of senescent cells both *in vitro* and *in vivo* (Dimri et al. 1995; Debacq-Chainiaux et al. 2009)It is derived from the lysosomal β-galactosidase enzyme whose activity is typically measured at acidic pH 4.5 in cells (fig. 4). Its activity becomes detectable at the suboptimal pH 6.0 in senescent cells, due to its increased protein abundance associated with the overexpression of the gene *GLB1,* coding for the β-galactosidase (Lee et al. 2006), and to the increase of the lysosomal mass during senescence (Kurz et al. 2000).

3.4.3. Telomeres shortening

The telomeres are located at each end of a chromosome and are constituted of a repetitive nucleotide sequence. They are aimed to protect the end of the chromosomes from deterioration (Epel et al. 2004). For vertebrates, the repeated sequence of nucleotides is TTAGGG. In humans, average telomere length is of about 11 kb at birth and reduces to about four kb in elderly, by losing 55 base pairs of telomeric DNA in the liver per year (Takubo et al. 2000). *In vitro*, human cells lacking telomerase lose on average 50-300 bp per cell division (Takubo et al. 2000). This shortening is related to the "end replication problem" due to the incomplete replication of fragments at the end of chromosomes by the DNA polymerase, leading to a critical telomere shortening. Indeed, when telomeres reached this critical length, it causes cell cycle arrest and by extension, cellular senescence or apoptosis (Capper et al. 2007). Interestingly, telomeres are not recognised by DNA damage or repair enzymes complexes because they form terminal loops in a "capped" state, stabilised by telomere-binding proteins. Several proteins can bind to single-stranded telomeric DNA to protect chromosome ends: TRF1/2 (telomeric repeat-binding factor 1/2) and POT-1 (protection of telomeres protein-1) (Deng et al. 2008). Nevertheless, it has been shown that telomere shortening destabilises these loops leading to telomere uncapping. In addition, ROS (reactive oxygen species) predominantly introduce DNA base damage leading to single-strand breaks (SSB). Telomeres acquire oxidative single-strand damage faster than other parts of the genome because sequences containing guanine triplets are more sensitive to oxidative stress and repair of SSB is less efficient in telomeres compared to the rest of the genome (Kawanishi and Oikawa 2004).
The senescence-associated telomere shortening can be counteracted by an ectopic expression of the catalytic subunit of the telomerase (hTERT). The telomerase, a reverse transcriptase expressed in tumour and germinal cells, is able to maintain constant the telomere length by filling the missing nucleotides (Adamus et al. 2014). As a result, the length of telomeres is maintained ensuring a continued proliferation allowing the immortalization of human cells (Jerry W. Shay and Wright 2005) (fig. 5).

3.4.4. Mitochondrial DNA deletion

Denham Harman was the first to propose that the generation of ROS by the mitochondria causes ageing. He developed the "free radical theory of ageing" (Harman 1972).Indeed, the major site of ROS production (approximately 90%) in the cell is the mitochondrial electron transport chain. Compared to nuclear DNA, mtDNA has limited DNA repair process and is, therefore, more sensitive to accumulation of damage. Moreover, several deletions of mtDNA are associated with ageing, including a specific 4,977 bp deletion called "common deletion" (Dumont et al. 2000). An age-dependent increase in mtDNA mutation frequency is observed

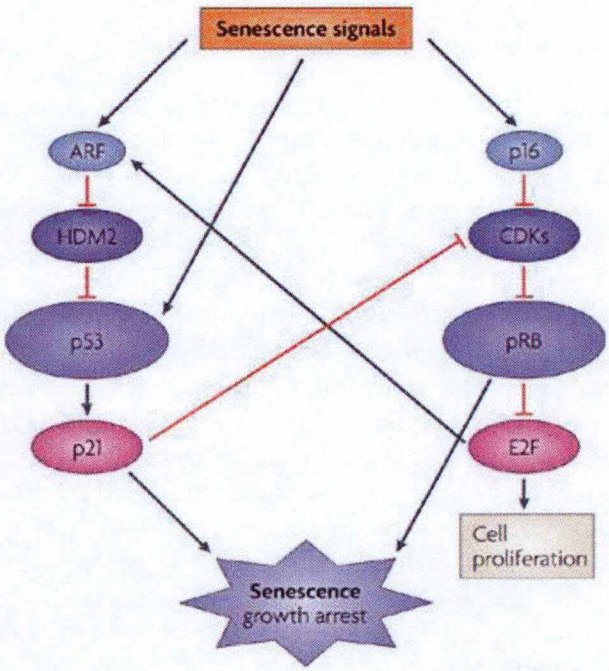

Fig. 6 – Growth arrest controlled by the p53/p21 and p16/pRB pathways. Some senescence signals can engage both pathways. ARF (alternative-reading-frame protein) regulates negatively HDM2 (E3 ubiquitin-protein ligase) that also regulates p53 negatively. Active p53 establishes and maintains the senescence growth arrest by inducing expression of p21, a cyclin-dependent kinase inhibitor (CDKI) that suppresses the phosphorylation and therefore inactivates the retinoblastoma tumor suppressor (pRB). p16, another CDKI keeps pRB in a hypophosphorylated form. pRB stops cell proliferation by suppressing the activity of E2F, a transcription factor which activates genes involved in cell-cycle progression (Campisi et al., 2007).

with deficient activity of respiratory chain enzymes such as cytochrome c oxidase, an enzyme converting molecular oxygen to two molecules of water (Dumont et al. 2000).
It was reported that the increased ROS generation combined with mitochondrial dysfunction affect and accelerate telomere shortening, increase probability of telomere uncapping, activate DNA damage response and finally induce irreversible cell cycle arrest (Passos et al. 2007).
Nevertheless, the process is not clear because a research hightlighted that mtDNA deletion does not change the lifespan and do not necessarily lead to increased mitochondrial ROS generation (Vermulst et al. 2007).

3.4.5. Cell cycle arrest

Senescent cells are mainly growth arrested in the G1/S cell cycle checkpoint. The senescence growth arrest is established and maintained by the p53/p21 and p16/pRb (retinoblastoma protein) pathways (fig. 6). These pathways are interconnected but can also stop independently cell-cycle progression. It results in expression of the cyclin-dependent kinase inhibitors (CDKI) p21 and p16.

The p53 pathway is regulated by multiple proteins such as the E3 ubiquitin-protein ligase HDM2 (MDM2 in mice) inducing p53 degradation and the alternate-reading-frame protein (ARF) which inhibits HDM2 activity (Sherr and McCormick 2002). Once activated, p53 can promote the expression of its transcriptional target p21, mediating a transient DNA-damage induced growth arrest. p21 is then expressed and induces cell cycle arrest.

The pRB protein is a tumour suppressor, which is responsible for a major G1 checkpoint by blocking S-phase entry and cell cycle progression (Dannenberg et al. 2000). p16 can maintain pRB in an active, hypophosphorylated form thereby suppressing the activity of E_2F, a transcription factor that stimulates expression of genes involved in cell-cycle progression (Sherr and McCormick 2002). Under certain conditions, this pathway could even be preferred to p53 pathway, but the activation of p16 in senescence is still not clear (Campisi and d'Adda di Fagagna 2007). One hypothesis suggests that the reduced expression of Polycomb INK4a repressors act on p16 (Itahana et al. 2003). The 16-pRB pathway is essential for SAHF (senescence-associated heterochromatic foci), containing heterochromatin proteins to repress expression of proliferation-promoting genes (Narita et al. 2003).

Experiments showed that senescence could also be triggered after G2 arrest in normal human fibroblasts (Mao et al. 2012).

Both pathways can be activated by DNA damage response (DDR), a pathway involved in the sensing of damaged DNA, resulting in the transient or permanent arrest of cell-cycle progression, allowing to repair the damage (Campisi and d'Adda di Fagagna 2007).

3.4.6. Persistent DNA damage and the DDR pathway

The DNA damage response (DDR) pathway is activated for maintaining cell cycle arrest as long as DNA damage is detected. Indeed, some lesions such as DNA mismatches or hydrolytic reactions can prevent genome replication and transcription and whether they are not repaired, lead to mutations or genome aberrations which threaten cell viability. For example, excessive reactive-oxygen compounds from oxidative respiration or redox-cycling

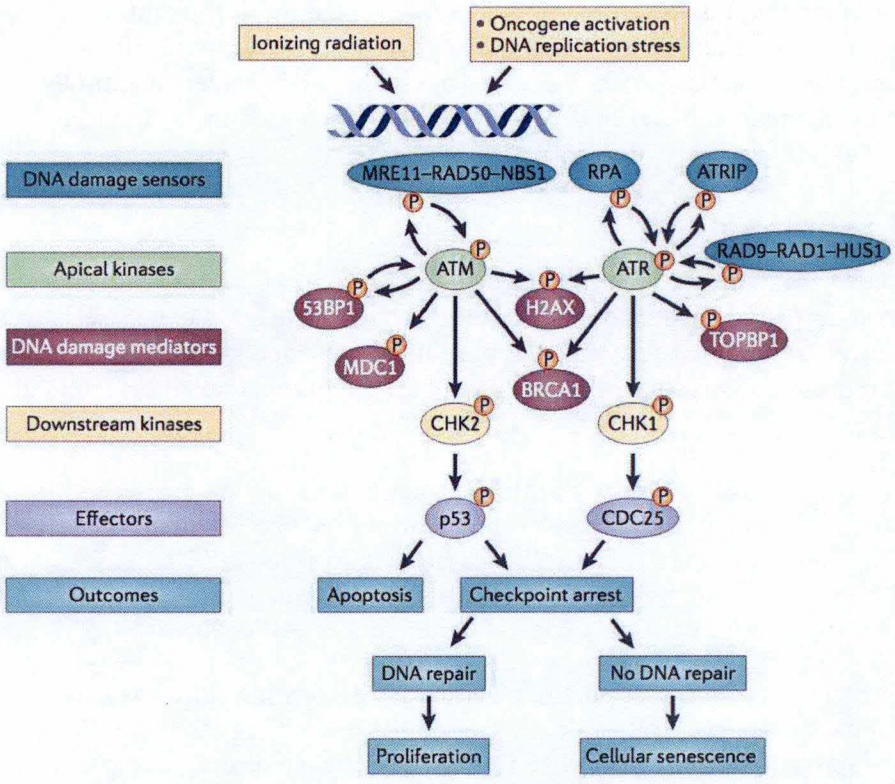

Fig. 7 – The DNA-damage response (DDR)- pathway. Different factors such as ionizing radiation or oncogene activation can generate single-stranded DNA and/or DNA double-strand breaks (DSBs). Damage are recognized by specialized complexes which recruit and activate protein kinases such as ataxia telangiectasia and Rad3-related (ATR) or ataxia-telangiectasia mutated (ATM). These activated apical kinases cause local phosphorylation of the histone H2AX (γ-H2AX) leading to a positive feedback loop by increasing local ATM. The mediator of DNA-damage checkpoint 1 (MDC 1) and p53-binding protein 1 (53BP1) mediate and facilitate this positive feedback loop. An increase of ATM and ATR activity activates and phosphorylates CHK2 and CHK1 (checkpoint kinase 2 and 1) respectively. Signalling pathways converge on cell-division cycle 25 (CDC25) phosphatases and p53 activation and cause an arrest of cell cycle. If DNA damage is repaired, cells can restart to proliferate while if damage is too severe, cells may undergo senescence or apoptosis (Sulli et al. 2012)

metabolism can produce DNA damage. Environmental agents including ultraviolet light, ionizing radiation and cancer-causing chemicals (tobacco) are also three main sources involved in the formation of single-strand and double-strand DNA breaks (SSBs and DSBs, respectively) (Rodier et al. 2009). DDR can sense these DNA damage through specific sensors, thereby protecting cell integrity (Zglinicki et al. 2005). At DSBs, γH2AX (the phosphorylated form of H2AX) allows the recruitment of ATM (Ataxia Telangiectasia Mutated) complexes, crucial for the establishment of a positive feedback loop along the chromatin (fig. 7). Importantly, ATM is activated by double-strand breaks (DSBs) in conjunction with the MRN (MRE11-RAD50-NBS1) sensor complex and γH2AX while ATR (ATM and Rad3 related) is activated in response to persistent single-stranded breaks (Rodier et al. 2009). DNA-binding protein replication protein A (RPA) binds to single-stranded DNA and generate a signal for ATR recruitment. ATR kinase activity is then boosted by the heterotrimeric 9-1-1 complex (composed of RAD9, RAD1 and HUS1) (Weiss et al. 2002). Once ATM is activated, CHK2 (checkpoint kinase 2) is phosphorylated and diffused in the nucleoplasm where DDR is spread. In parallel, ATR propagates the signal to CHK1 that diffuses throughout the nucleus (Bekker-Jensen et al. 2006). After phosphorylation, mediator proteins such as BRCA1 (breast cancer type-1 susceptibility) involved in single-stranded and double-stranded DNA repair are activated. The signal transduction converges to effector molecules such as CDC25 and the tumour suppressor p53. Inactivation of p53, p21 or some DDR proteins (ATM and CHK2) prevents replicative or stress-induced senescence and, in some conditions, can reverse the senescence growth arrest (Beauséjour et al. 2003). In this way, DDR and p53 pathway are necessary mechanisms preventing the proliferation of cells with serious DNA damage which could give rise to cancer development through oncogenic mutations (Bartkova et al. 2006). The result is a transient or a permanent (senescence) halt in cell cycle progression or, if damage are too important, apoptosis (Zglinicki et al. 2005). In addition to p53 activation pathway, DDR can also activate p16-pRB pathway, considered generally as secondary to engagement of the p53 pathway (Jacobs and De Lange 2004).

Thereby, cellular senescence is considered as a cell cycle arrest through persistent DDR. Indeed, several studies support the idea that cellular senescence is actively maintained by a high activity of signalling kinases such as ATM/ATR and Chk1/Chk2 (Rodier et al. 2009). This anti-proliferative response allows the suppression of damaged cells and is considered as a plausible tumour suppressor mechanism

3.4.7. Change in gene expression

Different studies have identified gene expression changes in senescent cells. This includes changes in cell-cycle regulators such as overexpression of p21 and p16 described above but genes coding for proteins stimulating cell-cycle progression are also shown to be repressed in senescent cells (for example, *cyclin A, cyclin B, c-FOS* or *PCNA* (*proliferating cell nuclear antigen*) (Cristofalo et al. 1998). Some of these genes are targets of the E_2F transcription factor, sequestered by hypophosphorylated pRB. Promoters of E_2F target genes acquire heterochromatic features in senescent cells (Narita et al. 2003).

The distinct morphological transition found between non-senescent and senescent cells is notably due to change in genes associated with the cytoskeleton. Indeed, supporting evidence have demonstrated an increase in expression of cytoskeletal genes such as *fibronectin* (Murano et al. 1991). Fibronectin is a glycoprotein found in connective tissue interacting with cell-surface receptors, integrins, that affect cell adhesion, growth, migration and survival.

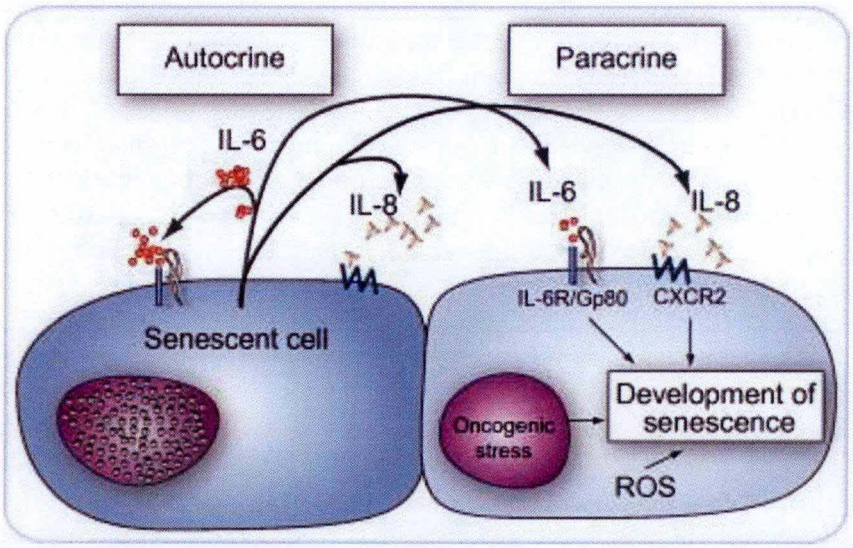

Fig. 8 – Senescent cells induce the senescence-associated secretory phenotype (SASP). Senescent cells secrete factors of the SASP such as IL-6 and IL-8 which both acted in an autocrine or paracrine manner to induce senescence in neighbouring cells. The combination of oncogenic stress and IL-6/IL-8 induces the senescent phenotype (Hoare et al 2010).

Experiments have shown an increase in *fibronectin* expression in culture and in *vivo* in human vascular endothelial cells and in skin fibroblasts (Kumazaki et al. 1993).
In addition, senescent cells can also secrete matrix metalloproteinases (MMPs). These enzymes play a significant role in cells by degrading the extracellular matrix (ECM). ECM remodelling is a crucial process for the regulation of cell differentiation, angiogenesis and wound healing (Streuli 1999; Sottile 2004; Guo and Dipietro 2010). For example, stromelysin-1 and -2 (MMP-3 and -10, respectively) and collagenase-1 (MMP-1) are upregulated in human and mouse fibroblasts undergoing replicative or stress-induced senescence. MMP-1 and -3 can regulate the activity of soluble factors in the SASP such as IL-8 (West et al. 1989).

3.4.8. Senescence-associated secretory phenotype (SASP)

Senescent cells are characterised by a specific secretory profile referred as the Senescence-Associated Secretory Phenotype or SASP (Coppé et al. 2010). Indeed, senescent cells were found to secrete many proteins able to modify their microenvironment. The SASP is divided into three different categories: soluble signalling factors (chemokines, interleukins and growth factors), secreted insoluble proteins (including extracellular matrix components) and secreted proteases (metalloproteinases).
Pro-inflammatory cytokines can trigger cellular responses through both autocrine and paracrine mechanisms (fig. 8). The autocrine feedback loop can reinforce the SASP through pro-inflammatory cytokines and the transcription factor NF-κB (Chien et al. 2011). Senescence can also be transmitted to neighbouring cells through paracrine effects of the SASP. For example, IL-6 secretion appears to be triggered by persistent DNA-damage pathway via phosphorylated ATM and CHK2 and is recognised as a major paracrine mediator of senescence reinforcement (Rodier et al. 2009). IL-1 is another cytokine more secreted by senescent cells and able to activate NF-κB and activator protein-1 (AP-1) pathways thereby promoting pro-inflammatory responses (Mantovani et al. 2001).
SASP factors are suspected to play both beneficial and deleterious roles. Cellular senescence is recognized as a tumour-suppressive mechanism that stops malignant transformation by inhibiting the proliferation of cells with accumulated damage. A study showed that senescent hepatic activated stellate cells (HSC) in fibrotic livers of mice treated with CCl_4, a chemical compound used to induce fibrosis, can limit the accumulation of fibrotic tissue caused by chronic liver damage through the secretion of pro-inflammatory cytokines and growth factors (Krizhanovsky et al. 2008). This result demonstrates that cellular senescence prevents the fibrogenic activation, thereby involving a pathophysiological role of the senescence process. Evidence showed that senescent cells seem to be implicated in wound healing and tissue repair through an efficient mechanism under temporal control, referred to as acute senescence (Burton and Krizhanovsky 2014) (Qin M Chen et al. 2000).
In contrast, chronic senescence is a different process compared to wound healing. During ageing-related senescence, cells can trigger a persistent cell cycle arrest leading to inflammation in tissue (Burton and Krizhanovsky 2014). Indeed, the proportion of senescent cells increases with age in mammalian tissues, which is correlated with an increased risk of cancer and age-related diseases. Other chemokines such as IL-8 or macrophage inflammatory protein (MIP)-1α and -3α are also overexpressed in senescent fibroblasts and showed to be involved in tumour progression (Begley et al. 2005). In addition, senescent fibroblasts may change the macrophage balance in the tumour environment. During angiogenesis, cells are stimulated by vascular endothelial growth factor (VEGF) and IL-8 thereby promoting

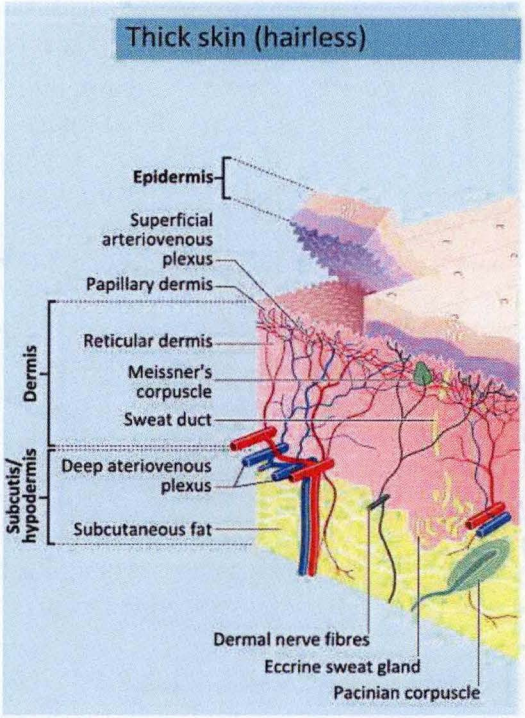

Fig. 9 – Schematic representation of the skin. The skin is composed of 3 layers: the epidermis, dermis and hypodermis. The epidermis is the outermost layer of skin providing a waterproof barrier. The dermis is subdivided into 2 layers: papillary dermis and reticular dermis containing Meissner's corpuscles. Thin skin is characterized by sebaceous glands and hair follicles. The deeper subcutaneous tissue is the hypodermis, made of connective tissue and fat (M.Komorniczak, 2012).

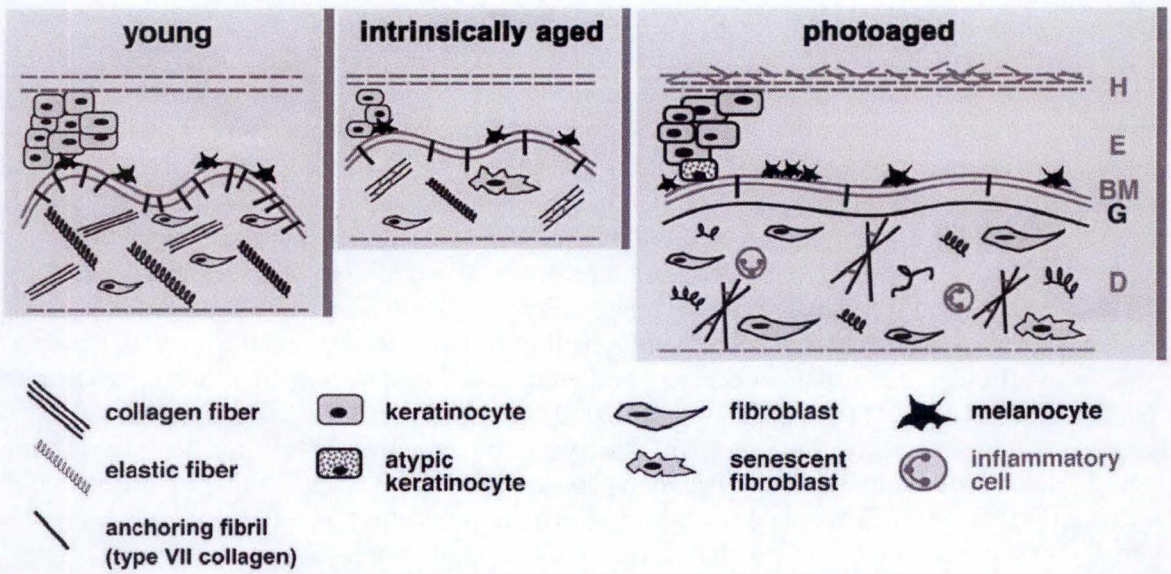

Fig. 10 – Differences between young, intrinsically aged and photoaged skin. Young skin is characterized by a balanced composition of keratinocytes in the epidermis (E), melanocytes adjacent to the basement membrane (BM), fibroblasts and different extracellular components within the dermis (D). Intrinsically aged skin presents a decrease in epidermal and dermal thickness due to a reduction of extracellular matrix and fibroblasts, linked to increased expression of matrix-degrading metalloproteases. Photoaged skin is often hyperplasic with an increase of epidermal and dermal thickness. The distribution of melanocytes is more heterogeneous, which is responsible of aged spots. Anchoring fibrils and interstitial collagen are reduced in number (Wlaschek et al. 2001).

proliferation. Models of mouse xenografts with breast cancer cells have shown the pro-angiogenic effects of the SASP (Coppé et al. 2006). Indeed, the blood vessel density was significantly higher when the tumour developed in the presence of senescent fibroblasts (Coppé et al. 2008).

4. Ageing of the skin

4.1. Histology of the skin

The skin is the largest organ of the human body with a surface area between 1.5 and 2.0 m^2, accounting for about 15% of the total body weight (Kanitakis 2002). Skin is composed of three layers: the hypodermis, the dermis and the epidermis, both separated by the dermal-epidermal junction (fig. 9) (Briggaman 1982; Tortora and Derrickson 2014).
The hypodermis is the innermost and thickest layer of the skin. It is mainly composed of adipocytes, fibroblasts and leukocytes.
The dermis is the layer of the skin between the epidermis and the hypodermis that is composed primarily of dense connective tissue (matrix) with different cell types. The matrix components are mainly type I and III collagens and elastic fibers. The dermis is composed of two layers: the papillary layer (upper layer) and the reticular layer (lower layer). The papillary dermis, connected with the epidermis, contains capillaries, elastic fibers, reticular fibers and thin arranged collagen fibers. It transmits nutrients to the epidermis via blood vessels and controls the temperature of the skin (Kanitakis 2002). The reticular dermis is made up of a thicker layer of dense connective tissue. It contains larger blood vessels, interlaced elastic fibers and collagen fibers parallel to the surface. The dermis also contains hair follicles, nerve endings such as Meissner's corpuscles, Pacinian corpuscles, sweat glands and sebaceous glands (Goldsmith et al. 2012).
Finally, the epidermis is composed of about 95 % of keratinocytes. Keratinocytes move slowly from the basal layer towards the skin surface (Kanitakis 2002).
According to the morphology and the position of keratinocytes, the epidermis can be divided into five distinct layers: *stratum basale, stratum spinosum, stratum granulosum, stratum lucidum* and *stratum corneum*.
Skin constitutes the physical barrier to the environment and preserves the homeostasis and the integrity of the body. It limits the inward and outward passage of water, electrolytes and others substances between the skin and external environment (Proksch et al. 2008). This is intended to prevent invasions of pathogens and damage from chemical and physical assaults (Proksch et al. 2008). However, physiological changes and extrinsic factors can alter the skin over time. Indeed, skin ageing is induced by intrinsic and extrinsic factors, both leading to decreased structural integrity and loss of physiological function associated with inflammation and impaired wound healing (Gosain and DiPietro 2004).

4.2. Intrinsic and extrinsic skin ageing

Skin deteriorates with age due to the synergistic effects of intrinsic and extrinsic factors. Intrinsic structural changes are a natural consequence of ageing. This intrinsic rate of skin ageing can also be influenced by environmental stressors, particularly the ultraviolet light exposure (fig. 10) (Wlaschek et al. 2001).

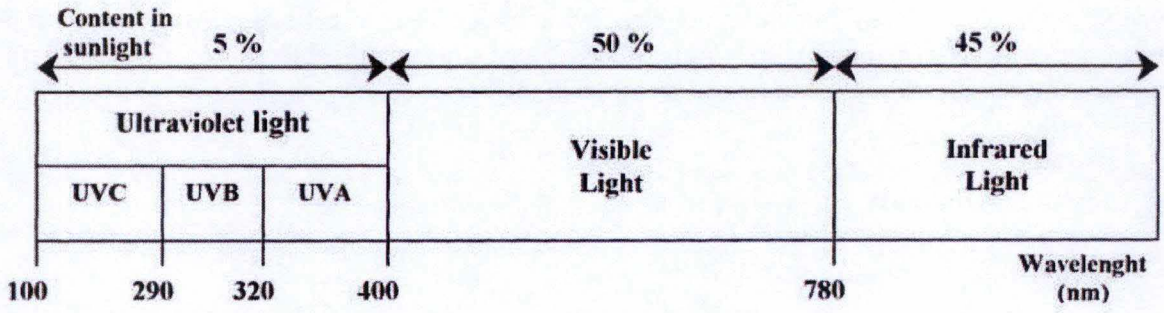

Fig. 11 – Electromagnetic spectrum. Sunlight is composed of a continuous spectrum of electromagnetic radiation subdivided according to the wavelength: ultraviolet (100-400 nm, 5 %), visible (400-780 nm, 50 %), and infrared (> 780 nm, 45 %). UV radiation is also divided into UVA, UVB and UVC rays (Svobodova, 2006).

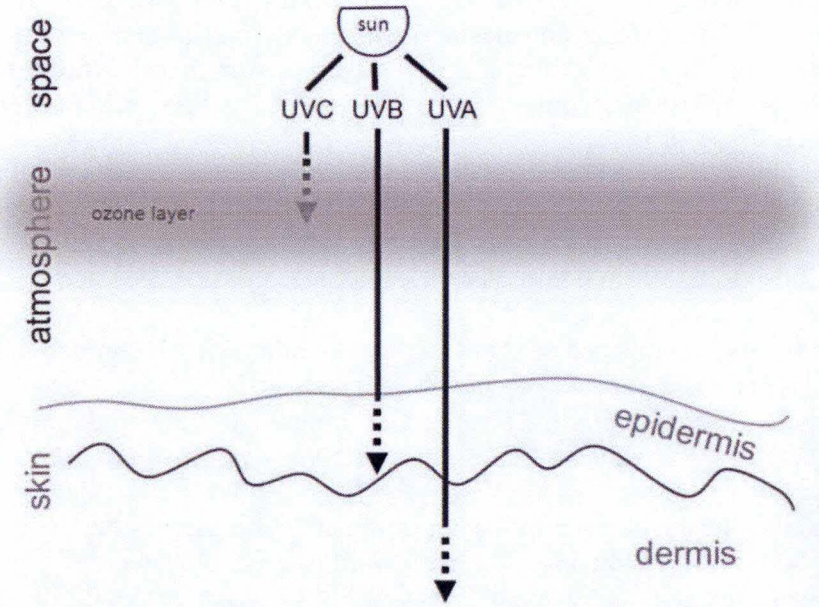

Fig. 12 – Penetration of solar UV radiation through atmosphere and skin. UVC is stopped by the ozone layer. Epidermis absorbs the major part of UVB while UVA penetrates into the dermis (Kammeyer and Luiten, 2015).

Intrinsic ageing of the skin is mainly genetically determined. The intrinsically aged skin is characterised by a thin and smooth aspect associated with a reduction in epidermal and dermal thickness (Farage et al. 2008). In fact, collagen and elastin content decreases while cross-links in collagen fibers appear (Werth et al. 1996). Fibroblasts of the dermis are less numerous and present a senescent phenotype. Moreover, atrophy of the extracellular matrix include a decrease of elastin content and a reduction in the fibrils of interstitial collagen thickness in photoaged skin (Werth et al. 1996) (fig. 10). These characteristic features in the intrinsically aged skin are induced by an increase of MMP degrading these different compounds (Wlaschek et al. 2001). Extrinsic ageing is superimposed to intrinsic ageing and is induced by environmental stress such as solar radiation (Byrne, Tainsky, and Fuchs 1994), cigarette smoke or pollution (Koh et al. 2002). It is clear that solar radiation and mainly its UV components are the most important inducer of extrinsic ageing (90% of visible skin ageing), which is then called "photoageing" (Hussein 2005). People exposed to chronic sun exposures show a rough and dry skin. In the photoaged skin, the thickness of the epidermis and the dermis is increased, due to hyperplasia (Wlaschek et al. 2001). Blood vessels are weakened leading to haemorrhage spot. The distribution of melanocytes is more heterogeneous and form aggregates responsible of the aged spots (fig. 10). Between dermis and epidermis, anchoring fibrils are reduced, and interstitial collagen is also greatly reduced and disordered after long-term sun exposures (Farage et al. 2008). This decrease is due to an increased activity of MMP-1, cleaving the type I procollagen. Moreover, elastic fibers and microfibrillar components are increased and can form a nonfunctional structure (Wlaschek et al. 2001).

4.3. Focus on photoageing

4.3.1. UV radiation

The continuous spectrum of electromagnetic radiation composing the sunlight is categorised into three different groups of wavelengths: ultraviolet (UV), visible light and infrared (fig. 11). According to the International Commission on Illumination, UV radiation is classified in function of the wavelength: UVA (320-400 nm), UVB (290-320 nm) and UVC (100-290 nm). UVC is stopped by the ozone layer while UVA and UVB radiation can reach Earth's surface (Matsumura and Ananthaswamy 2004) (fig. 12). Among ultraviolet radiation, the shortest wavelength radiation (UVC) is the most energetic and can consequently, causes severe biological damage. UVB radiation is the most energetic component of solar rays which can cross the ozone layer, but the proportion of UV rays reaching earth surface is composed of 95 % UVA and only 5 % UVB (Pattison and Davies 2006).

4.3.2. Damage induced by UV

UV radiation is known to be the most harmful and mutagenic part of the solar radiation spectrum (Ravanat et al. 2001). It causes various biological damage, depending on the wavelength. Histologically, the epidermis absorbs the major part of UVB whereas UVA are able to penetrate into the dermis (Wlaschek et al. 2001). UVA and UVB are responsible for skin tanning by activating the melanin production through melanocytes (Clydesdale et al. 2001). However, intense exposure can lead to sunburns and photoageing (Afaq and Mukhtar 2001). The adverse effects of UV radiation are mostly attributed to the UVB. UVB are responsible for sunburn after a short-term exposition, and cause ageing and wrinkling of the skin after a long-term exposition (Wlaschek et al. 2001). UV radiation can induce biological

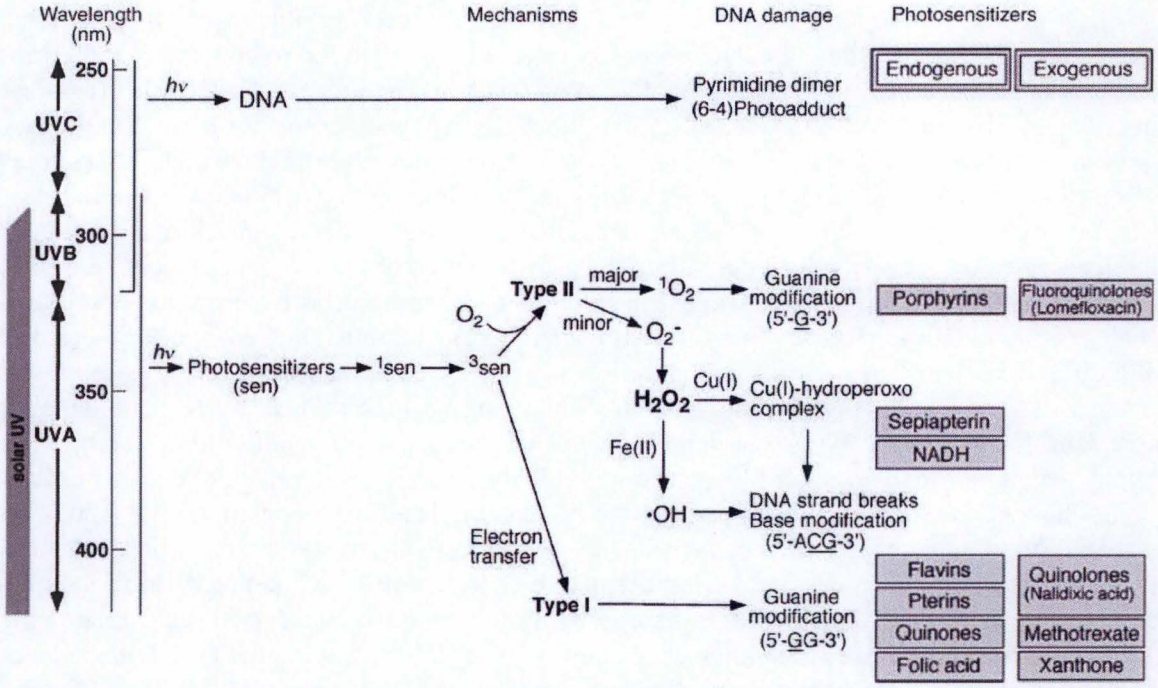

Fig. 13 – UV radiation induces direct and indirect DNA damage. Both UVB and UVC can directly react with DNA to generate pyrimidine dimers such as pyrimidine (6-4) pyrimidone photoadducts. UVA and also UVB induce DNA damage through the activation of photosensitizers. The excited photosensitizers can interact with DNA directly by one electron transfer (type I mechanism) and generate guanine modifications. On the other hand, photosensitizers can directly react with oxygen and generate the different reactive oxygen species, which can react with DNA bases (type II mechanism) (Hiraku et al. 2007).

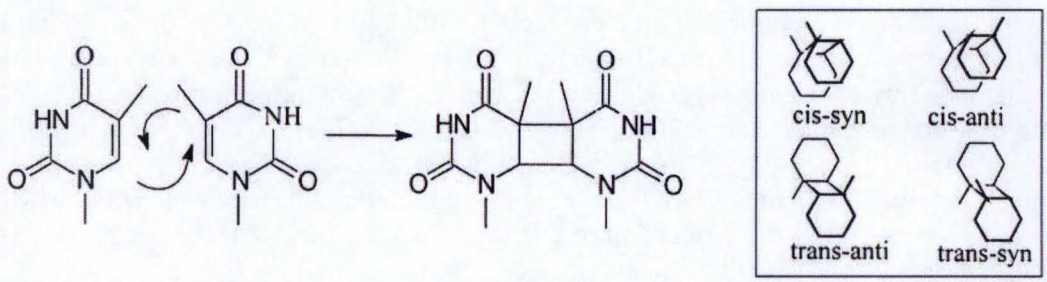

Fig. 14 – Formation of thymine cyclobutane dimers. The inset shows the different diastereoisomers (Ravanat et al., 2001).

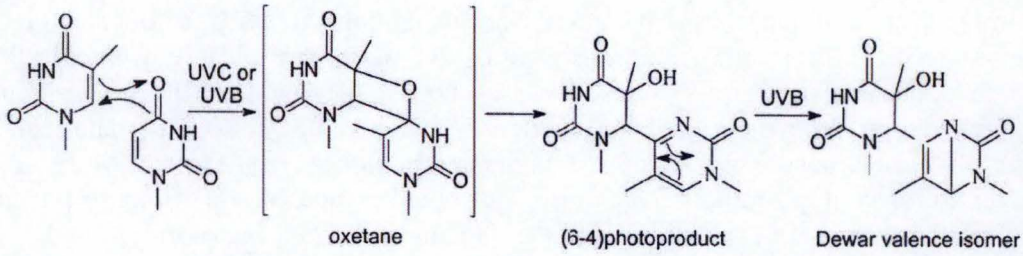

Fig. 15 – Formation and photoisomerization of the thymine (6-4) photoproduct (Ravanat et al., 2001).damage through two mechanisms: the direct absorption of the photon by cellular structures such as protein and DNA and the photosensitized processes (Sinha and Häder 2002).

a. Indirect DNA damage – UV radiation indirectly damages DNA through photosensitization mechanisms mediated by intracellular chromophores (Rastogi et al. 2010). Accordingly, a diversity of cellular compounds has been proposed to be endogenous photosensitizers such as porphyrins and flavins (Rastogi et al. 2010). Two types of reaction exist depending on the properties of the sensitizers as summarised in Fig. 13.
The type I reaction occurs when a photosensitizer (such as flavin, quinone or quinolone), activated by both UVA or UVB radiations, directly interacts with other biomolecules and form a deleterious product (Hanson and Simon 1998). Once the sensitizer is excited, it may directly reacts with DNA by one electron transfer. This reaction is based on the reduction of the excited photosensitizers and the oxidation potential of the DNA bases. Consequently, guanine residues of nucleic acids are most likely to be oxidised because of its lowest oxidation potential among the DNA bases (Hiraku et al. 2007). Also, the formation of 8-oxo-7,8-dihydro-2'-deoxyguanosine (8-oxodG), an oxidative form of DNA lesion is observed (Hiraku et al. 2007). 8-oxodG can pair with adenine during DNA replication, leading to GC/TA transversion. 8-oxodG has been defined as a biomarker of ageing because it accumulates with age (Farrell et al. 2011).
The type II mechanism is characterised by energy transfer from an excited photosensitizer to the oxygen molecule. This causes the generation of the different reactive oxygen species, which can then react with DNA bases and leads to base modification and DNA strand breaks.

b. Direct DNA damage – UVB and UVC irradiations induce dimerization of adjacent pyrimidines leading to cyclobutane pyrimidine dimers (CPDs) (75%) and (6-4) photoproducts (6-4PPs) (25%) (Pattison and Davies 2006) (fig. 14 & 15). CPDs are constituted from a [2+2] cycloaddition of the C5-C6 double bonds of adjacent pyrimidine bases. Different diastereomers may be generated, but only *syn* isomers are produced due to steric constraints (Ravanat et al. 2001). This dimeric photoproduct is able to distort the DNA helix (Kim et al. 1995). The formation of bi-pyrimidine photoproducts depends on the distribution of the pyrimidine bases because a higher number of pyrimidine bases induces a significant flexibility of the DNA. It has been reported that CPDs can inhibit the progress of the DNA polymerase and, consequently block the transcription and the replication (Mouret et al. 2006). Another photoproduct generated by UVB radiation is the conversion of two adjacent cytosines into the dimer of thymidine. It is recognised as a signature of exposure to UVB (Sage 1993).

5. Repair mechanisms

5.1. Antioxidants mechanisms

Reactive Oxygen Species (ROS) are chemical reactive species deriving from oxygen. They are characterised by their high reactive properties and include in particular $O_2^{\cdot-}$, H_2O_2 and $^{\cdot}OH$. They are detected mainly in three organelles: the mitochondria, the peroxisomes and the endoplasmic reticulum (ER). Briefly, mitochondria are the primary source of ROS. Peroxisomes are responsible for scavenging (via catalase-mediated decomposition of H_2O_2) and for the production of ROS (via β-oxidation of fatty acids). ER provides an oxidising environment thereby inducing disulphide bond and protein folding. ROS may act as a mediator involved in the proliferation, the differentiation and the stress-responsive survival

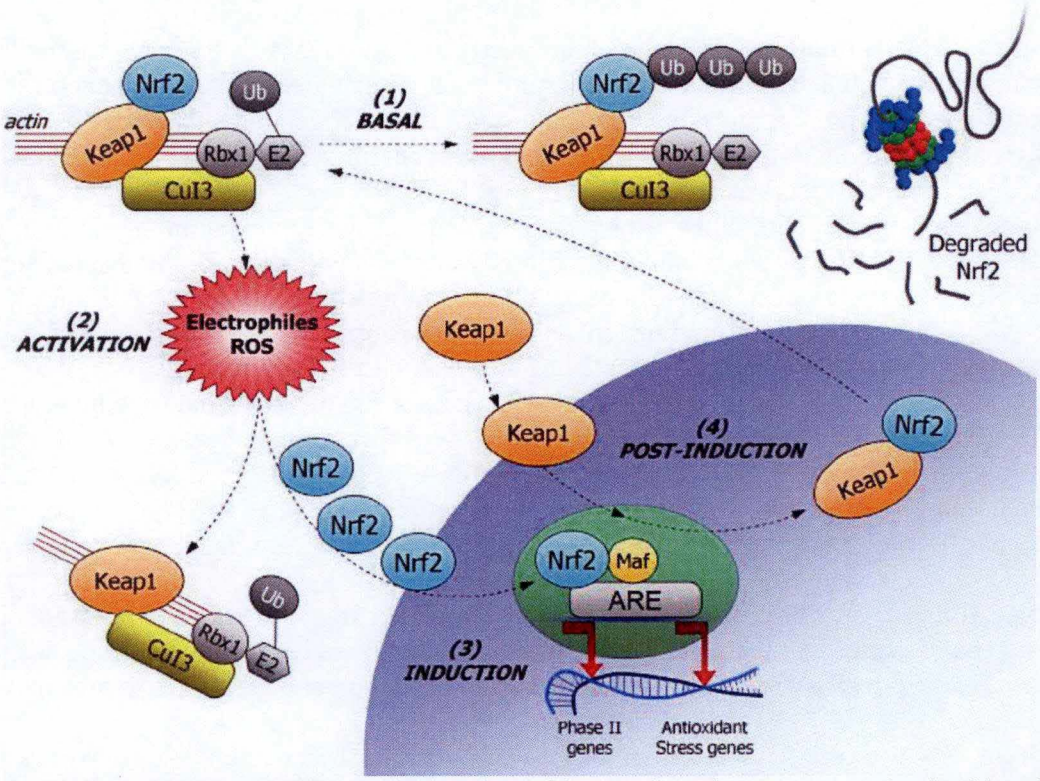

Fig. 16 – Nrf2 and Keap1 system. Under basal condition, Nrf2 and Keap1 are maintained by affinity within the cytosol, leading to ubiquitination and degradation of Nrf2 by the proteasome. Electrophiles or oxidative stress can separate Nrf2 from Keap1. After translocation to the nucleus, Nrf2 binds to AREs (antioxidant response elements) that are sequences found in the promoter region of genes coding for detoxification, antioxidant enzymes and stress proteins. After induction, Keap1 translocates to the nucleus and binds Nrf2 to transport it to the cytosol (Regoli and Giuliani 2014).

pathways. However, the main cellular components (DNA, lipids and proteins) may be damaged whether the production of ROS is excessive (Frohlich et al. 2008).
The transcription factor NF-E2-related factor 2 (Nrf2) is one of the most important regulator of the antioxidant response by maintaining cellular homeostasis (Nguyen, Nioi, and Pickett 2009). In normal condition, the level of Nrf2 is kept low by its inhibitor Keap1 (Kelch-like ECH-associated protein 1) associated to the Cullin 3 (CUL3) E3 ligase complex that facilitates its poly-ubiquitination and degradation by the proteasome (fig. 16). Under oxidative conditions, cysteine residues of Keap1 are oxidised which results in the release of Nrf2. Consequently, disengaged Nrf2 accumulates in the cytosol and can translocate to the nucleus where it recognises the Antioxidant Response Element (ARE) in the promoter of genes coding for antioxidant proteins, molecular chaperones or anti-inflammatory response proteins (Taguchi et al. 2011). In addition, it can dimerize with small Maf (masculoaponeurotic fibrosarcoma) proteins, and induce *Heme-oxygenase 1* (*HMOX1*) and *NAD(P)H:quinone dehydrogenase* (*NQO1*) gene expression (Nguyen et al. 2003).
HMOX1 is responsible for the breakdown of heme molecules to free Fe(II) and allows the activation of Fenton reaction (Gozzelino et al. 2010). At first glance, it seems to be counterintuitive because the Fenton reaction promotes oxidative stress via the production of $^{\bullet}OH$. However, in parallel, Nrf2 boosts the transcription of genes involved in the complex ferritin. This compound converts Fe(II) to Fe(III) and sequesters it to reduce the production of harmful $^{\bullet}OH$ radicals (Gozzelino et al. 2010).
NQO1 is a two-electron reductase able to use either NADH or NADPH as reducing factors. It was shown that NQO1 reduces endogenous quinones to protect cellular membranes against oxidative damage (Ross et al. 2000).
Nrf2 also supports the enzymes responsible for productive glutathione (GSH), which is the most abundant antioxidant cofactor within the cell (Taguchi et al. 2011).

5.2. DNA repair mechanisms

In response to diverse stresses such as UV radiation, chemical agents or pathogens, protective mechanisms such as cell-cycle checkpoint arrest, apoptosis or DNA repair are activated to preserve the genomic integrity. For example, to avoid the lethal effects of UV radiation, the cell has established different repair mechanisms including the base excision repair, the nucleotide excision repair and the double strand break repair (Rastogi et al. 2010).
The base excision repair (BER) is a pathway involved in removing damaged bases that could lead to mutations by mispairing or breaks in DNA during replication. BER occurs against lesions arising from hydrolytic deamination, ionising radiation, alkylating agents or also indirectly, by ultraviolet (Rastogi et al. 2010).
The DNA mismatch repair (MMR) is a highly conserved pathway involved in removing insertion/deletion that escapes polymerase proofreading during replication. The mismatch repair is a strand-specific process with a machinery that distinguishes the newly synthesised strand from the template (parental) (Lyer et al. 2006).
The nucleotide excision repair (NER) plays a crucial role in the repair of DNA lesions induced by solar radiation. Indeed, the most important lesions produced by UV radiation are CPDs and 6-4PPs. The NER pathway involves an interaction between specific enzymes to repair DNA lesions. After recognition of DNA damage by a specific factor (XPC-RAD23B), a protein complex (RAD23B) is recruited to the damaged site, which removes several nucleotides on either side of the damaged bases (Schärer 2013). The excised region is filled in by a DNA polymerase which replaces the excised region (directed by the complementary strand) (Rastogi et al. 2010). Two different pathways can then be distinguished: global

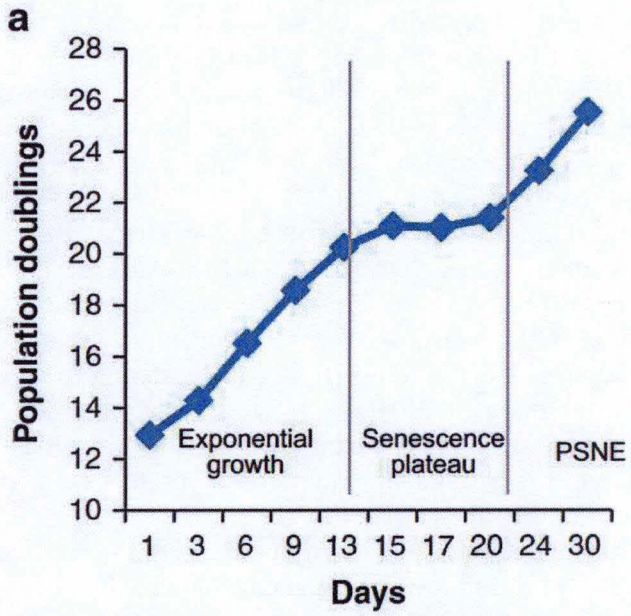

Fig. 17 – Growth curve of *in vitro* NHEKs (normal human epidermal keratinocyte). NHEKs undergo an exponential growth phase before reaching a plateau at which they exhibit biomarkers of senescence. Then, a small fraction of the cell population is able to re-enter in proliferation and to generate-post-senescence neoplastic emergence (PSNE) (Deruy et al., 2014).

genome NER (GG-NER) and transcription-coupled NER (TC-NER). GG-NER is a random process that works gradually by repairing lesions over the entire genome (non-transcribed and transcribed parts of the genome). Contrariwise, TC-NER repairs lesions blocking the transcription via RNA polymerase II in transcribed DNA strands with a high efficiency and specificity(Laat, Jaspers, and Hoeijmakers 1999). Although NER is not essential for survival, genetic disorders such as Xeroderma pigmentosum (XP), a rare hypersensitivity syndrome caused by homozygous defects in one of the effector proteins of NER, can induce a severe sensibility to UV irradiation (Limoli et al. 2003).

Recombination repair is a fundamental process involved in DNA repair. Double-strand breaks (DSBs) can appear due to ionising radiation, UV radiation, ROS or chemotherapeutic genotoxic chemicals. The deleterious effect of DSBs can be counteracted by two independent pathways including homologous recombination (HR) and non-homologous end joining (NHEJ). The NHEJ is an alternative pathway joining strands independent of sequence homology (Rastogi et al. 2010). In addition to the above repair mechanisms, cells may resort to other alternatives against cytotoxic and genotoxic agents by triggering apoptosis (programmed cell death) or cell-cycle arrest.

6. What's known about senescence in keratinocytes?

As told before, a majority of studies in senescence involve human fibroblasts since the discovery of RS by Hayflick in 1961. Senescent human fibroblasts are characterised by multiple features, termed biomarkers. In contrariwise, the senescence is less investigated for other cell types such as keratinocytes.

6.1. Replicative senescence in keratinocytes

Dermal fibroblasts grow *in vitro* for 50 to 60 PDs (according to the donor) before reaching a senescence growth plateau. In contrast, keratinocytes reach a senescence plateau after only 8 to 20 PDs according to the donors. Senescent keratinocytes present common characteristics of senescent fibroblasts such as SA-βgal activity at pH 6,0 and a specific enlarged morphology, as compared to non-senescent keratinocytes (Gosselin et al. 2009). Growth arrest of senescent fibroblasts triggers p53/p21 and p16/pRb pathways (Allsopp et al. 1992). In keratinocytes, the cell cycle arrest is more related to p16, expression as shown *in vitro* (Gosselin et al. 2009) and *in vivo* (Ressler et al. 2006). This observation is consistent with the report of Rheinwald, showing that keratinocytes expressing telomerase are not immortalized unless p16 expression is also abolished (Rheinwald et al. 2002).
Interstingly, it has been demonstrated that keratinocytes die by autophagic programmed cell death or that they can evade in the form of neoplastic post-senescence emergence (PSNE) (fig. 17) (Deruy et al. 2014). Indeed, Gosselin's team showed that normal human epidermal keratinocytes (NHEKs) can spontaneously escape from the senescent state, emerge to re-enter the cell cycle and undergo cell divisions. They also proved that these post-senescent emergence can rise to pre-transformed cells with tumorigenic potential (Gosselin et al. 2009). Moreover, experiments suggest that an increased autophagic activity may play a role in keratinocytes' senescence as fluorescence and electron microscopy revealed an enormous quantity of autophagic vacuoles (Gosselin et al. 2009). It turns out that the progenitors of PSNE have a lower autophagic activity, allowing to avoid autophagic cell death. PSNE is

correlated to their macroautophagy, which is itself also related to the activation of NF-κB/MnSOD/H_2O_2 pro-oxidant pathway. These results suggest that both macroautophagy and oxidative damage are involved in senescence evasion during ageing (Deruy et al. 2014).
Investigations on keratinocytes *in vitro* have shown that Rel/NF-κB factors are involved in cellular senescence. The increase in Rel/NF-κB (composed of RelA, cRel and p50) activity is combined with the increased expression of two Rel/NF-κB target genes: IkBα and MnSOD (manganese superoxide dismutase). The catalytic function of MnSOD is to detoxify the free radical superoxide, recognised as significant by-products of mitochondrial respiration.
In addition, senescent keratinocytes are also resistant to apoptosis caused by TNF-α (tumour necrosis factor). Similarly to previous reports on different cell types, Rel/NK-κB factors has a major protective effect against TNF-α-induced apoptosis (Bernard et al. 2004).
In addition, a recent study showed that senescent keratinocytes are not activated by ATM- or ATR-dependent DDR but rather by an accumulation of oxidative stress inducing SSBs. It was demonstrated that these breaks remain unrepaired and are caused by a decrease in poly(ADP-ribose) polymerase 1 (PARP-1) expression and activity (Deruy et al. 2014).

6.2. UV-SIPS

6.2.1. PUVA-SIPS in fibroblasts

Photochemotherapy employing 8-methoxypsoralen (8-MOP) combined with a long-wave ultraviolet-A (320 - 400 nm) irradiation, called PUVA therapy, is used to treat skin disorders such as psoriasis, T-cell lymphoma and other inflammatory skin disorders (Stern 2007). Psoralens are a group of photosensitizing drugs, which are excited by ultraviolet radiations and generate ROS like singlet oxygen and superoxide anion radicals. In addition to ROS, psoralen photoactivation generates DNA crosslinking inducing DNA fragmentation and chromosome breakage (Stern 2007).
A single non-toxic exposure of 8-MOP/UVA causes an arrest of proliferation of human dermal fibroblasts. At day 15 after irradiation, fibroblasts have a substantial increase in size (Ma et al. 2002). Moreover, the overexpression of interstitial collagenase/matrix metalloproteinase-1 (MMP-1) was induced while TIMP-1, its major inhibitor, was decreased. SA-βgal activity was also monitored and showed positive fibroblasts at day seven after PUVA treatment. Other experiments also showed an increase in hydrogen peroxide or superoxide anion radicals in senescent fibroblasts after PUVA treatment (Ma et al. 2002).

6.2.2. UVB-SIPS in fibroblasts

Different *in vitro* models have been developed to investigate many distinct mechanisms in response to UVB. An *in vitro* model of premature senescence of human diploid fibroblasts (HDFs) induced after repeated exposures to subcytotoxic dose of UVB has been previously set-up in our team (Debacq-Chainiaux et al. 2005). HDFs are exposed to a series of 10 exposures to a subcytotoxic dose of UVB. An irreversible growth arrest and an increased protein abundance of p53, p21 and $p16^{INK-4A}$ have been demonstrated, as well as an overexpression of several senescence-associated genes such as *c-Jun, c-fos, MMP-1, MMP-2, fibronectin, osteonectin* and *apo J* (*apolipoprotein J*) at 72 h after the last UVB exposure (Debacq-Chainiaux et al. 2005). Consequently, this model has highlighted changes in gene expression profiles and senescence-associated features.

6.2.3. UVB-SIPS in keratinocytes

It is assumed that fibroblasts are more sensitive to UVB irradiation than keratinocytes because they contain a less efficient system for genome repair (D'Errico et al. 2007). In the epidermis, keratinocytes are the first cells to be subjected to solar radiation including UVB. It has been shown that after chronic exposure of UVB on keratinocytes, alterations in genes will accumulate and consequently, change the normal process of differentiation (Melnikova and Ananthaswamy 2005). As a result, both oxidative stress and DNA damage are generated in keratinocytes.

Signal transduction controls the fate of keratinocytes depending on the intensity of UVB-induced DNA damage, changes in the cell membrane, and their subsequent. For example, the Insulin-like growth factor-1 receptor (IGFR-1) has been analysed 72 hours after an irradiation with a dose of $100J/m^2$, and results showed that IGFR-1 has a protective role for UVB-induced apoptosis (Lewis et al. 2008).

To better understand the biological effect of UVB-irradiated skin, we used an *in vitro* model set up by our team at a specific wavelength (312 nm) into the UVB spectrum. Experimentally, it has been demonstrated that keratinocytes can repair DNA damage at low doses of UVB while at high doses of UVB, DNA damage and the resulting oxidative stress are too severe thereby undergoing apoptosis (Lewis et al. 2008). At a defined wavelength of 312 nm, we ensure that DNA damage is significant for the keratinocytes, preventing the efficiency of the repair system. Consequently, keratinocytes undergo mitotic arrest and reach a state of premature senescence.

MATERIAL AND METHODS

Table 1: Material for isolation of normal human keratinocytes

Material	Firm, country
Leibowitz L15 medium (500 ml)	Gibco, USA
Antimycotic/antibiotic mix (5 ml)	Gibco, USA
Gentamycin (1 ml)	Gibco, USA
Ethanol (70 %)	Acros Organics, USA
PBS	
- NaCl 150 mM	Merck Millipore, USA
- phosphate buffer 10 mM, pH 7.4	Merck Millipore, USA
- H_2O	
Trypsin + 0.05 % EDTA	Gibco, USA
PBS + 10 % Fetal bovine serum (FBS)	Gibco, USA
Dispase II	Roche Applied Science, Switzerland
Penicillin-streptomycin 1 %	Gibco, USA
Keratinocytes Serum-Free Medium (K-SFM)	Gibco, USA
With keratinocytes supplements:	
- Human recombinant Epidermal Growth Factor (rEGF) (2,5 µg/500 ml)	
- Bovine Pituitary Extract (BPE) (25 mg/500 ml)	
Cell strainers (mesh size: 70 µm)	Greiner Bio One, Austria
75 cm^2 culture flasks	Greiner Bio One, Austria
Automated cell counter	ThermoFisher Scientific, USA
Centrifuge	Eppendorf, Germany

Table 2: Material for NHKs cultures

Material	Firm, country
Trypsin + 0.05 % EDTA	Gibco, USA
PBS + 10 % serum	
- PBS	Lonza, Switzerland
- Fetal bovine serum (FBS)	Gibco, USA
Keratinocytes Serum-Free Medium (K-SFM)	Gibco, USA
With keratinocytes supplements (see table I.I)	
75 cm^2 or 25 cm^2 culture flasks	Greiner Bio One, Austria
6-well or 24-well plates	Corning, USA
Centrifuge	Eppendorf, Germany
Automated cell counter	ThermoFisher Scientific, USA
Neubauer Chamber	Marienfeld, Germany
Trypan blue	Assistant, Germany

1. Cell culture

Normal human keratinocytes (NHKs) were isolated from foreskin biopsies of young donors and obtained from Saint Luc Hospital of Bouge (Belgium). Ethical committee of Saint Luc Hospital approves the procedure.

1.1 Isolation of NHKs

a. Material

Table 1.

b. Method

Skin biopsies are preserved at 4°C in Leibowitz L15 medium with antimycotic/antibiotic mix and gentamycin. After removing the adipose tissue, skin is cut in small pieces of above 5 mm^2. Pieces of skin are washed in three successive baths of PBS, ethanol 70 % and PBS respectively, before an overnight incubation at 4°C in Dispase II with 1 % penicillin-streptomycin. The epidermis is then separated from the dermis and incubated in trypsin-EDTA for 20 minutes at 37°C. To avoid aggregation of epidermis, sample is shaken every 5 minutes during incubation. Trypsin activity is then inhibited by the addition of PBS + 10% foetal bovine serum (FBS). NHKs are isolated using a Cell Strainer with a 70 µm mesh size. The cell suspension is centrifuged 8 minutes at 1200 rpm and then cultivated in 75 cm^2 culture flasks (T75) in 15 ml of Keratinocytes Serum-Free Medium (K-SFM) supplemented with human recombinant Epidermal Growth Factor (rEGF) and Bovine Pituitary Extract (BPE). NHKs are grown at 37°C in a 5% CO_2 humidified atmosphere.

1.2. NHKs cells culture

a. Material

Table 2.

b. Method

Cells are subcultured when they reach about 85 % of confluence. K-SFM medium is removed and trypsin + EDTA (2 ml/T75 or 1 ml/T25) is added. Cells are incubated for 5 minutes at 37°C to allow trypsin activity, which is afterwards inhibited by adding PBS supplemented with 10 % FBS (10 ml/T75 or 5ml/T25). Cells are harvested in the supernatant and centrifuged for 8 minutes at 1200 rpm. The supernatant is then removed, and cells are suspended in K-SFM medium and counted with an automated cell counter. The suspension is distributed in two T75 flasks and K-SFM medium is added to reach 15 ml per flask, before incubation at 37°C in a 5% CO_2 humidified atmosphere. Cumulative population doublings are calculated for each culture. Cells are subcultured (or medium changed) every 2 days. After thawing, the medium is replaced the next day. For replicative senescence, young cells are considered at passage 5 or 6, and cells are subcultured until they reach replicative senescence (around passage 12-13, depending on the donor). For UVB-SIPS, cells are plated in flasks (T25 or T75) or on coverslips with specific confluences (see below).

Table 3: Material for HepG2 cultures

Material	Firm, country
PBS	Merck Millipore, USA
Trypsin + 0.05 % EDTA	Gibco, USA
Dulbecco's modified Eagle's medium (DMEM) low glucose (1 g/l)	Gibco, Life Technologies, USA
+ 10 % Fetal bovine serum (FBS)	Gibco, USA
Centrifuge	Eppendorf, Germany
75 cm^2 culture flasks	Greiner Bio One, Austria
Automated cell counter	ThermoFisher Scientific, USA

Table 4: Material for UVB-Stress Induced Premature Senescence Model

Material	Firm, country
PBS	Merck Millipore, USA
Petri dishes	Greiner Bio-One, Austria
Narrowband Philips Lamps TL20W/01 RS	Philips, Netherlands
Radiometer	Vilber Lourmat, France
UVB sensor	Vilber Lourmat, France
Keratinocytes Serum-Free Medium (K-SFM) With keratinocytes supplements (see table I.I)	Gibco, USA

Table 5: Material for the detection of senescence associated-beta galactosidase (SA-βgal)

Material	Firm, country
PBS	Merck Millipore, USA
Fixation solution	
- 2 % formaldehyde	Belgolabo, Belgium
- 0.2 % glutaraldedyde	Merck Millipore, USA
- PBS	
Staining solution	
- phosphate buffer pH 6	
NaH_2PO_4 0.1 M	Merck, Germany
Na_2HPO_4 0.1 M	Merck, Germany
- potassium ferrocyanide 0.1 M	Merck, Germany
- potassium ferricyanide 0.1 M	Merck, Germany
- NaCl 5 M	Merck, Germany
- $MgCl_2$ 1 M	Merck, Germany
- x-gal solution (20 mg/ml) diluted into N, N, dimethylformamide	Eurogentec, Belgium Janssen Chimica, Belgium
- H_2O	
Methanol	Acros Organics, USA
Microscope	Leitz, Germany

1.3. HepG2 cells culture

a. Material

Table 3.

b. Method

Human liver cancer cells (HepG2 cells) are subcultured in Dulbecco's modified Eagle's medium (DMEM) supplemented with 10 % FBS. When cells reach 80 % of confluence, they are washed with warm PBS and trypsinized. Cells are then centrifuged for 5 min at 1000 rpm and added in 75 cm^2 culture flasks. Cells are growing at 37°C in a 5 % CO_2 humidified atmosphere.

2. UVB-Stress Induced Premature Senescence Model on NHKs

a. Material

Table 4.

b. Method

The UVB-stress Induced Premature Senescence (UVB-SIPS) model used consists of three repeated exposures of NHKs at 675 mJ/cm^2 to narrow-band UVB, in a three-hour interval. At 72 hours before UVB irradiation, NHKs at passage 4 or 5 were subcultured at a density of 12,000 cells/cm^2 for UVB condition and 8,500 cells/cm^2 for control condition (cells are then considered at passage 5 or 6 during the experiment). Before stresses, the medium was removed and cells are washed with 10 ml of sterile PBS. PBS is then removed and cells are incubated in 1 ml/T25 or 3 ml/T75 of PBS during UVB exposures. UVB exposures are made in an irradiation chamber containing three Philips Narrowband TL 20W/01 lamps positioned at about 30 cm above the flask. The emitted UVB radiations are measured with an UVB-sensor linked to a UV radiometer. Control cells are submitted to the same conditions without UVB exposure.

3. Senescence Associated β-galactosidase (SA-βgal) assay

a. Principle

Dimri *et al.* showed that SA-βgal activity is detected at pH 6.0 in senescent cells while normally detected at optimal pH 4.0 in non-senescent cells. Due to the overexpression of its gene and an increase in the biogenesis of lysosomes, this enzyme is overexpressed in senescent cells (Dimri et al. 1995). Therefore, SA-βgal activity is an easy and useful biomarker allowing detection of senescent cells in cultures and tissues.
Cells are incubated at pH 6.0 in a staining solution containing x-gal. Thereby, β-galactosidase cleaves x-gal to generate a blue precipitate noticeable in senescent cells at pH 6.0.

b. Material

Table 5.

Table 6: Material for total proteins extraction

Material	Firm Country
PBS	Merck Millipore, USA
DLA lysis buffer (pH 8.5)	
- Thiourea 2 M	Sigma-Aldrich, USA
- Urea 7 M	Merck Millipore, USA
- Chaps 2 %	Sigma-Aldrich, USA
- ASB 14 2 %	Sigma-Aldrich, USA
- Tris 30 mM	MP Biomedicals, USA
PIC (protease inhibitor cocktail)	
- Tablet dissolved into 2 ml of H_2O	Sigma-Aldrich, USA
PIB (phosphatase inhibitor buffer)	
- Na_3VO_4 25 mM	Sigma-Aldrich, USA
- PNPP (4-nitrophenylphosphate) 250 mM	Sigma-Aldrich, USA
- β-glycerophosphate 250 mM	VWR, USA
- NaF 125 mM	Merck Millipore, USA
Sonicator	Hielscher, Germany
Thermomixer	Eppendorf, Germany
Centrifuge	Eppendorf, Germany

Table 7: Material for nuclear proteins extraction

Material	Firm Country
Hypotonic buffer (HB) 10x	
- NaF 50 mM	Merck Millipore, USA
- Na_2MoO_4 10 mM	Sigma-Aldrich, USA
- Hepes 200 mM	Sigma-Aldrich, USA
- EDTA 1 mM	Merck Millipore, USA
Lysis buffer (100 ml)	
- HB 10x (10 ml)	
- NP-40 (500 µl)	Amresco, Australia
- H_2O (89.5 ml)	
RE (100 ml)	
- HB 10x (10 ml)	
- Glycerol 85 % (20ml)	Merck Millipore, USA
- H_2O (70 ml)	
RE buffer (1 ml)	
- RE (920 µl)	
- PIC (40 µl)	
- PIB (40 µl)	
SA (100 ml)	
- HB 10x (10 ml)	
- Glycerol 85 % (20 ml)	Merck Millipore, USA
- NaCl 4 M (20 ml)	Merck Millipore, USA
- H_2O (50 ml)	
SA buffer (1 ml)	
- SA (920 µl)	
- PIC (40 µl)	Sigma-Aldrich, USA
- PIB (40 µl)	
PBS	Merck Millipore, USA
Washing buffer	
- PBS (60 ml)	Sigma-Aldrich, USA
- Na_2MoO_4 (14.4 mg)	Merck Millipore, USA
- NaF (12.6 mg)	
Positive control	
- SIN-1 (3-Morpholinosydnonimine hydrochloride) (2.5 Mm)	Sigma-Aldrich, USA
- Dulbecco's Modified Eagle's Medium (DMEM), low glucose, GlutaMAX + 10 % serum	Thermo Fisher Scientific, USA
Centrifuge	Eppendorf, Germany

c. Method

At 72 h after the last UVB stress, or at appropriate passages for replicative senescence, SA-βgal assays are made to determine the percentage of senescent cells in the cultures. NHKs are subcultured at low density (1,200 cells/cm^2) in a 6-well plate in K-SFM medium. The day after, cells are washed twice in 2 ml PBS and fixed for 5 min at room temperature (RT) in a fixation solution. After two additional PBS washes, cells are incubated for 16 h at 37°C in freshly prepared SA-βgal staining solution. After incubation, cells are washed twice with 2 ml PBS and once with 1 ml methanol. Cells are observed under phase contrast of bright field illumination using Leitz Labovert FS Microscope. The percentage of SA-βgal positive cells is determined by counting 300 cells per well and 3 wells per conditions.

4. Protein extraction and western blotting

4.1 Total proteins extraction

a. Material

Table 6.

b. Method

Cell medium is removed and NHKs are washed with PBS. Cells are lysed in 150 µl/T75 or 50 µl/T25 of DLA lysis buffer supplemented with PIC and PIB. Cells are scratched and transferred in microtubes. Extracts are sonicated 3 times for 10 seconds at low amplitude (Hilscher Ultrasound Technology) to cleave chromatin. Lysates are incubated at 12°C and shaken at 1,250 rpm for 15 min. Lysates are finally centrifuged 10 min at 12°C at 10,000 rpm to remove cellular debris. Supernatants containing proteins are collected and stored at -80°C.
For positive control, HepG2 cells are incubated 6 h with SIN-1 (3-Morpholinosydnonimine hydrochloride) (2,5 mM) in DMEM before extraction.

4.2 Nuclear proteins extraction

a. Material

Table 7.

b. Method

Extraction of nuclear proteins is performed on NHKs at 1, 24, 48 and 72 hours after UVB-SIPS, or at suitable passages for replicative senescence. Culture flasks (T75) are put on ice. Growth medium is removed and cells are washed with fresh rinse solution. Cells are incubated in 10 ml 1x Hypotonic Buffer (1x HB) for 10 minutes. Once keratinocytes are swollen, 1x HB is removed and replaced by 200 µl of lysis buffer for breaking down cytoplasmic membrane. After scratching, extracts are transferred into microtubes and centrifuged for 30 seconds at 13,000 rpm at 4°C. The supernatants are carefully removed and

Table 8: Material for protein assay

Material	Firm, country
96-well plates	Greiner Bio-One, Austria
H_2O	
Bovine Serine Albumin (BSA) 2 µg/µl	Santa Cruz Biotechnology, USA
Pierce 660 Protein Assay reagent	Thermo Scientific, USA
Ion Detergent Compatibility reagent	Thermo Scientific, USA
Mark Microplate Spectrophotometer	Bio-Rad, USA
Microplate Manager 6 software	Bio-Rad, USA

Table 9: Material for western blot

Material	Firm, country
Loading buffer 5x	
- SDS 20 %	MP Biomedicals, USA
- Glycerol 85 %	Merck Millipore, USA
- Bromophenol blue	GE Healthcare, UK
- β-mercaptoethanol	Fluka, USA
- Tris HCl 0.5 M pH 6.8	Merck Millipore, USA
H_2O	
Centrifuge	Eppendorf, Germany
Running buffer pH 8.3/8.5	
- Tris 25 mM	Merck Millipore, USA
- Glycine 0.192 M	Merck Millipore, USA
- SDS 0.1 %	MP Biomedicals, USA
- H_2O	
10- and 15- well precast protein gels	BioRad, USA
PVDF membrane	Thermo Scientific, USA
Protein standard	Novex, USA
- See Blue Plus 2 protein standard	Invitrogen, USA
- HiMark Pre-Stained, HMW protein standard	BioRad, USA
	BioLabs, USA
- Precision Plus Kaleidoscope Standard	
- Blue Prestained Protein Standard	
Methanol 85 %	Acros Organics, USA
Transfer buffer (pH 8.3)	
- Tris 25 mM	Merck Millipore, USA
- Glycine 150 mM	Merck Millipore, USA
- Methanol 20 %	Acros Organics, USA
- H_2O	
PBS	Merck Millipore, USA
Blocking solution Licor	LI-COR, USA
Tween 20	Bio-Rad, USA
Odyssey scanner	LI-COR, USA
Odyssey V3.0 software	LI-COR, USA

Table 10: Antibodies used for western blot

Primary Antibodies	Firm	Clonality	Source	Dilution	Reference
P-ATM	Cell Signaling Technology	monoclonal	rabbit	1:1,000	#5883
P-ATR	Cell Signaling Technology	polyclonal	rabbit	1:1,000	#2853
P-BRCA	Cell Signaling Technology	polyclonal	rabbit	1:1,000	#9009
P-CHK1	Cell Signaling Technology	monoclonal	rabbit	1:1,000	#2348
P-CHK2	Cell Signaling Technology	monoclonal	rabbit	1:1,000	#2197
P-BRCA	Cell Signaling Technology	polyclonal	rabbit	1:1,000	#9009
P-p53	Cell Signaling Technology	monoclonal	mouse	1:1,000	#9286
ATM	Genetex	monoclonal	mouse	1:1,000	GTX70103
ATR	GeneTex	monoclonal	mouse	1:1,000	GTX70109
CHK1	Cell Signaling Technology	monoclonal	mouse	1 :1,000	#2360
CHK2	Cell Signaling Technology	polyclonal	rabbit	1:1,000	#2662
p53	Millipore	monoclonal	mouse	1:1,000	#05-224
Nrf2	Cell Signaling Technology	monoclonal	rabbit	1:1,000	#12721
Nrf2	Santa Cruz	monoclonal	rabbit	1 :1,000	Sc-13032
Nrf2	ABCAM	monoclonal	rabbit	1 :1,000	AB62-352
HMOX-1	ABCAM	monoclonal	rabbit	1 :500	AB52947
NQO 1	ABCAM	monoclonal	mouse	1 :1,000	AB28947
Secundary Antibody	**Firm**	**Clonality**	**Source**	**Dilution**	**Reference**
IRDye680RD Goat anti-mouse IgG	LI-COR	polyclonal	Goat	1/10,000	#926-32211
IRDye800CW Goat anti-mouse IgG	LI-COR	polyclonal	Goat	1/10,000	#926-32210
IRDye800CW Goat anti-rabbit IgG	LI-COR	polyclonal	Goat	1/10,000	#926-32211

transferred into a new microtube. These supernatants contain the cytoplasmic fractions while the pellets contain the nuclear ones. The pellets are suspended in 50 µl of RE and 50 µl of SA supplemented with PIC and PIB. Microtubes are placed on a wheel for 30 minutes at 4 °C. The last centrifuge is performed for 10 minutes at 13,000 rpm at 4°C. The supernatants containing nuclear proteins are carefully removed and collected into new microtubes to be stored at -80°C.

For positive control, HepG2 cells are incubated 6 h with SIN-1 (2.5 mM) in DMEM before extraction.

4.3 Protein assay

a. Material

Table 8.

b. Method

Protein concentrations were determined by using the colorimetric Thermo Scientific Pierce 660 nm assay reagent. The assay is performed on 96-well plate. Every sample is analysed in duplicate. 9 µl of water and 1 µl of sample are added per well. Bovine serum albumin (BSA) is used for the standard curve from 0 to 10 µg (0, 1, 2.5, 5, 7.5 and 10 µg). A blank sample is also used and composed of 1 µl of lysis buffer and 9 µl of water. 150 µl of the Protein Assay Reagent supplemented with the ionic detergent compatibility reagent (IDCR) is added to each well. After incubation at room temperature for 5 minutes, absorbance is measured at 660 nm by spectrophotometry.

4.4 Western blot analysis

a. Principle

Western blot (WB) is a technique used to detect and quantify specific proteins on samples (tissue homogenate, cells extracts) by the use of specific antibodies. Proteins migrate under denaturing conditions in a SDS-page, allowing a separation by molecular weight. Proteins are next transferred to polyvinylidene fluoride (PVDF) membrane. The use of specific primary antibodies, itself recognised by a secondary labelled antibody, allows the revelation of proteins of interest.

b. Material

Table 9.

Table 10.

c. Method

Protein samples are firstly prepared with loading buffer and 15 µg proteins are used in 20 µl of total volume. Samples are boiled 5 min at 100°C and centrifuged 10 min at 13,400 rpm. Proteins are then loaded on 10- or 15-wells precast polyacrylamide gel (Mini- Protean TGX,

BioRad, USA) with respectively 30 or 20 µl of total volume. Electrophoresis is running for 2 hours under 70 volts in a running buffer. A PVDF membrane is activated into methanol for 1 min and successively washed with PBS for 10 min. The transfer to PVDF membrane is made under liquid condition in transfer buffer. The gel is placed on the membrane inside a "sandwich" system composed of 4 filter papers and 2 sponges previously humidified in the transfer buffer. Transfer takes place for 2 hours under 70 volts electric current.
After transfer, membrane is blocked for 1 hour in a PBS-Licor blocking solution (50 % - 50 %) and then washed 3 times with a PBS-Tween 20 0.1 % solution. Next, membrane is incubated overnight at 4°C with specific primary antibody (Table 10), which is previously diluted in Licor-Tween 20 0.1 % solution. After three successive washings with PBS-Tween 20 0.1 % for 5 min, membrane is incubated for 1 hour at room temperature with secondary antibody (Table 10) diluted 1/10,000 in a Licor-Tween 20 0.1 % solution. Membrane is finally washed three times with PBS-Tween 20 0.1 % and twice with PBS, and protein of interest is revealed and quantified by scanning with an Odyssey V3.0 program (LI-COR, USA). For normalisation, β-actin is used as a protein loading control for cytoplasm and total extracts while lamin A/C is used for nuclear extracts.

5. Analysis of gene expression

5.1 RNA extraction

a. Method

To avoid degradation of RNA, bench and material are cleaned with a solution of 1 % of sodium dodecyl sulfate (SDS). RNA extraction is performed at 1, 24, 48 and 72 hours after the last UVB stress or at adequate passage for replicative senescence.
RNA extraction is performed using the RNeasy mini kit (procedure with DNAse digest) according to supplier's instructions. NHKs are lysed in RLT lysis buffer (600 µl / T25 and 1200 µl / T75). Samples can be stored at -80°C or directly processed. Total RNA samples are isolated with Qiacube (Qiagen). RNA concentration is obtained by absorbance at 260 nm using the ND-1000 (NanoDrop Technologies). The quality of samples is determined by the 260/230 ratio (salts contamination) and 260/280 ratio (protein contamination).

5.2 Reverse transcription

a. Method

Total RNA is reverse transcribed using first Strand cDNA Synthesis kit (Roche Life Science, Switzerland) according to supplier's instructions. Two µg RNA are mixed in RNAse-free water to reach 12 µl. Oligo(dT) primers are added and samples are incubated at 62°C for 10 minutes. Then, 7 µl of RT mix (4 µl reverse transcriptase buffer, 0.5 µl reverse transcriptase, 0.5 µl ribonuclease inhibitor and 2 µl deoxynucleotides) are added per sample followed by an incubation of 30 minutes at 55°C. The reaction is finally stopped on ice, and enzymes are degraded 5 minutes at 95°C. Samples are stored at -20°C.

Table 11: Material for real time PCR

Material	Firm, country
96-well plates	Greiner Bio-One, Austria
H_2O	
SYBR Select Master Mix	Applied Biosystems, USA
Centrifuge	Thermo Scientific, USA
StepOne Plus	Applied Biosystem, USA
SDS software 2.2	Applied Biosystems, USA

Table 12: PCR primers used for real-time PCR

Genes	Abbreviation	Forward Primer	Reverse Primer
Glyceraldehyde-3-phospate-dehydrogenase	GAPDH	ACC CAC TCC ACC TTT GAC	GTC CAC CAC CCT GTT GCT GTA
Interleukin-6	IL-6	TCC AGG AGC CCA GCT ATG AA	CCC AGG GAG GAA CTT CAG GTG ATT
Interleukin-8	IL-8	CTG GCC GTG GCT CTC TTG	GGG TGG AAA GGT TTG GAG TAT G
Ribosomal protein L13	RPL 13	GCC TAC AAG AAA GTT TGC CTA	TGA GCT GTT TCT TCT TCC GGT
Vascular endothelial growth factor	VEGF	CCA AGG CCA GCA CAT AGG AG	TGC TCT ATC TTT CTT TGG TCT GC
Insulin-like growth factor binding-protein 3	IGFBP3	CAG AGC ACA GAT ACC CAG AAC TTC	CAC ATT GAG GAA CTT CAG GTG ATT
Heme oxygenase-1	HMOX-1	GCA GTC AGG CAG GGT GAT A	CAA CTC CTC AAA GAG CTG GAT GTT
NAD(P)H dehydrogenase (quinone 1)	NQO1	GGG ATC CAC GGG GAC ATG AAT G	ATT TGA ATT CGG GCG TCT GCT G
Superoxide dismutase 2	SOD 2	CAA ATT GCT GCT TGT CCA AAT C	CGT CTC CCA CAC ATC AAT C

5.3 Real-time PCR

a. Principle

Quantitative Polymerase chain reaction (qPCR) is a technique based on the polymerase chain reaction (PCR). The method uses the linearity of DNA amplification to determine the relative or absolute amounts of a sequence. An intercalating dye (SYBR Green) is used to be incorporated into double-stranded DNA. The level at which the fluorescence is measurable is called the threshold cycle (Ct), and the amount of target DNA/cDNA can be compared to the amount of a housekeeping gene knows to be equally expressed in the various conditions tested.

b. Material

Table 11.
Table 12.

c. Method

Real-time PCR is performed on 96-well plate, on 5 µl of 100 X diluted cDNA per sample (in duplicate). 20 µl of a master mix containing forward and reverse primers (Table 12), and Power SYBR Green PCR Master Mix are added to cDNA per well. Real-time PCR is performed by using the StepOnePlus instrument. The thermal cycling conditions consists of an initial denaturation step at 95°C for 5 min, followed by 40 cycles at 95°C for 30 seconds and 65°C for 1 min.
Data are analysed by using the SDS software 2.2. Relative abundance of transcripts is determined by delta Ct and normalised with GAPDH (glyceraldehyde 3-phosphate dehydrogenase) expression as housekeeping gene.

6. Analysis of ROS level by flow cytometry

a. Principle

Flow cytometry is a technique that is widely used to measure and analyse the physical and chemical characteristics of particles, usually cells, in a fluid through a beam of light. The properties analysed include cell size, cytoplasmic complexity, DNA or RNA content and membrane-bound and intracellular proteins. These characteristics are defined from an optical-to-electronic coupling system that records how the particle emits fluorescence and scatters incident laser light.
For this master thesis, generation of reactive oxygen species (ROS) is analysed in keratinocytes under UVB-SIPS condition. The DCH probe used is firstly under DCFH-DA form (2',7'-dichlorofluorescein diacetate - DCFH-DA), a stable non-fluorescent dye which can passively enter into cells, before being captured when its acetate groups are cleaved by esterases. The probe could be converted to the fluorescent 2',7'-dichlorofluorescein (DCF) upon oxidation of ROS. The intensity signal at 488 nm is proportional to the intracellular level of ROS.
The MitoSOX Red reagent is a fluorogenic dye highly specific of superoxide anion, also used to analyse mitochondrial ROS. Once in mitochondria, the dye is oxidised by superoxide but

Table 13: Material for detection by flow cytometry

Material	Firm, country
Trypsin + 0.05 % EDTA	Gibco, USA
PBS + 10 % Fetal bovine serum (FBS)	Gibco, USA
Hanks' Balanced Salt Solution (HBSS)	Life technologies, USA
Flow cytometry tube	In Vitro Technologies, USA
SIN-1 (3-Morpholinosydnonimine hydrochloride),	ThermoFisher Scientific, USA
CM-H_2DCF	Life Technologies, USA
MitoSOX Red Mitochondrial Superoxide Indicator	Thermo Scientific, USA
Antimycin A	Sigma-Aldrich, USA
FCCP	Sigma-Aldrich, USA
Centrifuge	Eppendorf, Germany
flow cytometer (BD FACSCalibur)	BD Biosciences, USA

Table 14: Material for immunocytochemistry

Material	Firm, country
Paraformaldehyde	Merck Millipore, USA
PBS	Merck Millipore, USA
Triton X100	Sigma-Aldrich, USA
BSA	Santa Cruz Biotechnology, USA
TO-PRO 3	Molecular Probes, USA
RNAse	Sigma, USA
Coverslips	VWR, USA
Mowiol	Sigma-Aldrich, USA
Confocal microscopy	Leica, Germany

Table 15: Antibodies used for immunocytochemistry

Primary Antibodies	Firm	Clonality	Source	Dilution	Reference
P-ATM	Cell Signaling Technology	monoclonal	rabbit	1:1,000	#5883
P-ATR	Cell Signaling Technology	polyclonal	rabbit	1:1,000	#2853
P-BRCA1	Cell Signaling Technology	polyclonal	rabbit	1:1,000	#9009
P-CHK1	Cell Signaling Technology	monoclonal	rabbit	1:1,000	#2348
P-CHK2	Cell Signaling Technology	monoclonal	rabbit	1:1,000	#2197
P-p53	Cell Signaling Technology	monoclonal	mouse	1:1,000	#9286
p53	Millipore	monoclonal	mouse	1:1,000	#05-224
Nrf2	Santa Cruz	polyclonal	rabbit	1:500	Sc-13032
Secundary Antibodies	**Firm**	**Clonality**	**Source**	**Dilution**	**Reference**
Goat anti-rabbit IgG, Alexa Fluor 488 conjugate	Molecular Probes	polyclonal	goat	1:10,000	#A11008
Goat anti-mouse IgG, Alexa Fluor 488 conjugate	Molecular Probes	polyclonal	goat	1:10,000	#A11001

not by other ROS or RNS. The oxidation product becomes highly fluorescent and exhibits red fluorescence upon binding to nucleic acids.

b. Material

Table 13.

c. Method

At 24, 48 and 72h after the last UVB stress, NHKs are cultured into 6-well plates at a density of 200,000 cells per well. Next day, the medium is removed and 1 ml of trypsin-EDTA 0.05% is added to each well. When cells detach, trypsin activity is stopped by adding 2 ml of PBS + 10 % FBS. Cell suspensions are centrifuged for 8 min at 1,200 rpm in flow cytometry tubes.
For DCF probe: supernatants are removed and pellets are suspended in 100 µl Hanks' Balanced Salt Solution (HBSS) mixed with DCF probe (2.5 µM). As positive control, SIN-1 (3-Morpholinosydnonimine hydrochloride) (2.5 mM) is suspended with the DCF probe (2.5 µM) in 100 µl of HBSS. As negative control, cells are incubated in HBSS without probe. Cells are incubated with respective mixes for 20 min in the dark at 37°C and 5 % CO_2. Then, cells are washed twice with 500 µl cold HBSS and centrifuged 8 min at 1,200 rpm. Pellets are finally suspended in 500 µl HBSS and directly analysed by flow cytometry, considering 10,000 events for each sample.
For MitoSOX probe: the probe is dissolved in dimethylsulfoxide (DMSO) (5 mM) and the stock solution is furthermore diluted in HBSS to make a 5 µM MitoSOX solution. The experimental procedure is identical compared to DCF probe. Antimycin A (AA) and Carbonyl cyanide-4-(trifluoromethoxy)phenylhydrazone (*FCCP*) are dissolved in ethanol to make respectively 20 and 40 mM stock solution. As positive controls, pellets are suspended in HBSS with AA (1, 2.5, 5, 10 µM) and FCCP (20 µM). As negative control, pellets are suspended in 100 µl of HBSS without dye.

7. Immunocytochemistry

a. Principle

For immunocytochemistry, the protein of interest is first preserved in the cells by fixation. It is a technique used to localise a protein into cells by using specific primary antibody, that binds to the antigen and whose excess is washed off with buffer. This primary antibody is recognised by a second fluorophore-conjugated antibody. The secondary antibody can also be labelled to enzyme such as the horseradish peroxidase, which is the most efficient label for second antibody. Following further washing, the peroxidase reacts with its substrate. Cells and fluorescent signal are observed using a confocal microscope.

b. Material

Table 14.
Table 15.

c. Method

At 24 hours before fixation, NHKs are seeded at a density of 40,000 cells per glass coverslip (or 24 hours before UVB stresses directly on coverslips for 1 hour and 24 hours UVB-SIPS

Table 16: Material for enzyme linked-immunosorbent assay

Material	Firm, country
VEGF DVE00 kit	R&D Systems, USA
IL-6 D6050 kit	R&D Systems, USA
IL-8 D8000C kit	R&D Systems, USA

condition). Cells are fixed with PBS-4 % paraformaldehyde (PFA) solution for 10 min at room temperature (RT). Cells are washed 3 times with cold PBS and permeabilised with a solution of PBS-Triton X-100, for 5 min at room temperature. To avoid non-specific staining, every coverslip was rinsed three times (10 min) with PBS-2 % BSA (Bovine Serum Albumin). Primary antibodies (30 µl) diluted in PBS-2% BSA solution (Table 15) are added onto coverslips. Incubation with the primary antibody takes place overnight at 4°C in a wet chamber. Coverslips are washed three times with PBS-2 % BSA solution, before the one-hour incubation with secondary antibodies, at RT in a wet chamber and in the dark. Secondary antibodies (30 µl) are diluted 1/1,000 in PBS-2 % BSA (Table 15). Cells are washed three times with PBS- 2 % BSA solution and once with H_2O. To stain nuclei, cells are incubated with 30 µl of TO-PRO-3 diluted 1/80 in PBS + RNAse (2 mg/ml) for 35 min at RT. Finally, cells are rinsed 3 times with PBS. Coverslips are mounted with Mowiol (prewarmed at 56°C) on glass microscope slides, and observed by confocal microscopy, using a constant multilayer.

8. ELISA (Enzyme-linked Immunosorbent Assays)

a. Principle

Enzyme-linked Immunosorbent Assays (ELISA) is a technique used for the quantitative assessment of an antigen in a sample. This assay requires a compatible antibody that recognises epitopes. A first specific antibody is coated onto a microplate and used to immobilise a specific protein. Samples, including a standard and control are added to each well. After washing, an enzyme-linked polyclonal antibody specific for the protein of interest is added into the wells. Following a wash to remove any unbound antibody-enzyme reagent, a substrate is added to the plate. The reaction is then converted into a coloured product that can be measured using a plate reader. The concentration of antigen in a sample is calculated using the optical density (OD). Using a protein of a known concentration, a standard curve is required to determine the antigen concentration in a sample.

b. Material

Table 16.

c. Method

Conditioned media are collected at 1, 24, 48 and 72 hours after the last stress and centrifuged at 12,000 rpm for 8 min. Supernatants are collected and directly used or stored at -80°C. Different kits are used depending on the protein of interest: VEGF (Vascular Endothelial Growth Factor, R&D Systems, USA, DVE00), IL-6 (Interleukin-6, R&D Systems, USA, D6050) and IL-8 (Interleukin-8, R&D Systems, USA, D8000C). For each ELISA assay, a standard curve is established in accordance with supplier's instructions. All standards, samples and controls are assayed in duplicate. Assay diluents (100 µl for IL-6 and IL-8 and 50 µl for VEGF) are added to each well. Conditioned media (100 µl) are then suspended to assay diluent. The microplate is covered with adhesive strip and samples are incubated for 2 hours at RT. After 4 washes with washing buffer, human IL-6 antibodies and VEGF antibodies conjugated to horseradish peroxidase (HRP) are added in respective wells and incubated for 2 h (1 hour for IL-8) at RT. Wells are washed before incubation for 30 min in

Table 17: Material for TransAM assay

Material	Firm, country
StreptaWell, High Bind	Sigma-Aldrich, USA
PBS	Merck Millipore, USA
PBS 50	
- NaCl 50 mM	Merck Millipore, USA
- phosphate buffer 10 mM, pH 7.4	Merck Millipore, USA
- 0.1 % tween 20	Bio-rad, USA
- H_2O	
BSA	Santa Cruz Biotechnology, USA
Binding buffer (pH 7.5)	
- Hepes 2 mM	Sigma-Aldrich, USA
- EDTA 0.2 mM	Merck Millipore, USA
- NaCl 8 mM	Merck Millipore, USA
- Glycerol 12 %	Merck Millipore, USA
- DTT (dithiothreitol) 1 M	Sigma-Aldrich, USA
- H_2O	
Hypotonic buffer (HB) 2x	
- NaF 50 mM	Merck Millipore, USA
- Na_2MoO_4 1 mM	Sigma-Aldrich, USA
- Hepes 1 M, pH 7.9	Sigma-Aldrich, USA
- EDTA 0.5 M	Merck Millipore, USA
- H_2O	
RE (1 ml)	
- HB 2x (500 µl)	Merck Millipore, USA
- Glycerol (200 µl)	
- H_2O (300 µl)	
RE buffer (1 ml)	
- RE (920 µl)	
- PIC (40 µl)	
- PIB (40 µl)	
SA (1 ml)	
- HB 2x (500 µl)	Merck Millipore, USA
- Glycerol (200 µl)	Merck Millipore, USA
- NaCl 4 M (20 ml)	
- H_2O (50 ml)	
SA buffer (1 ml)	
- SA (920 µl)	Sigma-Aldrich, USA
- PIC (40 µl)	
- PIB (40 µl)	

Dilution buffer - RE buffer (800 µl) - SA buffer (200 µl) - PIC (40 µl) - PIB (40 µl)	Sigma-Aldrich, USA
GLORIA (powdered milk)	
TMB one component substrate	VWR, USA
Stop solution for TMB substrates	ThermoFisher Scientific, USA
Mark Microplate Spectrophotometer	Bio-Rad, USA

the dark with Color Reagents A and B mix. Stop solution (50 µl) (R&D Systems, USA, #895032) is finally added and a spectrophotometer is used to read plates at 450 nm, with the correction wavelength set at 540 nm or 570 nm.

9. TransAM (Transcription Factor ELISAs)

a. Principle

The tranAM method combines both ELISA techniques and the sensitivity and the specificity of transcription factors assays. Kits contain 96-well plates coated which oligonucleotides containing the binding sites of the protein of interest (consensus sequences). After incubation with the samples, a primary antibody is used to bind the protein of interest upon DNA binding site. The HRP-conjugated secondary antibody recognises primary antibody and provides a sensitive colorimetric readout quantified by spectrophotometry.

b. Material

Table 17.

c. Method

Plates are firstly coated with the nucleotide-binding Nrf2 sequence (5' - GTCACAGTGACTCAGCAGAATCTG- 3'). For this, 4 pM of nucleotide-binding Nrf2 in 50 µl of PBS 50 tween 0.1 % are added per well. An adhesive cover is used to seal the plate before incubation for 1 hour at 37°C. Each well is washed twice with PBS 50 tween 0.1 % and once with H_2O. Plates are dried at 37°C and can be kept many weeks at 4°C.
Binding buffer (30 µl) is added to each well. For each well, 10 µg of nuclear extracts are suspended in dilution buffer for a total volume of 20 µl. An adhesive cover seals plate before incubation for 1 hour at RT with mild agitation. After incubation, each well is washed 3 times with PBS 50 tween 0.1 % and 100 µl of Nrf2 antibody (1:500 dilution in PBS + BSA 1 %) is then added to each well. The plate is covered and incubated for 1 hour at RT without agitation. After incubation, wells are washed 3 times with PBS 50 tween 0.1 %. 100 µl of diluted HRP-conjugated antibody (1:1,000 dilution in PBS + Gloria 1 %) is then added and the plate is covered for 1 hour at RT without agitation. After, 4 washes with PBS 50 tween 0.1 %, TMB substrate solution (100 µl per well) is incubated for 10 min at RT in the dark. The blue colour turns yellow by adding 100 µl of stop solution per well. After 5 min, absorbance is read at 450 nm with a reference wavelength of 655 nm.
The nuclear extract from HepG2 incubated 6 hours with SIN-1 (2.5 mM) is used as positive control and lysis buffer is used as negative control.

10. Statistical tests

Pairwise comparisons were performed by using unpaired and paired t-test or two-way ANOVA and Tukey post-hoc tests (NS: not significant, *: $0.01<P<0.05$, **: $0.001<P<0.01$, *** $P<0.001$).

Results

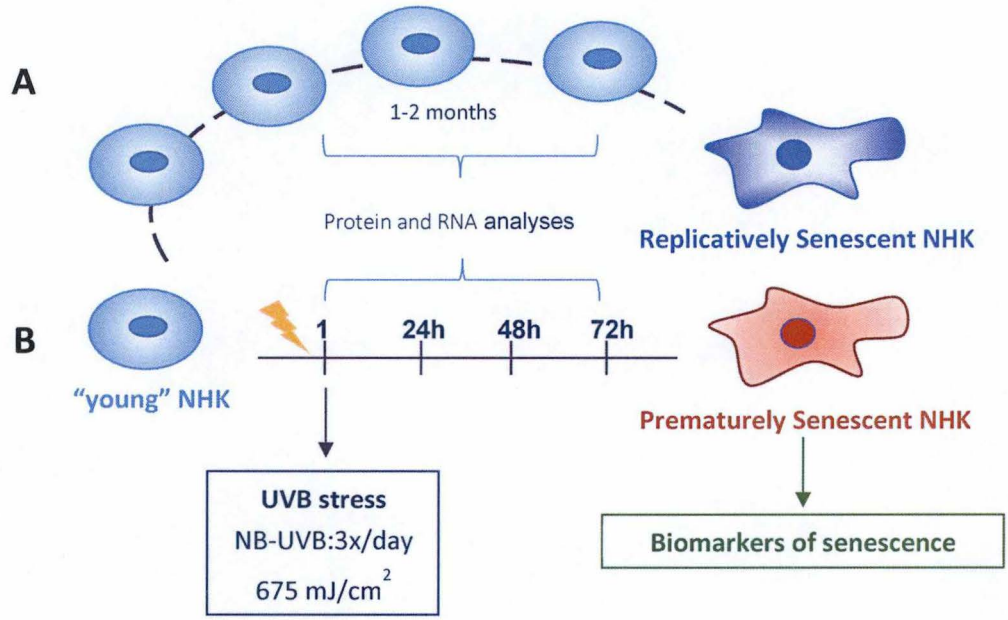

Figure 1: Replicative senescence (RS) and UVB-SIPS model in normal human keratinocytes (NHKs). **A.** NHKs were subcultured from passage 4 to 10-12. Protein and RNA analyses were performed for each passage. Senescence biomarkers were checked at each passage.

B. 72 hours before UVB stresses, NHKs were subcultured at passage 5 or 6. Cells were exposed 3 times to NB-UVB at 675 mJ/cm^2, in a three-hour interval. Control cells were not exposed to UVB. Cells were analyzed at 1, 24, 48, 64 and 72 hours after the last UVB stress, and senescence biomarkers were checked at 72 hours.

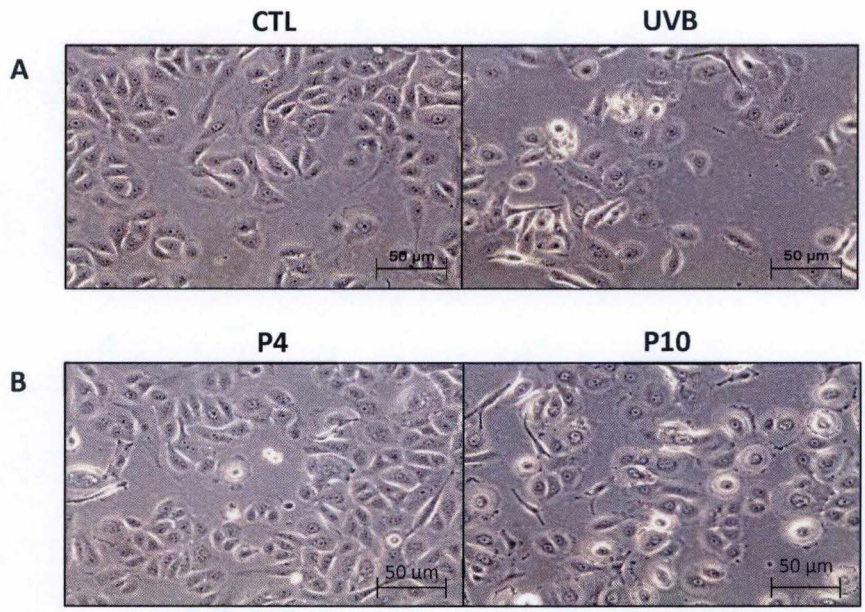

Figure 2: Morphological changes in UVB-SIPS (A) and in RS (B) in NHKs. A. Morphological changes observed in UVB-SIPS in NHKs. NHKs were exposed (or not: CTL) to UVB at 675 mJ/cm^2 three times a day, in a three-hour interval. Micrographies were taken 72 hours after the last UVB stress with phase contrast microscopy at 200x magnification. **B.** Micrographies were taken at two passaging cells (P4 and P10) with phase contrast microscopy at 200x magnification.

The objective of our project is to investigate the senescence-associated secretory phenotype, the DNA Damage Response (DDR) pathway, and the oxidative stress of normal human keratinocytes in UVB-stress induced premature senescence (UVB-SIPS).
The UVB-SIPS model used consists of three repeated exposures of NHKs at 675 mJ/cm^2 to narrow-band UVB (peaking at 312 nm) in a three-hour interval for one day.
This model was previously set up in our team and allows the induction of premature senescence. By comparison, replicative senescence (RS) is obtained by a growth plateau phase when cell proliferation exhaustion is reached, after about ten passages in culture (fig. 1).
First, we compared different biomarkers of senescence in both senescent models including morphological changes and senescence-associated β-galactosidase activity (SA-βgal). Then we studied the expression of IL-6, IL-8 and VEGF, three main components of the senescence-associated secretory phenotype (SASP), at the mRNA and protein levels in UVB-SIPS. Then, we analysed the DNA damage response (DDR) pathway as well as the oxidative stress and the related activation of Nrf2 in UVB-SIPS.

1. Biomarkers of senescence in RS and in UVB-SIPS

1.1. Morphology

When cells enter in senescence, they are characterized by morphological changes, considered as a biomarker of senescence. Senescent keratinocytes show an increased cell and organelles size. Indeed, the number and size of lysosomes and of autophagic vacuoles was reported to increase gradually *in vitro* in fibroblasts during senescence process. In addition, nucleus is often larger and irregularly shaped probably leading to larger cells (Kang et al. 2000).
Micrographies were taken at 72 hours after the last UVB stress and at the beginning and at the end of the culture for RS (P4 and P10) in NHKs (fig. 2). First we observed that NHKs exposed to UVB have an irregular shape and became enlarged compared to control NHKs, which are small polygonal cells. For RS, small polygonal cells are observed at early passage (P4) while NHKs become also larger, irregular and flattened at late passages (P10).
These results show that NHKs in UVB-SIPS and in RS have similar morphological changes specific of senescence. However, this biomarker is not sufficient to establish that NHKs *in vitro* develop a senescent phenotype.

1.2. Growth arrest

Cellular senescence is characterised by an irreversible growth arrest that occurs *in vitro*. Indeed, this limited growth of human cells in culture is notably due to telomere shortening at each cell division.
A primary cell culture has a finite lifespan expressed in the number of cumulative population doublings (CPDs). Population doubling was measured at each passage after thawing frozen cells.

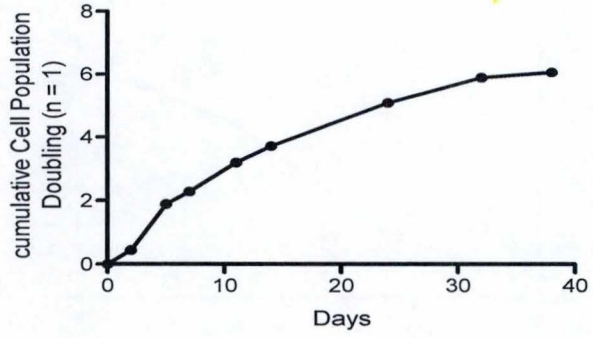

Figure 3: Cumulative Population Doublings in NHKs with time in culture (days). Cumulative Population Doublings were evaluated at each passage by manual counting (n = 1).

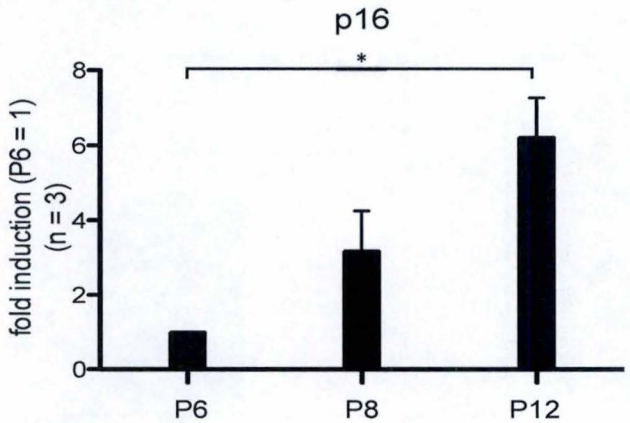

Figure 4: Expression of p16 gene in NHKs. Total RNA was extracted at P6, P8 and P12, then reverse transccription and qPCR were performed. Results are expressed as fold induction compared to P6. GAPDH (glyceraldehyde 3-phosphate deshydrogenase) was used as housekeeping gene. NHKs isolated from three different donors have been analysed (n=3). Statistical tests were carried out by using unpaired *t*-test (*: $P < 0.05$).

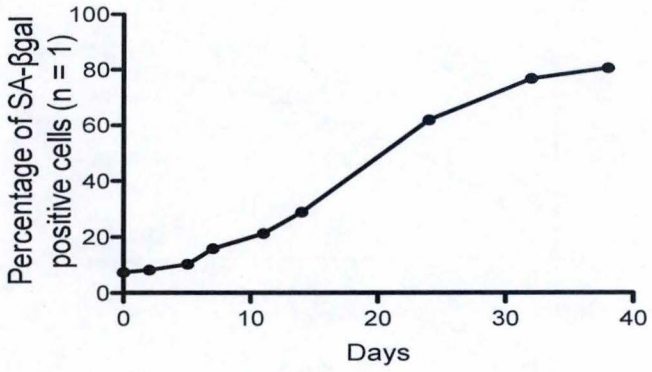

Figure 5: Proportion of cells positive for the SA-βgal assay in NHKs with time in culture (days). SA-βgal positive cells were counted for each passage, and percentage was determined compared to total cells (300 cells counted per well, 3 wells per condition) (n=1).

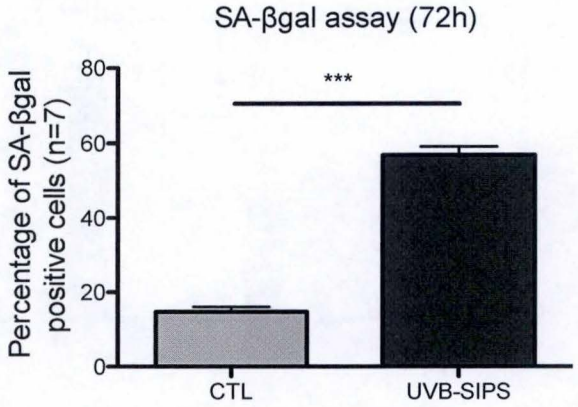

Figure 6: Proportion of cells positive for the SA-βgal assay in NHKs in UVB-SIPS. NHKs were exposed (or not: CTL) to UVB at 675 mJ/cm^2 three times a day in a three-hour interval. SA-βgal positive cells were counted 72 hours after the last UVB stress, and percentage was determined compared to total cells (300 cells counted per well, 3 wells per condition) (n=7). Statistical tests were carried out by using unpaired *t*-test (***: $P < 0.001$).

Results showed an exponential phase of proliferation at the beginning of the culture, slowing down to approach a growth arrest plateau in the last passages (fig. 3).
P16 is an important cyclin-dependent kinase inhibitor known to initiate and to maintain cellular senescence in different cell types. This regulator of the cell cycle prevents phosphorylation of pRb, thereby inducing an irreversible growth arrest leading to senescence. We performed a qPCR to determine p16 mRNA level at different passages in culture, in NHKs isolated from 3 different donors. Our results show an increased expression of p16 gene from 3.2-fold in P8 to 6.2-fold in P12 compared to P6 (fig. 4).

1.3. Senescence Associated β-galactosidase (SA-βgal)

Senescence Associated β-galactosidase (SA-βgal) is probably the most widely used marker of cellular senescence for the detection of senescent cells both *in vitro* and *ex vivo* (Dimri, Lee et al. 1995, Debacq-Chainiaux et al. 2009). By using the chromogenic substrate 5-bromo-4-chloro-3-indolyl β-D-galactopyranoside (X-Gal), lysosomal β-galactosidase activity can be detected at suboptimal pH 6.0 in senescent cells.
Therefore we estimated the proportion of cells positive for the SA-βgal assay. It was performed for each passage from passage 4 to passage 11 in RS (n = 1) (fig. 5) and 72 h after the last UVB stress in our model of UVB-SIPS (n = 7) (fig. 6).
In RS, the percentage of SA-βgal positive cells increases to reach a plateau after about 10 passages (fig. 5). Indeed, a low percentage of cells are positive at passage 4 (8 %) while NHKs are highly positive to SA-βgal assay (81 %) at passage 11. We can also observe that, at early passages (4 to 8), the proportion of positive cells for SA-βgal activity remain relatively low whereas a significant increase is observed at later passages.
For UVB-SIPS, results show also a higher percentage of SA-βgal positive cells at 72 hours after UVB exposures (fig. 6), from 17 % in the control cells to 58 % in the cells exposed to UVB (n = 7).
These results indicate that both NHKs in RS and in UVB-SIPS are senescent in our two models. Both models can be used to investigate the cellular senescence.

1.4. SASP

One of the major traits of senescent cells is their senescence-associated secretory phenotype, called SASP. SASP comprises in particular growth factors, interleukins and inflammatory cytokines (Rodier et al., 2009). These factors are known to contribute and to maintain cellular senescence thereby affecting neighbouring cells. If the SASP is well characterized in replicative senescence, few are known on its composition in SIPS models.
We checked the expression of three of the prominent factors of the SASP: interleukin-6 (IL-6), interleukin-8 (IL-8) and vascular endothelial growth factor (VEGF), in NHKs in UVB-SIPS. We isolated RNA and collected conditioned media at 1, 24, 48 and 72 hours after the last UVB stress. We then performed qPCR and ELISA (Enzyme-linked Immunosorbent

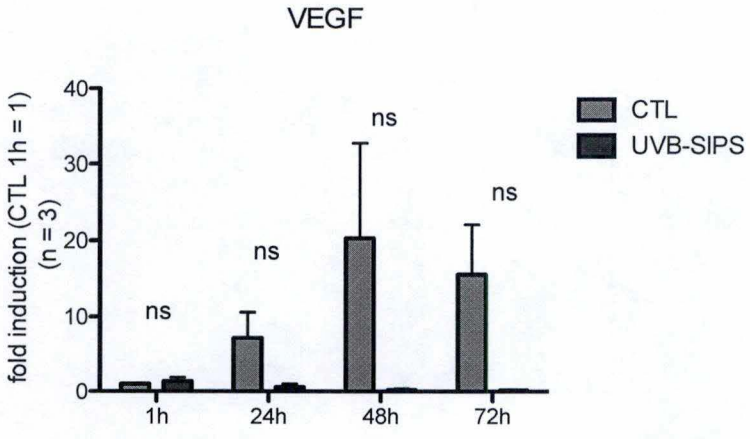

Figure 7: Expression of VEGF gene in NHKs in UVB-SIPS. NHKs were exposed three times a day to UVB at 625 mJ/cm^2 (or not: CTL) in a three-hour interval. Total RNA was extracted at 1, 24, 48 and 72 hours after the last stress, then reverse transccription and qPCR were performed. Results are expressed as fold induction compared to control NHKs at 1h. GAPDH (glyceraldehyde 3-phosphate deshydrogenase) was used as housekeeping gene. Three different donors have been analysed (n=3). Statistical tests were carried out by using two-way ANOVA and Bonferroni post-tests.

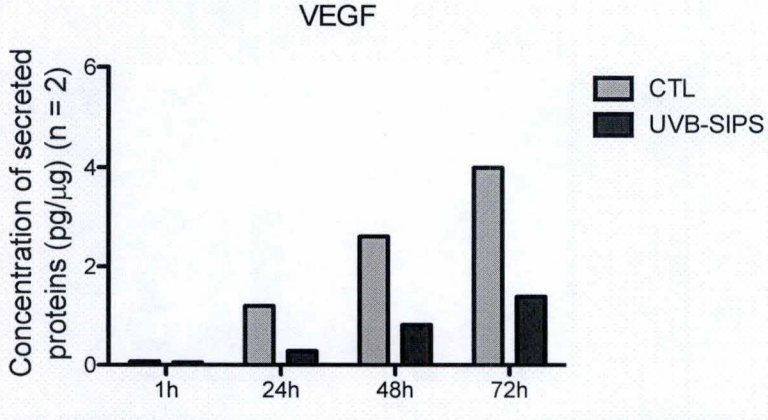

Figure 8: Quantification of VEGF secreted proteins in NHKs in UVB-SIPS by indirect ELISA. NHKs were exposed three times a day to UVB at 625 mJ/cm^2 (or not: CTL) in a three-hour interval. Supernatants have been harvested at 1, 24, 48 and 72 hours after the last stress. Results (means of two donors for 1, 24 and 48 h for and four donors for 72 h) are expressed as quantity of secreted proteins reported to the concentration of total proteins of the cell lysates.

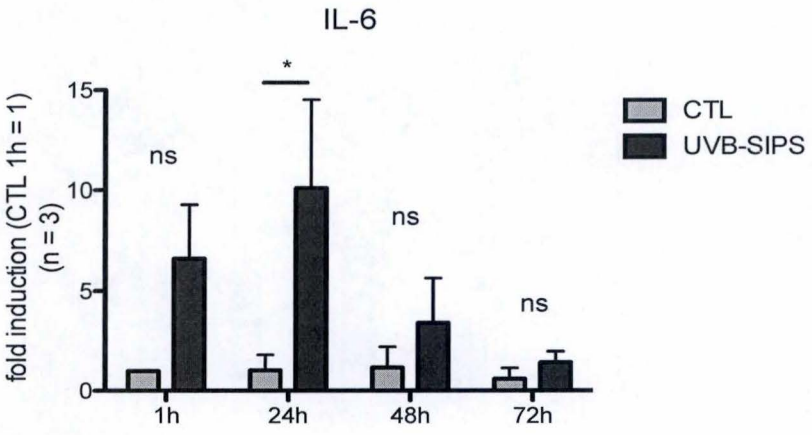

Figure 9: Expression of IL-6 gene in NHKs in UVB-SIPS. NHKs were exposed three times a day to UVB at 625 mJ/cm^2 (or not: CTL) in a three-hour interval. Total RNA was extracted at 1, 24, 48 and 72 hours after the last stress, then reverse transccription and qPCR were performed. Results are expressed as fold induction in UVB stressed NHKs compared to control NHKs. GAPDH (glyceraldehyde 3-phosphate deshydrogenase) was used as housekeeping gene. Three different donors have been analysed (n=3). Statistical tests were carried out by using two-way ANOVA and Bonferroni post-tests (*: $P < 0.05$).

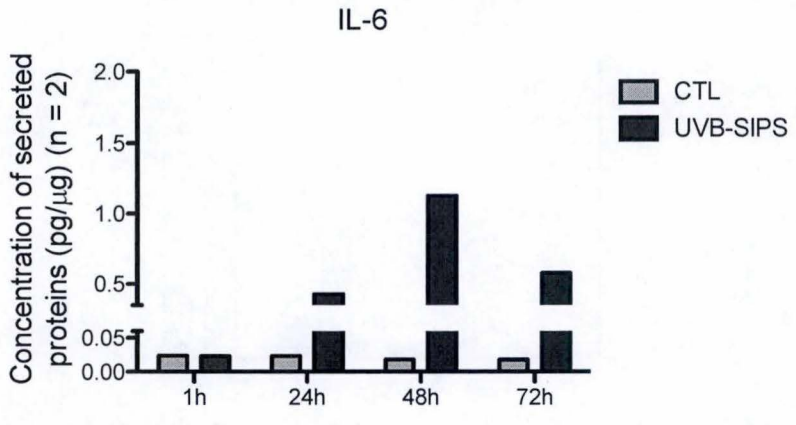

Figure 10: Quantification of IL-6 secreted proteins in NHKs in UVB-SIPS by ELISA). NHKs were exposed three times a day to UVB at 625 mJ/cm^2 (or not: CTL) in a three-hour interval. Supernatants have been harvested at 1, 24, 48 and 72 hours after the last stress. Results (mean of two donors) are expressed as quantity of secreted proteins reported to the concentration of total proteins of the cell lysates.

Assays) to quantify their expression. We studied the mRNA level of NHKs from 3 different donors and the secreted proteins from 2 independent donors.

VEGF is secreted by many cell types including keratinocytes. It is an essential contributor to tumour angiogenesis, but also plays a role in wound healing. It is recognised as a major actor of the SASP (Coppé et al., 2009). Results from the qPCR on 3 different donors indicated that the gene expression of VEGF in controls varies from 24h to 72h (7.1-, 20.3- and 17.2-fold, respectively) (fig. 7). In contrariwise, fold induction was almost unchanged and remains comparatively low in UVB-stressed cells compared to controls.
In parallel, we investigated the abundance of VEGF protein secreted, by ELISA assay. At 1 hour after the last UVB stress, concentration was very low and no difference is distinguished between control and UVB-SIPS cells. After, the same trend is observed, namely an increase in the secretion of VEGF in control cells at 24, 48 and 72 h, of 1.2, 2.7 and 4.1 pg/µg respectively. This time, we also observed an increase of secreted VEGF at 24, 48 and 72 h after the last stress of 0.3, 0.8 and 1.3 pg/µg respectively in UVB-exposed cells, but these levels remain lower than in control cells (fig. 8). These results show that VEGF, both at the mRNA and at the protein level, is overexpressed in the control cells from 24h onwards, and that its expression appears to be unchanged in cells exposed to UVB, at each time point when compared to control cells. However, although a trend is emerging, caution should be exercised as these results are not statistically significant, given the variability between donors.

We then studied interleukin-6 (IL-6) expression because it is considered as one of the most prominent cytokine of the SASP. IL-6 has been shown to be a pleiotropic pro-inflammatory cytokine in many cell types including human keratinocytes.
We observed increased IL-6 mRNA levels in UVB-exposed cells at each time point, when compared to its expression in control cells in which it remains stable and less expressed. As presented in figure 9, IL-6 gene expression was elevated at 1 hour (6.6-fold) and becomes significantly higher at 24 hours (10.1-fold) after UVB exposures compared to the controls. The peak value in IL-6 expression was observed at 24 hours after UVB stress before a decline at 48 and 72 hours with 3.4- and 1.4-fold increase respectively.
In parallel, the level of IL-6 secreted protein remained unchanged and low for control cells at each time point (n = 2) (fig. 10). At 1 hour, no difference was observed and levels of IL-6 secreted proteins was low both in UVB-SIPS and in control NHKs. In contrariwise, results indicated a major increase at 24 and 48 hours after UVB stresses (0.5 and 1.2 pg/µg respectively) followed by a slow decrease at 72 hours (0.6 pg/µg) but its level is still higher than in the controls (fig. 10).
Despite a high variability among donors, we observed a tendency for an increase in the expression of IL-6 as well at the mRNA level from 1 h to 48 h and at the protein level from 24 to 72 h in the cells exposed to UVB.

Finally we studied the expression of IL-8. Interleukin-8 (IL-8) is a chemokine produced by macrophages and several other cell types such as epithelial cells. IL-8 binds to CXCR1 and CXCR2 receptors and is an important regulator of the immune reaction in the innate immune

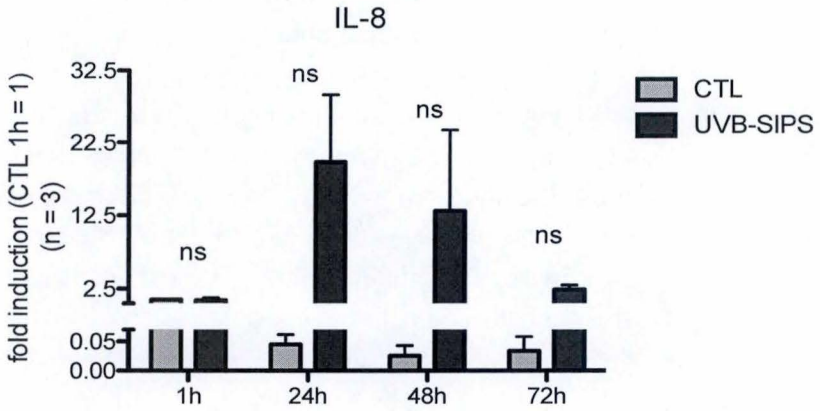

Figure 11: Expression of IL-8 gene in NHKs in UVB-SIPS. NHKs were exposed three times a day to UVB at 625 mJ/cm^2 (or not: CTL) in a three-hour interval. Total RNA was extracted at 1, 24, 48 and 72 hours after the last stress, then reverse transccription and qPCR were performed. Results are expressed as fold induction in UVB stressed NHKs compared to control NHKs. GAPDH (glyceraldehyde 3-phosphate deshydrogenase) was used as housekeeping gene. Three different donors have been analysed (n = 3). Statistical tests were carried out by using two-way ANOVA and Bonferroni post-tests.

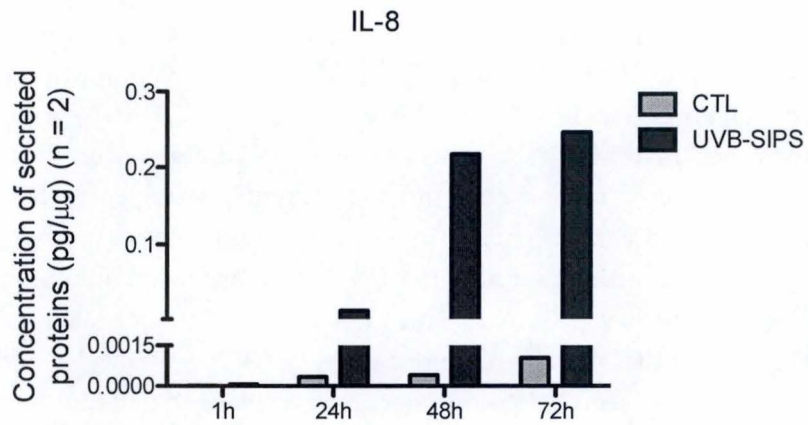

Figure 12: Quantification of IL-8 secreted proteins in NHKs in UVB-SIPS by ELISA. NHKs were exposed three times a day to UVB at 625 mJ/cm^2 (or not: CTL) in a three-hour interval. Supernatants have been harvested at 1, 24, 48 and 72 hours after the last stress. Results (mean of two donors) are expressed as quantity of secreted proteins reported to the concentration of total proteins of the cell lysates.

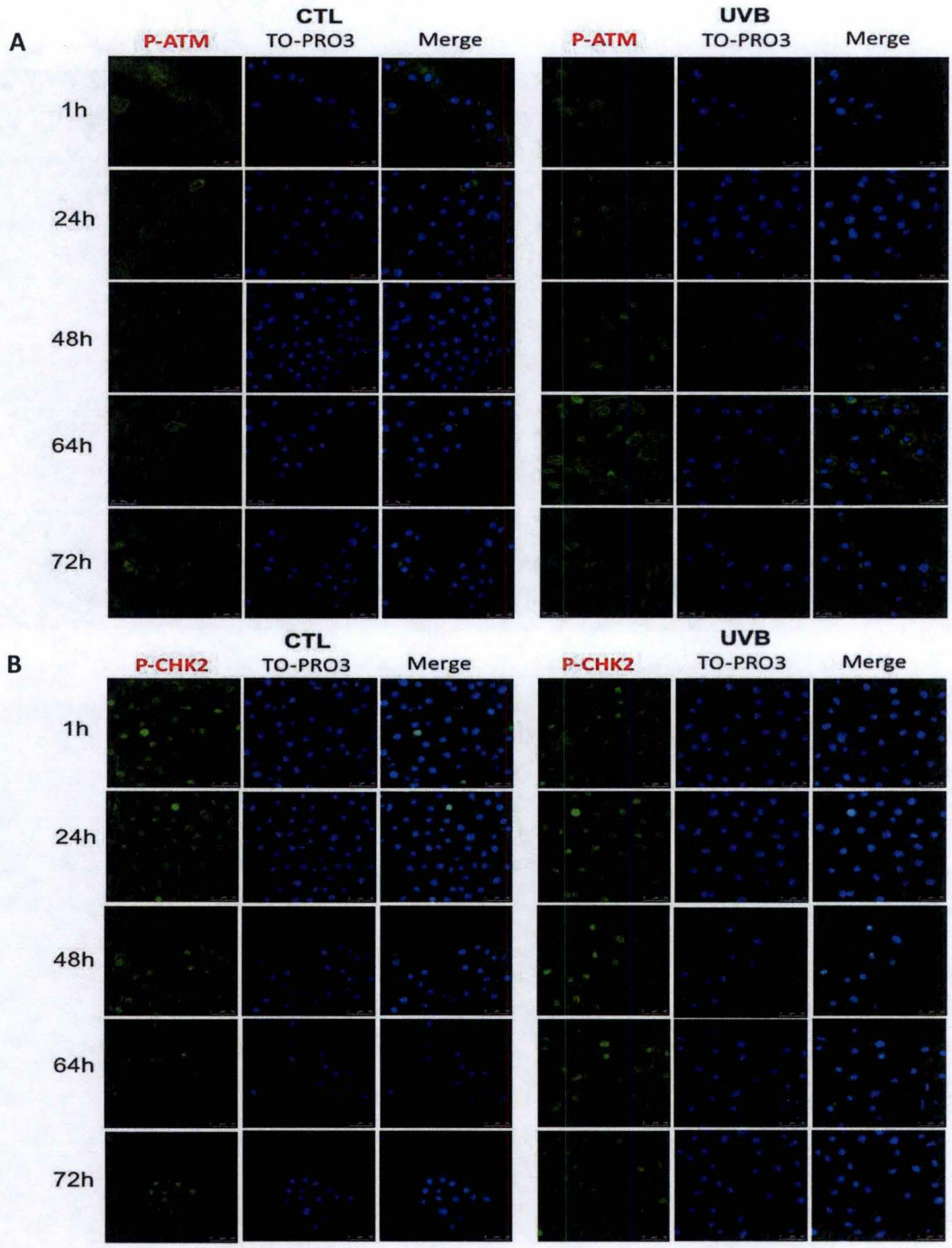

Figure 13: Localisation and abundance of P-ATM and P-CHK2 in UVB-SIPS in NHKs by immunocytochemistry. Cells were exposed three times a day to UVB at 675 mJ/cm^2 in a three-hour interval. Cells were prepared for immunocytochemistry at 1, 24, 48, 64 and 72 hours after the last stress with corresponding antibodies. Proteins of interest were revealed in green by alexa 488 antibodies. Nuclei were stained in blue with TO-PRO3. **A**. P-ATM **B**. P-CHK2. Observation was done with confocal microscopy (Leica). Scale bar : 50 μm.

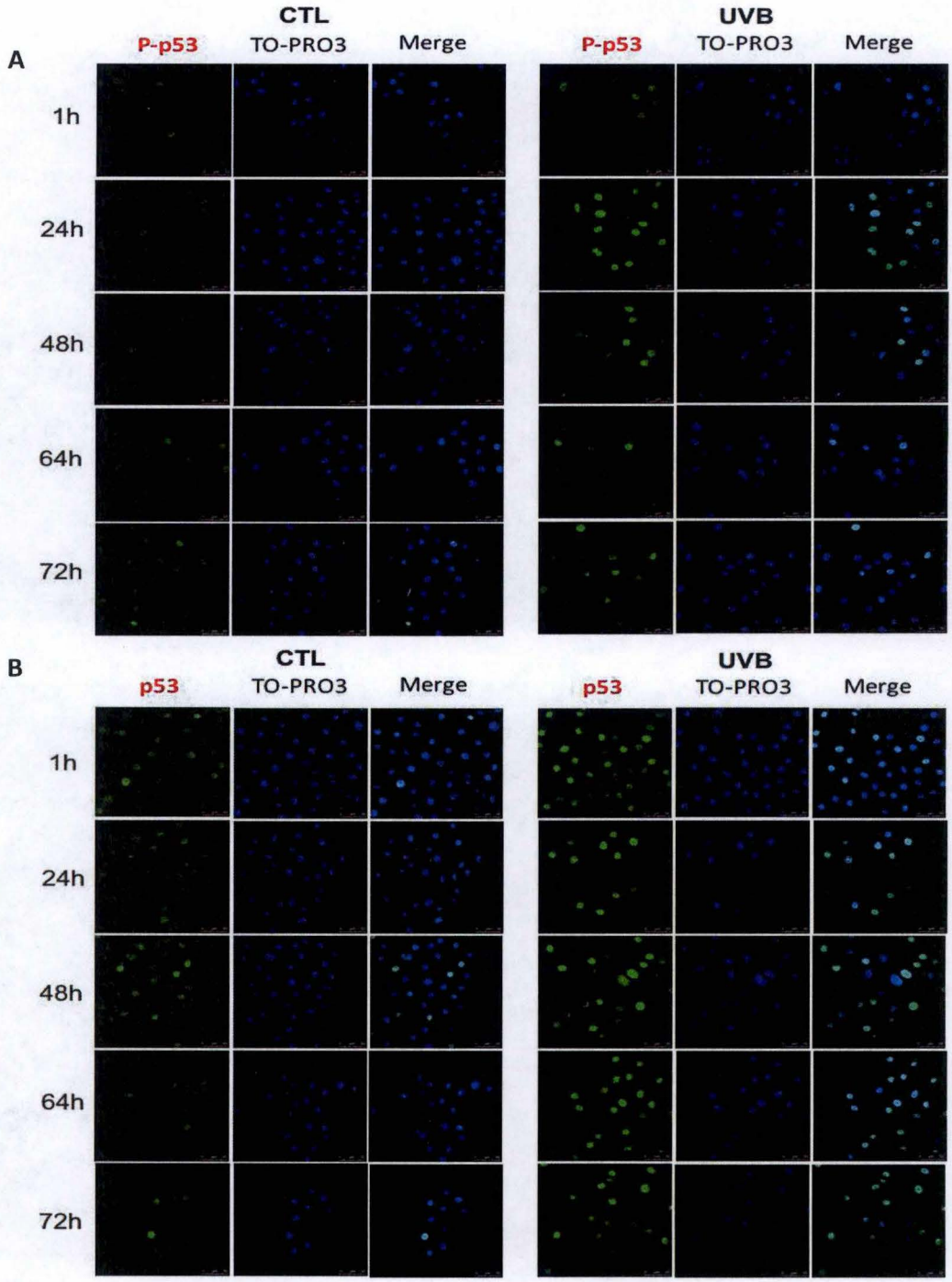

Figure 14: Localisation and abundance of P-p53 and p53 in UVB-SIPS in NHKs by immunocytochemistry. Cells were exposed three times a day to UVB at 625 mJ/cm^2 in a three-hour interval. Cells were prepared for immunocytochemistry at 1, 24, 48, 64 and 72 hours after the last stress with corresponding antibodies. Proteins of interest were revealed in green by alexa 488 antibodies. Nuclei were stained in blue with TO-PRO3. **A.** P-p53 **B.** p53. Observation was done with confocal microscopy (Leica). Scale bar : 50 µm.

system response. IL-8 is also a major actor of the SASP, overexpressed in in senescent cells (Coppé et al. 2009).
The IL-8 mRNA and protein levels in NHKs in UVB-SIPS were also evaluated by qPCR and ELISA.
If the IL-8 mRNA fold induction decreased in control cells at 24, 48 and 72 hours (less than 0.1-fold), it increased in UVB-stressed cells from 24 to 72 h, reaching values of 19.8-, 13.1- and 2.4-fold respectively (fig. 11).
In addition, the level of secreted IL-8 remained low at each time (3.10^{-4}, 4.10^{-4} and 1.10^{-3} pg/µl at 24, 48 and 72 hours) for control cells compared to UVB-treated cells. Secreted IL-8 proteins are very low at 1 hour in both control and UVB-SIPS conditions (fig. 12), but the concentration of secreted IL-8 rises at 24 hours (0.016 pg/µg) followed by an important increase at 48 and 72 hours (0.23 and 0.25 pg/µg) after the last stress.

In conclusion, the expression of VEGF is decreased both at mRNA and protein level in UVB-stressed cells, and the expression of IL-6 and IL-8 is increased at mRNA and protein level in UVB-stressed cells. But we have to note that these data are essentially trends observed because a high variability has been demonstrated between NHKs isolated from different donors. These results seem however to confirm that a SASP is well associated with UVB-SIPS in NHKs.

2. DNA damage repair (DDR) pathway

UVB radiation can damage DNA, leading to the DDR activation. The DDR pathway is a signaling cascade activated by DNA damage to arrest cell-cycle progression, transiently or permanently, allowing the repair of damage. The severity of the damage and the long-term activation of this pathway could result in induction of cellular senescence, or apoptosis. As UVB-SIPS NHKs display long-term DNA damage, including cyclobutane pyrimidine dimers (CPDs) detectable until 72 hours after the last UVB stress (E. Bauwens and L. Ernst previous data), we investigated by immunofluorescence and by western blotting, if the main DDR actors (ATM, ATR, CHK2, CHK1, BRCA1 and p53) were activated in response to repeated UVB exposures. To follow the kinetics of activation, we performed analyses at 1, 24, 48, 64 and 72 hours after the last UVB stress. The activation of some DDR actors had already been shown for two donors in a previous work (L. Ernst master thesis), we used in the present study a third donor to validate the data.
We first noticed abundance and localisation of these actors by immunocytochemistry (Fig. 13 and Fig. 14). We observed a slight increase of P-ATM with a nuclear localisation at 24 and 48 hours after the last UVB stress. At 64 hours, staining was more important in the cytoplasm in UVB-exposed cells compared to controls (Fig. 13A). For P-CHK2, from 1 to 24 hours, we didn't observe any difference between controls and UVB-exposed cells, as the staining is important in both conditions. However, we could see a higher nuclear staining in UVB-exposed cells, especially at 48 and 64 hours (Fig. 13B). Results are more evident for P-p53, with a clear increase of the staining in the nuclei of UVB-exposed NHKs as compared to controls, at each

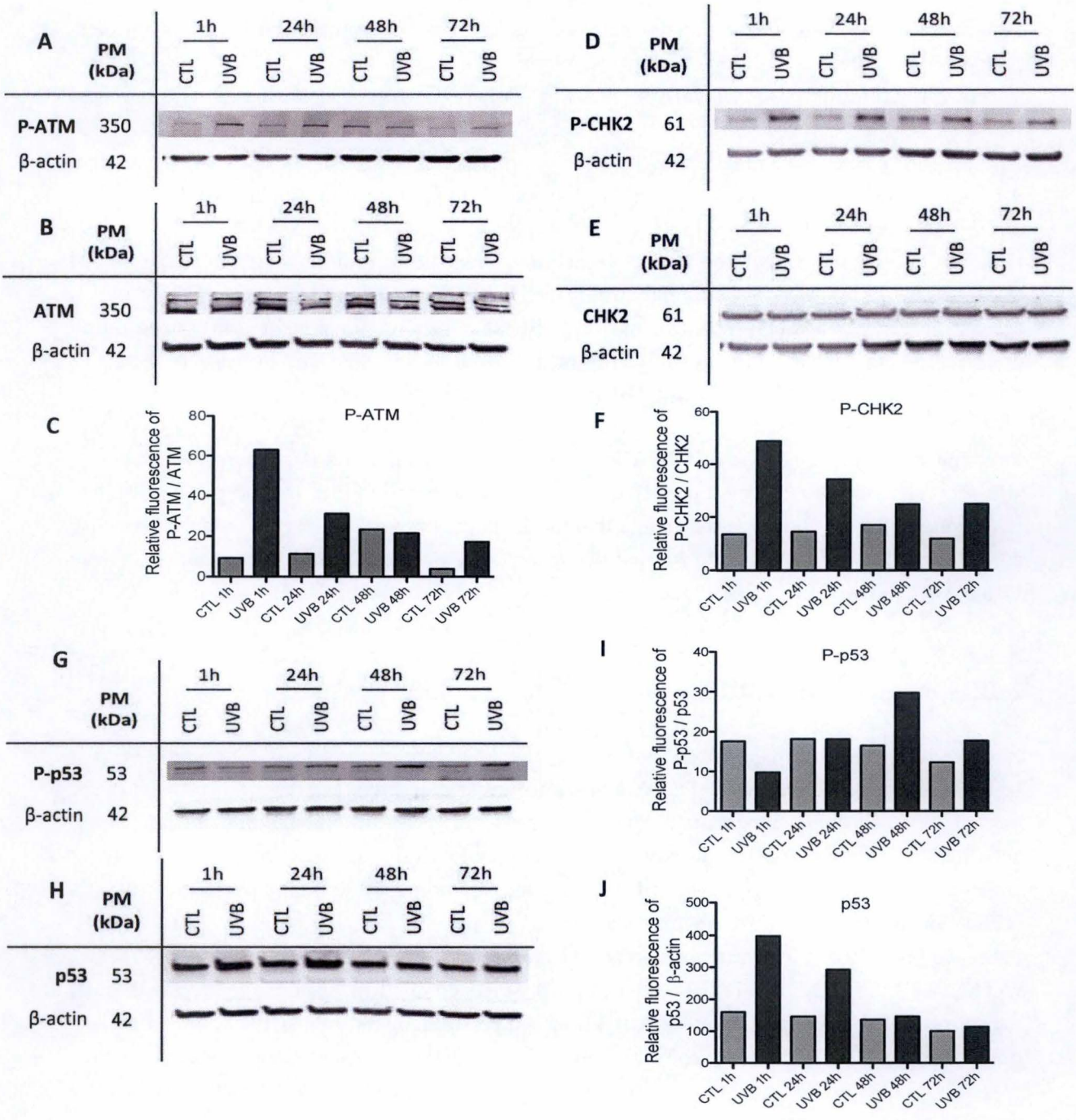

Figure 15: Protein abundance of DDR actors in NHKs in UVB-SIPS by Western Blot. NHKs were exposed three times a day to UVB at 625 mJ/cm^2 (or not: CTL) in a three-hour interval. Proteins were extracted at 1, 24, 48 and 72 hours after the last stress. β-actin was used as loading control. Abundance of P-ATM (**A**) and ATM (**B**) in control and UVB cells. Relative fluorescence of P-ATM was normalized to total ATM (**C**). Abundance of P-CHK2 (**D**) and total CHK2 (**E**) in control and UVB cells. Relative fluorescence of P-CHK2 was compared to CHK2 (**F**). Abundance of P-p53 (**G**) and p53 (**H**) in control and UVB cells. Relative fluorescence of P-p53 (**I**) and p53 (**J**) were compared to β-actin.

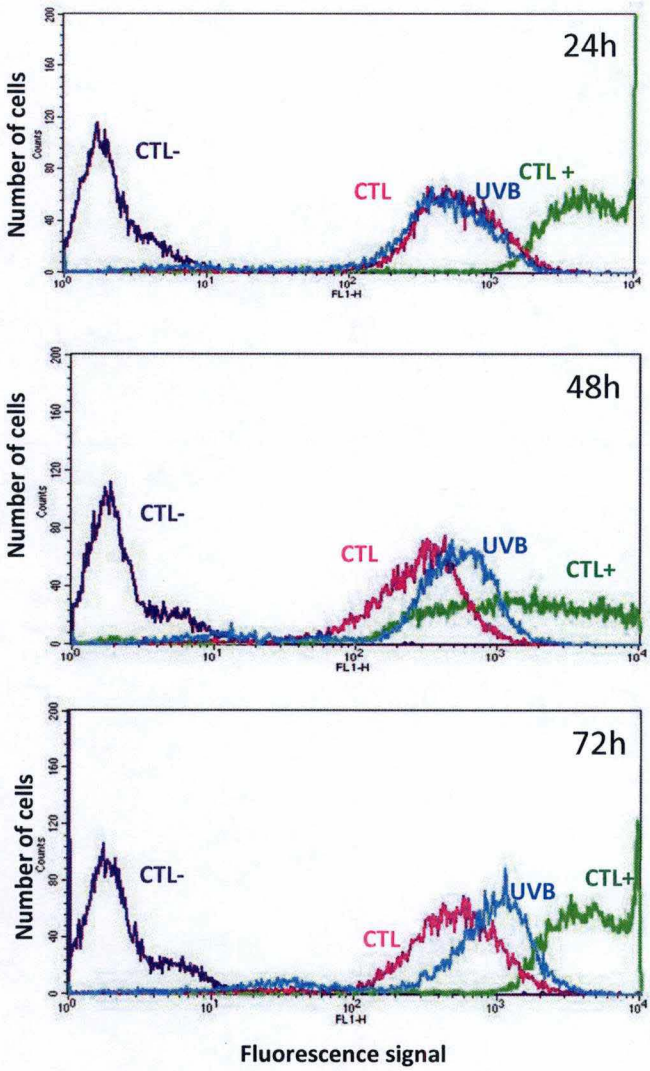

Figure 16: ROS level in UVB-SIPS NHKs at 24, 48 and 72 hours after the last stress by flow cytometry. NHKs were exposed three times a day to UVB at 625 mJ/cm^2 (or not: CTL) in a three-hour interval. At 24, 48 and 72 hours after the last stress, NHKs were incubated with CM-H_2DCF probe. Control NHKs condition is presented in pink and UVB-SIPS NHKs condition in blue. Negative control of the test (without probe) is shown in purple. Positive control of the test, which consists of NHKs incubated with hydrochloride SIN-1, is shown in green. 10,000 events are counted with BD FACSCalibur.

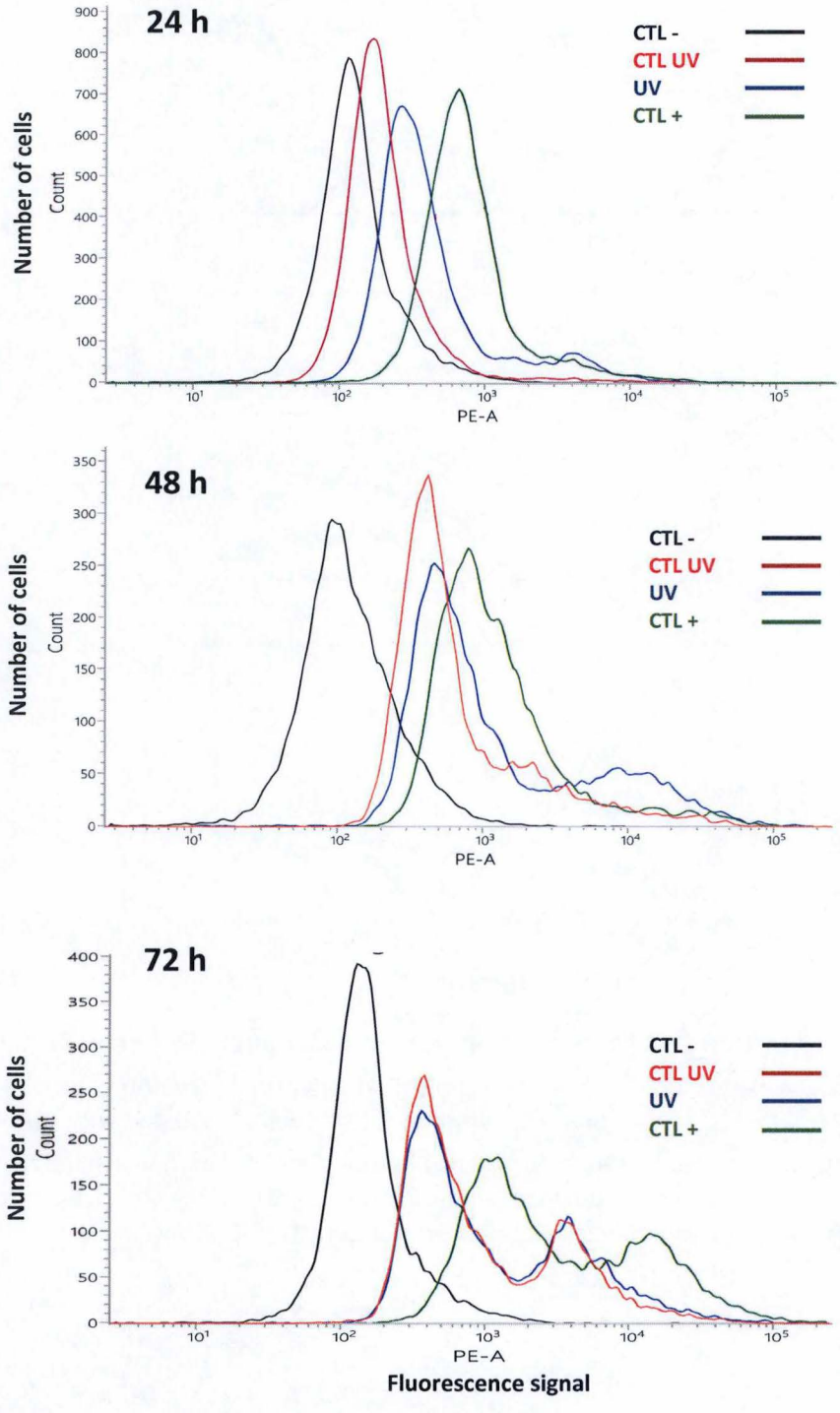

Figure 17: Superoxide level in UVB-SIPS NHKs at 24, 48 and 72 hours after the last stress by flow cytometry. NHKs were exposed three times a day to UVB at 625 mJ/cm^2 (or not: CTL) in a three-hour interval. At 24, 48 and 72 hours after the last stress, NHKs were incubated with MitoSOX probe. Control NHKs condition is presented in red and UVB-SIPS NHKs condition in blue. Negative control of the test (without probe) is shown in black. Positive control of the test, which consists of NHKs incubated with hydrochloride FCCP and antimycin A is shown in green. 10,000 events are counted with BD FACSCalibur.

total p53 from 1 to 72 hours (Fig. 14B). For ATR pathway, no difference of abundance was highlighted for P-ATR and P-BRCA1, but a slight increase was observed for P-CHK1 at each time points (data not shown).
We then performed western blots to check expression of these proteins at the same time points (Fig. 15). In UVB-exposed cells, a high abundance of P-ATM was observed at 1 hour after the last UVB stress followed by a slow decrease at 24 and 72 hours but it is still higher than in the controls (Fig. 15A, B and C). For P-CHK2, an important increase was detected at 1 hour after the last UVB exposure followed also by a slow decrease but abundance is still higher in UVB-treated cells at 24, 48 and 72 hours (Fig. 15D, E and F). An increased abundance of P-p53 was observed at 48 and 72 hours in NHKs exposed to UVB (Fig. 15G and I). We also observed a high abundance of total p53 at 1 and 24 hours in UVB-exposed NHKs, followed by a return to identical abundance as controls. These results confirmed the previous data already obtained in our team on a third independent donor and suggested an activation of ATM pathway induced by repeated UVB exposures in NHKs, probably associated with growth arrest.

3. Oxidative stress and Nrf2 pathway in UVB-SIPS

3.1. Generation of ROS

Generation of intracellular ROS after UVB exposures was monitored by flow cytometry after incorporation of CM-H_2DCF probe at different times after the last UVB stress. This probe is oxidized by ROS and yields a fluorescent adduct that is trapped inside the cell. Negative control consisted on NHKs without probe and positive control on NHKs incubated with the probe and hydrochloride SIN-1 releasing nitric acid as a ROS-inducing agent. We showed that generation of ROS was detectable at 24, 48 and 72 hours in our samples (fig. 16).
If no difference between control and UVB-exposed cells was detected at 24 hours, we highlighted a difference between both conditions at 48 and 72 hours, with a higher ROS signal in UVB-exposed cells. Previous data obtained at 72 hours on two different donors strengthened our results (L. Ernst master thesis). Production of ROS can contribute to activate some important regulators such as the Nrf2 pathway.

3.2. Generation of superoxide

The cellular content of superoxide anion was carried out by flow cytometry at different times after the last UVB stress. Superoxide level was measured with MitoSOX probe, a highly specific dye oxidized by superoxide but not by other mitochondrial ROS. Negative control used is NHKs without probe (black) while positive control is NHKs incubated with the probe FCCP (Carbonyl cyanide-4-(trifluoromethoxy)phenylhydrazoneor) and AA (antimycin A) (green) (fig. 17). Graphs indicated UVB-exposed cells in blue and control cells in red. We showed that generation of superoxide was detectable at 24, 48 and 72 hours in our samples. A difference between both conditions was detected at 24 hours, with a higher superoxide signal

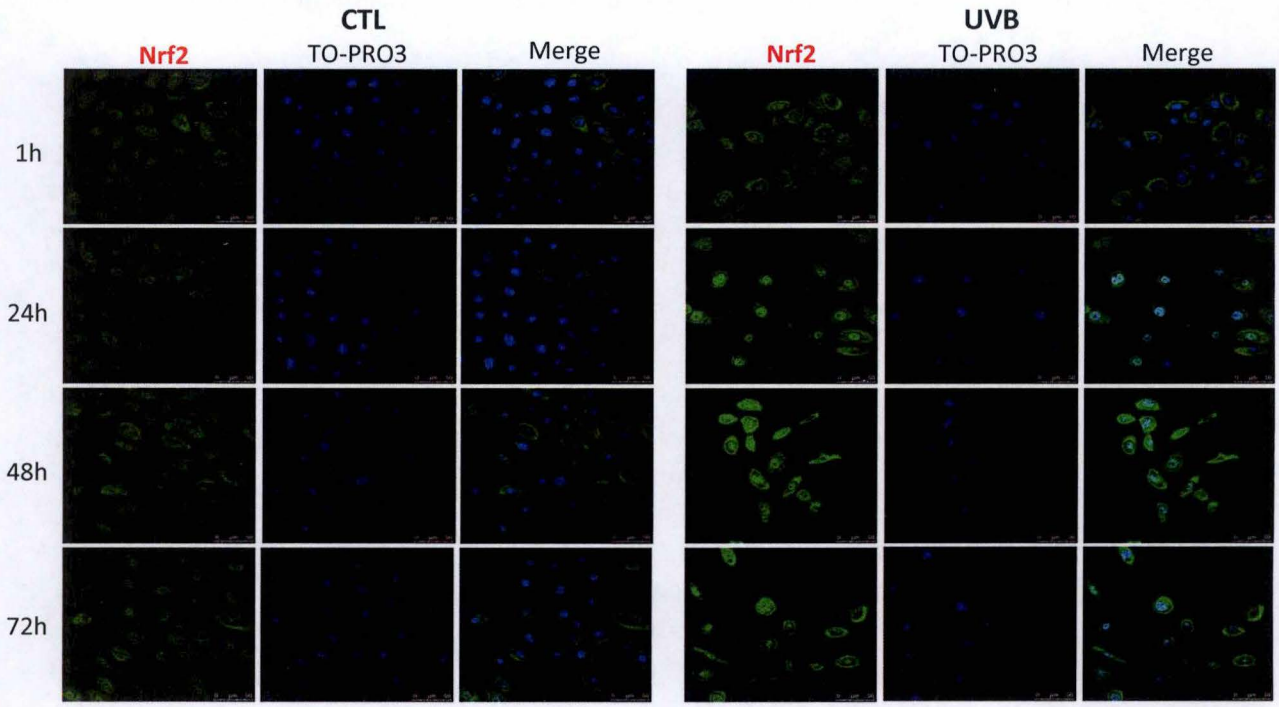

Figure 18: Localisation and abundance of Nrf2 in NHKs in UVB-SIPS by immunocytochemistry. NHKs were exposed three times a day to UVB at 625 mJ/cm^2 (or not: CTL) in a three-hour interval. Cells were prepared for immunocytochemistry at 1, 24, 48 and 72 hours after the last stress with Nrf2 antibody. Protein of interest was revealed in green by alexa 488 antibodies. Nuclei were stained in blue with TO-PRO3. Observation was done with confocal microscopy (Leica). Scale bar : 50 µm.

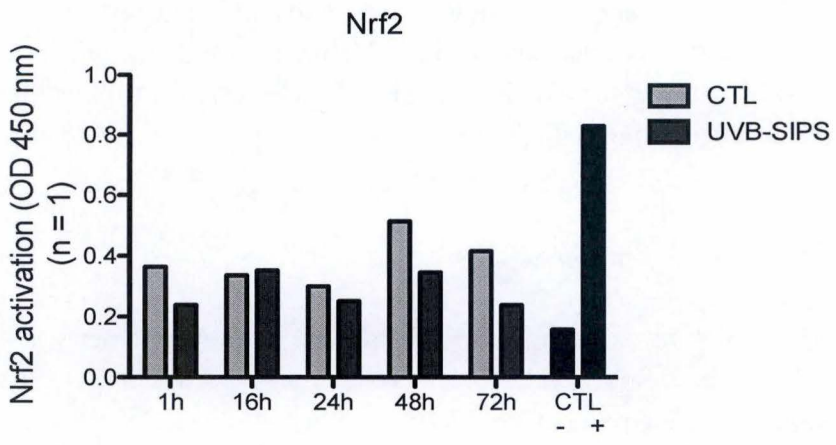

Figure 19: Nrf2 activation in NHKs in UVB-SIPS by TRANS-AM. Nuclear protein extraction is performed on NHKs at 1, 16, 24, 48 and 72 hours after UVB-SIPS (or not: CTL) in a three-hour interval. For positive control, HepG2 cells are incubated 6 hours with SIN-1. For negative control, proteins are extracted in lysis buffer without SIN-1. After coating with nucleotide-binding Nrf2 sequence, 10 µg of proteins from samples are incubated into wells. Nrf2 antibody and HRP-conjugated antibody are added before TMB substrate solution. Stop solution is needed before reading absorbance at 450 nm with a reference wavelength of 655 nm (n = 1).

in UVB-treated cells. However, results showed a very weak increase at 48 hours in the UVB-exposed cells, and no difference at 72 hours between control and UVB-exposed NHKs.

We can therefore conclude that the UVB-SIPS model induces an increase of ROS production in NHKs, with a superoxide generation detectable at short term (24 h), whereas, more generally, an increase in ROS is observed from 48 h in UVB-exposed cells.

3.3. Expression and activity of Nrf2

Nrf2 is an important regulator of cellular resistance, involved in the regulation of antioxidant defense. In addition to its direct involvement in ROS detoxification, Nrf2 can regulate ROS levels by modulating free Fe(II) homeostasis. In normal condition, Nrf2 is sequestered in the cytosol by the Keap1 homodimer, which facilitates its degradation by the proteasome. Under stress conditions, Nrf2 is no longer targeted for degradation by Keap1 and then translocates to the nucleus.
We studied the localisation and the abundance of Nrf2 at 1, 24, 48 and 72 hours after the last UVB stress.
As presented in Fig. 18, a very low staining in both nuclear and cytoplasmic compartments is observed in control conditions from 1 to 72 hours. We observed an important staining in cell nuclei at 24 hours in UVB stressed cells. The fluorescence signal, distributed into the cytoplasm and nuclei, was still more intense in UVB stressed cells condition at 48 and 72 hours as compared to controls. This result seems to indicate that Nrf2 translocates into the nucleus after 24h, and that its expression is higher after repeated UVB stresses.

To investigate furthermore the activity of transcription factor Nrf2, we used the TransAM method to study the binding of this transcription factor to its target sequence ARE (Antioxidant Response Element). The levels of Nrf2-ARE binding in NHKs in our model of UVB-SIPS were measured in nuclear proteins at each time using a specific TransAM kit. Nuclear proteins were incubated in 96-well plates pre-coated with ARE consensus oligonucleotides. The active form of Nrf2 that bound to this sequence was detected by incubation with anti-Nrf2 antibody and HRP-conjugated secondary antibody. HepG2 cells incubated 6 hours with SIN-1 are positive controls. For negative control, nuclear proteins are extracted in a mix of RE and SA buffers.
As indicated in figure 19, optical density was measured for each time point and is correlated with Nrf2 binding. We observed a slight activation at 1, 48 and 72 hours in control NHKs compared to UVB-exposed cells. In contrast to immunocytochemistry, we didn't detect any activation of Nrf2 in NHKs after repeated exposures to UVB.
We can note that the Nrf2 protein recognized by the antibody from Santa Cruz used in TransAM has a molecular weight of 55-65 kDa. Recently, evidence supported that the relevant size of Nrf2 is 95-110 kDa in Western blot (Lau et al., 2013). We then decided to compare three different Nrf2 antibodies from different companies (Santa Cruz, Cell signaling and ABCAM) in Western blot. We didn't find any differences between these antibodies (data not shown).

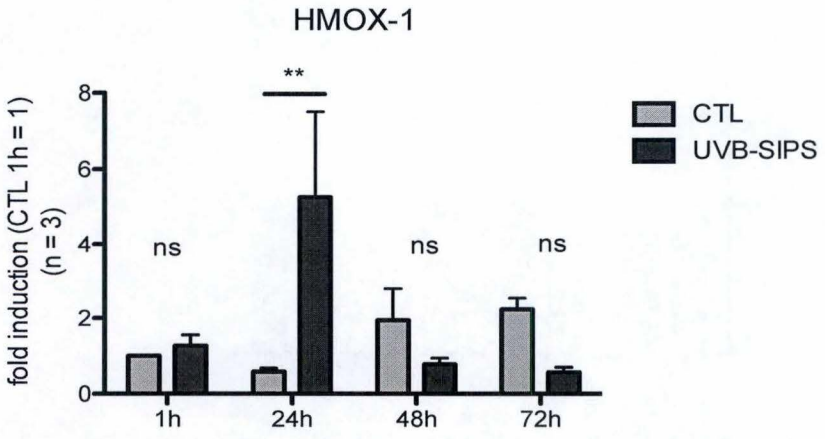

Figure 20: Expression of HMOX-1 gene in NHKs in UVB-SIPS. NHKs were exposed three times a day to UVB at 625 mJ/cm^2 (or not: CTL) in a three-hour interval. Total RNA was extracted at 1, 24, 48 and 72 hours after the last stress, then reverse transccription and qPCR were performed. Results are expressed as fold induction in UVB stressed NHKs compared to control NHKs at 1h. GAPDH (glyceraldehyde 3-phosphate deshydrogenase) was used as housekeeping gene. Three different donors have been analysed (n=3). Statistical tests were carried out by using two-way ANOVA and Bonferroni post-tests (**: $P < 0.01$).

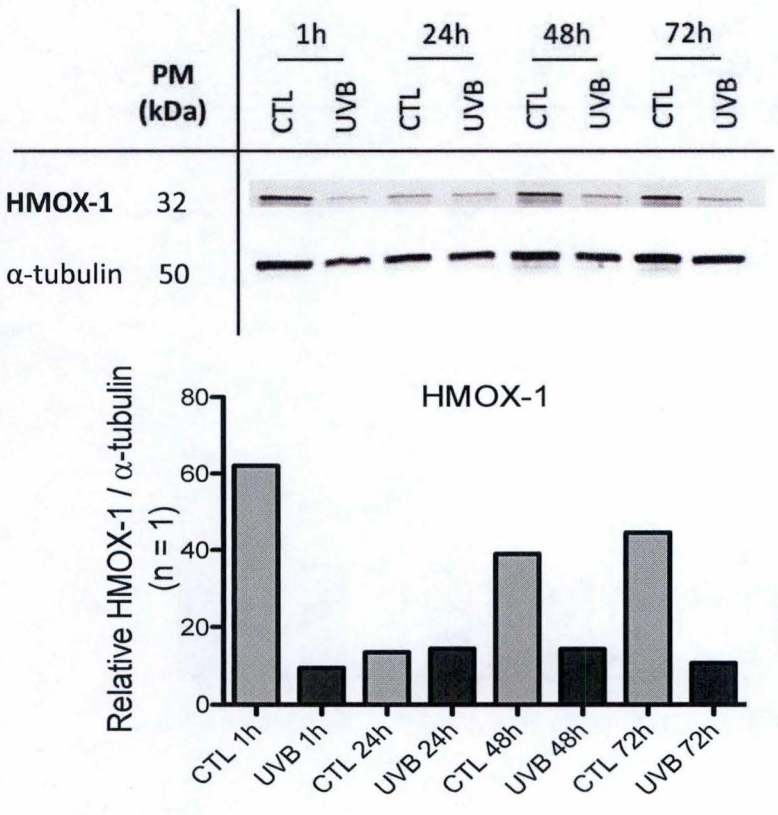

Figure 21: Protein abundance of HMOX-1 in NHKs in UVB-SIPS by Western Blot. NHKs were exposed three times a day to UVB at 625 mJ/cm^2 (or not: CTL) in a three-hour interval. Proteins were extracted at 1, 24, 48 and 72 hours after the last stress. a-tubulin was used as loading control. Relative fluorescence was compared to α-tubulin.

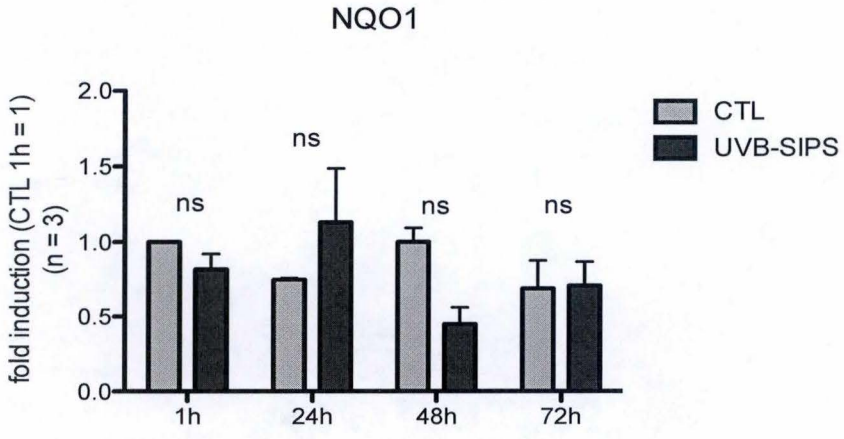

Figure 22: Expression of NQO1 gene in NHKs in UVB-SIPS . NHKs were exposed three times a day to UVB at 625 mJ/cm^2 (or not: CTL) in a three-hour interval. Total RNA was extracted at 1, 24, 48 and 72 hours after the last stress, then reverse transccription and qPCR were performed. Results are expressed as fold induction in UVB stressed NHKs compared to control NHKs at 1h. GAPDH (glyceraldehyde 3-phosphate deshydrogenase) was used as housekeeping gene. Three different donors have been analysed (n=3). Statistical tests were carried out by using two-way ANOVA and Bonferroni post-tests.

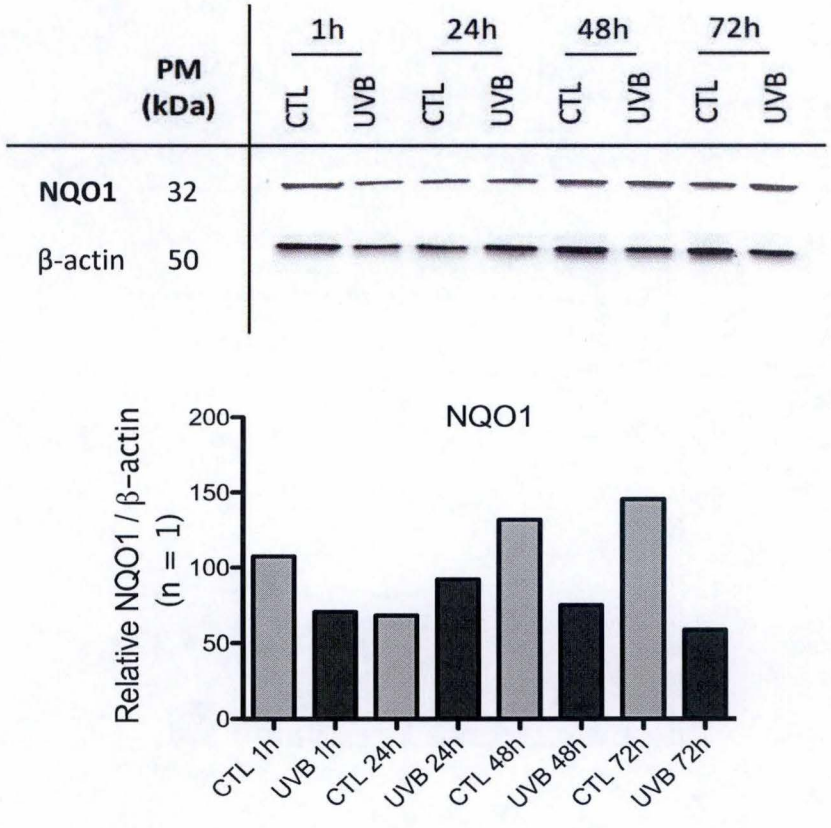

Figure 23: Protein abundance of NQO1 in NHKs in UVB-SIPS by Western Blot. NHKs were exposed three times a day to UVB at 625 mJ/cm^2 (or not: CTL) in a three-hour interval. Proteins were extracted at 1, 24, 48 and 72 hours after the last stress. (-actin was used as loading control. Relative fluorescence was compared to β-actin.

3.4. Antioxidant genes expression

Nrf2 activation can lead to the expression of several antioxidant genes, such as *Heme Oxygenase-1 (HMOX-1)* and *NAD(P)H quinone dehydrogenase-1 (NQO1).*
We studied the mRNA and protein expression of these two Nrf2-targeted genes by western blots and qPCR in NHKs in UVB-SIPS.
HMOX1 is a rate limiting enzyme in heme degradation thereby acting as a potent anti-oxidative and anti-inflammatory factor (Yoshida et al 2001). It is one of the main effector of cellular defense against oxidative stress, regulated by Nrf2.
We detected a significant overexpression of HMOX-1 (5.2-fold) at 24 hours in UVB-exposed cells (fig. 20), compared to control cells (0.6-fold). This is followed by an important decrease of its expression at 48 and 72 hours (0.8 and 0.6-fold), even lower than in control cells (1.9 and 2.2-fold).
We performed western blots to check the expression of HMOX-1 at the same time points for NHKs isolated from one donor (fig. 21). Results showed a higher protein abundance at 1, 48 and 72 hours in control cells compared to UVB-exposed cells. No difference of abundance was highlighted in UVB-exposed cells at each time points. The increased mRNA abundance at 24 hours is therefore not verified at the protein level. It would be useful to make protein extracts of NHKs from independent donors and to repeat this experiment.

NQO1 is a cytosolic homodimeric flavoprotein that reduces quinones to hydroquinones in a two-electron step reduction. NQO1 can protect cells from oxidative stress, neoplastic lesion and redox cycling. It is known that Nrf2 regulates expression of NQO1 gene in many tissues (Ross et al. 2000).
We also performed quantitative PCR and western blot to investigate NQO1 expression in NHKs in UVB-SIPS. Results showed no difference at the mRNA level between controls and UVB-exposed NHKs from 1 to 72 hours (fig. 22).
For NQO1 protein abundance, we didn't observe any changes at each time except in control cells, in which an increased expression is detected at 48 and 72 hours compared to UVB-treated cells (fig. 23). The expression of NQO1 therefore does not appear to be modified following UVB stresses.

DISCUSSION, CONCLUSION & PERSPECTIVES

DISCUSSION

Increasingly evidence shows that cellular senescence is involved in the progressive loss of organ function and is associated with the development of some aged-related diseases. However, it is unclear how senescent cells appear in tissues and what is the impact of senescence on aged-related diseases. Several types of senescence exist: replicative senescence (RS), linked to proliferative potential exhaustion, senescence induced by oncogenes and senescence induced by stress. In our work, we used a model of premature senescence induced by UVB stress (UVB-SIPS) in normal human keratinocytes (NHKs) to better understand the molecular mechanisms activated following these stresses and potentially involved in the appearance of the senescent phenotype. Despite steady progress in senescence and ageing, little is known about all the mechanisms involved in this ageing process induced by solar radiation. It is why it is important to better learn the mechanisms underpinning the establishment and maintenance of senescent keratinocytes after UVB exposures.

First, we checked the morphological changes between keratinocytes in UVB-SIPS and in RS conditions. Phase contrast microscopy revealed irregular and flattened cells in UVB-SIPS and in RS compared to cells at early passage, in agreement with previous observations in the literature. Indeed, it was reported that senescent epidermal keratinocytes are irregular-shaped, enlarged and flattened, with vacuoles in the perinuclear cytoplasm (Kang et al. 2000). The size is also modified with some larger keratinocytes for the late passage in RS, but the difference is less obvious for NHKs in UVB-SIPS. This fits with the observation that small polygonal keratinocytes (10 – 20 μm in diameter) were found at early passages while cells get irregular in size and shape thereby reaching up to 50 μm in diameter at late passages (Soroka et al. 2008). This morphological change could be explained by an increased lysosomal mass which reflects a general increase in cytoplasmic constituents (Kurz et al. 2000). A recent study highlighted that UPR (unfolded protein response) activation could represent a basic pathway involved in changes in cell size (Druelle et al. 2016). Indeed, experiments showed that ER (endoplasmic reticulum) stress characterised by both expansion and biogenesis through ATF6α (cyclic AMP-dependent transcription factor), an ER stress sensor, induces morphological changes. It could be explained by an increasing production of senescent pro-inflammatory secretome, since the invalidation of ATF6α has an impact on the production of IL-6 (Druelle et al. 2016). In addition, it appears that ATF6α-controlled ER expansion is also linked to thicker and longer packed bundles of vimentin, an intermediate filament cytoskeleton, in senescent cells (Nishio et al. 2001; Druelle et al. 2016).

We also checked the cumulative cell population doublings (CPD) curve and the expression of p16 in RS in NHKs, in order to confirm the cell cycle arrest (Rheinwald et al. 2002). Our results showed an exponential phase of proliferation followed by a plateau after five weeks. In addition to proliferation curve, the increased expression of p16 confirms the cell growth arrest.

DISCUSSION

To confirm the senescent state of our model, we also used the SA-βgal assay, a widely used marker induced at senescence (Dimri et al. 1995). Indeed, this biomarker can be used in culture or *ex vivo*, and it is linked to the increased lysosomal biogenesis (Debacq-Chainiaux et al. 2009). Consequently, this increased enzymatic activity is detectable at a suboptimal pH (pH 6.0) in senescent cells (Dimri et al. 1995). Our RS model showed a high percentage of SA-βgal positive cells at late passages compared to early passages. Moreover, in NHKs exposed to UVB-SIPS, a high percentage of positive cells for SA-βgal was also detected, suggesting that our model is appropriated for our experiments.

One of the major features of senescent cells is that they secrete many factors. These factors include inflammatory, growth and remodeling factors and can potentially explain how senescent cells can attract immune cells, modify tissue microenvironments, and, paradoxically, reinforce tumor growth of nearby cells (Coppé et al. 2010; Xue et al. 2007). Moreover, the SASP is also the main driver of age-related inflammation thereby promoting immune clearance of the damaged cells (Chien et al. 2011). Secreted factors such as IL-6 and IL-8 are required for the induction and maintenance of cell cycle arrest of cells exposed to oncogenic stress (Kuilman et al. 2008). Here we show in our experiments that IL-6 is quickly overexpressed after the last UVB stress, and then its expression decreases from 48 hours. This peak of increased abundance is delayed at the protein level, with a maximum secreted abundance at 48 hours. It has been speculated that UVB light induces the release of IL-6 by keratinocytes after UVB exposure through IL-1 (Chung et al. 1996). Research found that IL-6 can activate cells via two different mechanisms, called classic and trans-signaling. In classic signaling, IL-6 binds to the non-signaling membrane-bound IL-6 receptor (IL-6R), and the IL-6/IL-6R complex then recruits two signal-transducing glycoprotein 130 (gp130) receptor proteins. Once gp130 is dimerized, it activates the Jak/STAT, PI3K, and MAPK signaling pathways (Simpson et al. 1997). It would be interesting to investigate the molecular pathway involved and/or IL-6R to know whether the NHKs under UVB stresses are responsive to IL-6 or not. In addition to classic signal, the trans-signaling pathway includes IL-6 and a soluble form of IL-6R thereby activating the neighbouring cells. This form is considered as the primary driving force of pro-inflammatory response in chronic inflammatory diseases (Jones, Scheller, and Rose-John 2011). To extend these analyses to an inflammatory setting, we could investigate EGFR (Epidermal Growth Factor Receptor) signaling and mTOR (mammalian Target Of Rapamycin) activation because these actors induce IL-6 secretion, which contributes to tumour development through STAT3 (Signal transducer and activator of transcription 3) activation (Gao et al. 2007).

In addition to IL-6, we also studied the expression of IL-8, a pro-inflammatory mediator, in NHKs after UVB stresses. Our results showed an increased IL-8 expression at 24 and 48 hours, followed by a decreased expression, but still higher than in the controls. At the protein level, we highlighted a constant increase of IL-8 secretion in NHKs from 24 hours. It has been demonstrated that inflammatory stimuli such as tPA (tissue plasminogen activator) increases the expression of IL-8 in keratinocytes (Cataisson et al. 2006). *In vivo* studies provide evidence that IL-8 has a potential role as a chemotaxis factor, indicating a major role in wound healing (Devalaraja et al. 2000).

Finally, we studied the expression of VEGF, another component of the SASP. This potent angiogenic factor is known to drive tumour growth and metastasis. Interestingly, VEGF also stimulates angiogenesis in cutaneous wound repair (Bao et al. 2009). A variety of mitogens and chemotactic factors such as epidermal growth factor (EGF), transforming growth factor-β (TGF-β) and tumour necrosis factor-α (TNF-α) have been shown to be stimulating during cutaneous wound repair (Pakyari et al. 2013). We found that VEGF levels were drastically decreased in keratinocytes after UVB stresses compared to controls, both at the mRNA and protein levels. Interestingly, a previous model of UVB-induced premature senescence in human skin fibroblasts suggested that low dose UVB irradiation (five repeated UVB exposures at a dose of 10 mJ/cm^2) leads to a strong increase in VEGF mRNA and protein, which is an opposite results compared to our data (W. Chen et al. 2008).

Our data suggest that the level expression of many secreted factors change when keratinocytes senesce after UVB exposures. These secreted factors may influence the tissue microenvironment *in vivo* by attracting immune cells, leading to immune surveillance through elimination of senescent cells. Depending on the biological context, this process may improve the resolution of wound healing or tumor regression responses (Krizhanovsky et al. 2008). Despite the potential major role of the SASP, little is known about how the process is modulated.

A significant finding was that the DNA damage response (DDR) is required for the increased secretion of a variety of SASP factors (Rodier et al. 2009). Indeed, both DDR and SASP activate and promote a pro-inflammatory environment impacting neighbouring cells. UVB irradiation induces direct or indirect DNA damage through generation of ROS and leads to the formation of DNA double-strand breaks (Sinha and Häder 2002). Some sensors of this pathway can recognise DNA damage and activate ATM and ATR kinases, two major central regulators. Consequently, to further explore the impact of UVB on NHKs, we investigated the activation of the main DDR actors at different times after the last UVB stresses. Our data revealed a high abundance of P-ATM at 1 hour after the last UVB stress and a prominent nuclear staining at 24 hours followed by a decrease of the phosphorylated form. Similar results were obtained for P-CHK2 with a high abundance at 1 hour after the last UVB stress, and still detectable in UVB-exposed cells until 72 hours.

One target of CHK2 is p53, a tumour suppressor and transcriptional regulator that manage DNA repair and cell cycle arrest. We observed an increased abundance of P-p53 and p53 by immunocytochemistry and western blot in the UVB-SIPS condition. Data showed that if DSBs are not repaired, constitutive DDR signaling is triggered, and activates p53, inducing an irreversible growth arrest. On the other hand, we didn't detect in our model any activation of ATR and CHK1, a distinct kinase signaling pathway. We can assume that UVB exposure causes DSBs in DNA (previous results from E. Bauwens and L. Ernst) and ATM pathway is favoured compared to ATR pathway following our stress model.

ATM and ATR are the master transducers of DNA signals, which maintain genomic integrity through a vast network of cellular processes. While ATM is primarily activated by DSBs, ATR responds to a large spectrum of DNA damage, including a variety of DNA lesions that interfere with replication. In the signal cascade, ATM phosphorylates the DDR kinase CHK2

that promotes growth arrest. A study reported that CHK-2 is quickly dephosphorylated probably after exposition with phosphatases (Ahn et al. 2002). In contrariwise, our results showed a persistent activation of P-CHK2 after UVB irradiation. Importantly, CHK-2 and ATM have been described as important activators of inflammatory cytokines such as IL-6 and IL-8 in senescent cells (Rodier et al. 2009). Taken together, these observations suggest a potential activation of IL-6 and IL-8 cytokines through activation of ATM pathway.

In parallel, we investigated the generation of reactive oxygen species (ROS) in the UVB-SIPS model. By using the DCF probe by flow cytometry, we showed a clear difference at 48 and 72 hours, with an increase of ROS generation in UVB-exposed cells compared to control cells.
Indeed, it was reported that an excessive generation of ROS occurs through exposures to various exogenous agents such as UV, cytokines, chemotherapeutic drugs and macrophages during the inflammatory response (Finkel and Holbrook 2000). Moreover, photosensitizers such as $NADH^{-}$/NADPH, riboflavin, tryptophan and porphyrin can be excited by UVB radiations and transmit energy to oxygen molecules leading to the overproduction of ROS (Hiraku et al. 2007).
It has been proved that ROS is associated with p53-dependent cell cycle arrest, apoptosis and DNA repair, but the mechanisms involved in the interaction between ROS and p53 are still elusive (Sablina et al. 2005).
Current data show that overexpression of p53 transactivates p53-induced genes (PIGs) including ROS-generating enzymes, NQO1 and proline oxidase (POX) (Polyak et al. 1997).
To extend theses analyses, we monitored the superoxide level in NHKs in our model by flow cytometry. Our experiments showed a quick increase of superoxide level at 24 hours after UVB stresses compared to controls while no significant differences were observed at 48 or 72 hours after UVB-treated cells.
Based on different studies, activation of the major effectors of the DDR checkpoint can induce ROS production (Borodkina et al. 2014; Xue et al. 2007). The electron membrane chain can generate superoxide anion through redox reactions into various harmful ROS including hydroxyl radical, hydrogen peroxide or peroxynitrite anion (Brand 2010). In addition, a significant increase in mitochondrial superoxide anion has been reported in human senescent fibroblasts (Saitoh et al. 2013). Moreover, it is important to note that the production of ROS seems to be an earlier event than the onset of other senescent biomarkers in human fibroblasts (J.-M. Kim et al. 2013).
To further explore the impact of ROS, we evaluated the activation of Nrf2. Indeed, Nrf2 is a major transcription factor that controls the expression of both antioxidants and detoxification enzymes to maintain homeostasis. Under non-stress conditions, Nrf2 is constantly degraded in the cytoplasm, keeping protein levels low. By opposite, Nrf2 is upregulated and translocated to the nucleus in stress condition, thereby allowing the expression of specific factors in stress conditions. We focused on Nrf2 and our experiments showed an important staining in cell nuclei at 24 hours in UVB stressed cells. The fluorescence signal is then distributed and more intense into the cytoplasm and nuclei after 24 hours in UVB stressed cells condition. These results may suggest an activation of Nrf2 combined with a translocation caused by excessive production of ROS. However, the quantification of the binding of this transcription factor to its consensus sequence revealed no differences between controls and UVB stressed cells.

We therefore sought to confirm the relevance of Nrf2 activity, by evaluating antioxidant gene expression. Indeed, Nrf2 regulates the expression of genes in response to oxidative stress such as NQO1, HMOX-1 and glutamate cysteine ligase (GLC). HMOX-1, is an antioxidant and anti-inflammatory factor which catalyses the oxidation of heme to biliverdin, carbon monoxide and free iron. NQO1 is a flavoenzyme that catalyzes the two-electron reduction of quinones and aromatic compounds by using NAD(P)H as an electron donor, and can protect cells from oxidative stress.

We report here a significant increase of gene expression of HMOX-1 at 24 hours after UVB stresses while the protein abundance remains low in UVB-SIPS compared to controls. In addition, expression of NQO1 in our model doesn't change, both at the mRNA and protein levels.

If our results clearly show an increase in oxidative stress following UVB stresses, the activation of Nrf-2 is not confirmed, whether at the level of the binding assay (TransAM), and at the level of the expression of the target genes.

Major findings on the change of HMOX-1 expression with ageing showed an increased basal HMOX-1 mRNA, protein levels or enzymatic activity in various tissues such as liver, lung, brain or spleen. For example, liver HMOX-1 mRNA is increased in old rats (Patriarca et al. 2007). In contrast, some studies reported a decreased expression with ageing. For example, HMOX-1 is decreased in the aorta of the hippocampus of old rats compared to young ones (Ewing and Maines 2006; Ungvari et al. 2011). Importantly, it should be important to note that most studies on HMOX-1 used rodents while studies of human tissues or cells are rare. Many research have also investigated the change of NQO1 expression in different models in order to understand how this antioxidant gene is involved in senescent process. For example, it was demonstrated that NQO1 was increased in liver of aged mice compared with young adults (Fu, Csanaky, and Klaassen 2012). In contrast, another study showed a decrease of NQO1 expression in astrocytes of old mice (Duan et al. 2009). It remains unclear whether the difference in the age-dependent change of the basal expression of NQO1 is due to tissues, cell types, species, or ageing phases.

Our results highlighted various mechanisms potentially involved in the model of UVB-SIPS in NHKs. However, several experiments have to be planned to confirm our results, notably due to the variability between donors.

Indeed, DDR pathway, if implicated, is probably not the only regulator of senescence because it is activated quickly after the damage while senescence phenotype such as SA-βgal, develops only after 72 hours in our model. One such actor may be $p38^{MAPK}$, a member of the mitogen-activated protein kinase (MAPK) family. It has been demonstrated that constitutive $p38^{MAPK}$ is sufficient to induce growth arrest by p53 and pRb/p16 (Freund, Patil, and Campisi 2011). Moreover, $p38^{MAPK}$ regulates the SASP by increasing NF-κB transcriptional activity independently of the DDR (Freund, Patil, and Campisi 2011). It was also shown that NF-κB is involved in cellular responses following ultraviolet radiation, cytokines and free radicals (Brasier 2006). It would be interesting to analyse the expression and activation of $p38^{MAPK}$ and NF-κB in NHKs in response to UVB-SIPS.

DISCUSSION

Recently, a publication suggested that a feedback pathway between persistent DDR activation and the increased of ROS production was necessary for cellular senescence (Borodkina et al. 2014). After investigation of ROS and superoxide levels, we detected some changes in NHKs after UVB stresses. However, it would be substantial to understand what is the molecular pathway behind oxidative stress in senescence.

Accumulation of ROS can mediate damage to cellular components during ageing process (López-Otín et al. 2013). Indeed, it has been proposed that both increased protein oxidative damage and decreased elimination of oxidized proteins cause an accumulation of oxidized proteins (Bota and Davies 2002). Age-related impairment of oxidized protein elimination seems to be involved in a decline of protein homeostasis and accumulation of oxidative modified proteins. For example, a decreased proteasome subunit expression has been found in senescent human keratinocytes, thereby leading to a decrease of proteasome activity (Chondrogianni et al. 2003). Interestingly, UV irradiation of human keratinocytes also induces a loss of proteasome peptidase activities, which has been associated with damaged proteins, such as the proteins modified 4-hydroxy-2-nonenal (a major cytotoxic product of lipid peroxidation) (Bulteau et al. 2002). Concerning oxidized repair systems, it turns out that impaired expression and/or activity of the peptide methionine sulfoxide reductases (MsrA), which catalyzes the reduction of methionine sulfoxide in proteins back to methionine, may explain an accumulation of unrepaired proteins (Picot et al. 2004). Oxidized protein degradation and repair system appears to play a critical role in senescence. Consequently, understanding its implication in our model would represent an important step to confirm our investigations.

Our data therefore seem to show that DDR is activated in UVB-SIPS, while Nrf2 pathway must be confirmed by further experiments. Are these pathways involved in the onset of senescent phenotype including SASP?

Previous experiments showed that some DDR actors are involved in the SASP (Coppé et al. 2010). Indeed, it was shown that ATM and CHK2 depletion prevents the high IL-6 secretion in senescent following X-radiation (Rodier et al. 2009). It would be interesting to determine whether in our model, DDR pathway is also linked to the expression of some factors of the SASP. We could deplete ATM or CHK2 expression in NHKs by using shRNA, and then exposed them to repeated UVB stress inducing senescence. So we could confirm if the ATM pathway is essential for senescence in our model.

Finally, to elucidate the role of the secretome produced by NHKs in our model, we could investigate the interaction between senescent keratinocytes and other cell types (non-senescent keratinocytes, cancer cells or immune cells). Co-cultures have been used to analyse secreted factors produced by different cells and can be interesting in our model.

Furthermore, we also could investigate various specific factors in the healing process of cutaneous wounds. Indeed, our results showed a high activation of IL-8 but also a major decrease of VEGF expression. However, a study showed that VEGF stimulates angiogenesis in cutaneous wound repair (Bao et al. 2009). To further explore the wound healing induced by UVB in senescent keratinocytes, a variety of mitogens and chemotactic factors such as epidermal growth factor (EGF), transforming growth factor-β (TGF-β) and tumour necrosis factor-α (TNF-α) could be investigated because these actors have been shown to be stimulated during cutaneous wound repair (Pakyari et al. 2013).

REFERENCES

Adamus, Jean, Sirpa Aho, Helen Meldrum, Carol Bosko, and Jian-Ming Lee. 2014. "p16INK4A Influences the Aging Phenotype in the Living Skin Equivalent." *Journal of Investigative Dermatology* 134 (4): 1131–33. doi:10.1038/jid.2013.468.

Afaq, Farrukh, and Hasan Mukhtar. 2001. "Effects of Solar Radiation on Cutaneous Detoxification Pathways." *Journal of Photochemistry and Photobiology B: Biology* 63 (1–3): 61–69. doi:10.1016/S1011-1344(01)00217-2.

Ahn, Joon Young, Xianghong Li, Heather L. Davis, and Christine E. Canman. 2002. "Phosphorylation of Threonine 68 Promotes Oligomerization and Autophosphorylation of the Chk2 Protein Kinase via the Forkhead-Associated Domain." *Journal of Biological Chemistry* 277 (22): 19389–95. doi:10.1074/jbc.M200822200.

Allsopp, R. C., H. Vaziri, C. Patterson, S. Goldstein, E. V. Younglai, A. B. Futcher, C. W. Greider, and C. B. Harley. 1992. "Telomere Length Predicts Replicative Capacity of Human Fibroblasts." *Proceedings of the National Academy of Sciences* 89 (21): 10114–18. doi:10.1073/pnas.89.21.10114.

Ameur, Adam, James B. Stewart, Christoph Freyer, Erik Hagström, Max Ingman, Nils Göran Larsson, and Ulf Gyllensten. 2011. "Ultra-Deep Sequencing of Mouse Mitochondrial DNA: Mutational Patterns and Their Origins." *PLoS Genetics* 7 (3). doi:10.1371/journal.pgen.1002028.

Baker, Darren J, Karthik B Jeganathan, J Douglas Cameron, Michael Thompson, Subhash Juneja, Alena Kopecka, Rajiv Kumar, et al. 2004. "BubR1 Insufficiency Causes Early Onset of Aging-Associated Phenotypes and Infertility in Mice." *Nature Genetics* 36 (7): 744–49. doi:10.1038/ng1382.

Bao, Philip, Arber Kodra, Marjana Tomic-Canic, Michael S Golinko, H Paul Ehrlich, Harold Brem, and D Ph. 2009. "The Role of Vascular Endothelial Growth Factor in Wound Healing." *The Journal of Surgical Research* 153 (2): 347–58. doi:10.1016/j.jss.2008.04.023.

Bartkova, Jirina, Nousin Rezaei, Michalis Liontos, Panagiotis Karakaidos, Dimitris Kletsas, Natalia Issaeva, Leandros-Vassilios F. Vassiliou, et al. 2006. "Oncogene-Induced Senescence Is Part of the Tumorigenesis Barrier Imposed by DNA Damage Checkpoints." *Nature* 444 (7119): 633–37. doi:10.1038/nature05268.

Beauséjour, Christian M., Ana Krtolica, Francesco Galimi, Masashi Narita, Scott W. Lowe, Paul Yaswen, and Judith Campisi. 2003. "Reversal of Human Cellular Senescence: Roles of the p53 and p16 Pathways." *EMBO Journal* 22 (16): 4212–22. doi:10.1093/emboj/cdg417.

Begley, Lesa, Christine Monteleon, Rajal B. Shah, James W. MacDonald, and Jill A. Macoska. 2005. "CXCL12 Overexpression and Secretion by Aging Fibroblasts Enhance Human Prostate Epithelial Proliferation in Vitro." *Aging Cell* 4 (6): 291–98. doi:10.1111/j.1474-9726.2005.00173.x.

Bekker-Jensen, Simon, Claudia Lukas, Risa Kitagawa, Fredrik Melander, Michael B Kastan, Jiri Bartek, and Jiri Lukas. 2006. "Spatial Organization of the Mammalian Genome Surveillance Machinery in Response to DNA Strand Breaks." *The Journal of Cell Biology* 173 (2): 195–206. doi:10.1083/jcb.200510130.

Bernadotte, Alexandra, Victor M. Mikhelson, and Irina M. Spivak. 2016. "Markers of Cellular Senescence. Telomere Shortening as a Marker of Cellular Senescence." *Aging* 8 (1): 3–11. doi:10.18632/aging.100871.

Bernard, David, Karo Gosselin, Didier Monte, Chantal Vercamer, Fatima Bouali, Albin Pourtier, Bernard Vandenbunder, and Corinne Abbadie. 2004. "Involvement of Rel/Nuclear Factor-κB Transcription Factors in Keratinocyte Senescence." *Cancer Research* 64 (2): 472–81. doi:10.1158/0008-5472.CAN-03-0005.

Bischoff, Claus, Hans Christian Petersen, Jesper Graakjaer, Karen Andersen-Ranberg, James

W Vaupel, Vilhelm A Bohr, Steen Kølvraa, et al. 2006. "No Association between Telomere Length and Survival among the Elderly and Oldest Old." *Epidemiology* 17 (2): 190–94. doi:10.1097/01.ede.0000199436.55248.10.

Borodkina, Aleksandra, Alla Shatrova, Polina Abushik, Nikolay Nikolsky, and Elena Burova. 2014. "Interaction between ROS Dependent DNA Damage, Mitochondria and p38 MAPK Underlies Senescence of Human Adult Stem Cells." *Aging* 6 (6): 481–95. doi:10.18632/aging.100673.

Bota, Daniela a, and Kelvin J a Davies. 2002. "Lon Protease Preferentially Degrades Oxidized Mitochondrial Aconitase by an ATP-Stimulated Mechanism." *Nature Cell Biology* 4 (9): 674–80. doi:10.1038/ncb836.

Brand, Martin D. 2010. "The Sites and Topology of Mitochondrial Superoxide Production." *Experimental Gerontology* 45 (7–8): 466–72. doi:10.1016/j.exger.2010.01.003.

Brasier, Allan R. 2006. "The NF-kappaB Regulatory Network." *Cardiovascular Toxicology* 6 (2): 111–30. doi:CT:6:2:111 [pii].

Briggaman, Robert a. 1982. "Epidermal-Dermal Interactions in Adult Skin." *Journal of Investigative Dermatology* 79 (s1): 21s–24s. doi:10.1111/1523-1747.ep12544628.

Bulteau, Anne Laure, Marielle Moreau, Carine Nizard, and Bertrand Friguet. 2002. "Impairment of Proteasome Function upon UVA- and UVB-Irradiation of Human Keratinocytes." *Free Radical Biology and Medicine* 32 (11): 1157–70. doi:10.1016/S0891-5849(02)00816-X.

Burtner, Christopher R, and Brian K Kennedy. 2010. "Progeria Syndromes and Ageing: What Is the Connection?" *Nature Reviews. Molecular Cell Biology* 11 (8): 567–78. doi:10.1038/nrm2944.

Burton, Dominick G A, and Valery Krizhanovsky. 2014. "Physiological and Pathological Consequences of Cellular Senescence." *Cellular and Molecular Life Sciences*. doi:10.1007/s00018-014-1691-3.

Byrne, C, M Tainsky, and E Fuchs. 1994. "Programming Gene Expression in Developing Epidermis." *Development (Cambridge, England)* 120 (9): 2369–83.

Calamini, Barbara, Maria Catarina Silva, Franck Madoux, Darren M. Hutt, Shilpi Khanna, Monica A. Chalfant, Christophe Allais, et al. 2010. *ML346: A Novel Modulator of Proteostasis for Protein Conformational Diseases. Probe Reports from the NIH Molecular Libraries Program*. http://www.ncbi.nlm.nih.gov/pubmed/23833797.

Calderwood, Stuart K, Ayesha Murshid, and Thomas Prince. 2009. "The Shock of Aging: Molecular Chaperones and the Heat Shock Response in Longevity and Aging--a Mini-Review." *Gerontology* 55 (5): 550–58. doi:10.1159/000225957.

Campisi, Judith, and Fabrizio d'Adda di Fagagna. 2007. "Cellular Senescence: When Bad Things Happen to Good Cells." *Nature Reviews. Molecular Cell Biology* 8 (9): 729–40. doi:10.1038/nrm2233.

Capper, Rebecca, Bethan Britt-Compton, Maira Tankimanova, Jan Rowson, Boitelo Letsolo, Stephen Man, Michele Haughton, and Duncan M. Baird. 2007. "The Nature of Telomere Fusion and a Definition of the Critical Telomere Length in Human Cells." *Genes and Development* 21 (19): 2495–2508. doi:10.1101/gad.439107.

Cataisson, Christophe, Andrea J. Pearson, Margaret Z. Tsien, Francesca Mascia, Ji Liang Gao, Saveria Pastore, and Stuart H. Yuspa. 2006. "CXCR2 Ligands and G-CSF Mediate PKCα-Induced Intraepidermal Inflammation." *Journal of Clinical Investigation* 116 (10): 2757–66. doi:10.1172/JCI27514.

Chainiaux, Florence, Joao-Pedro Magalhaes, François Eliaers, José Remacle, and Olivier Toussaint. 2002. "UVB-Induced Premature Senescence of Human Diploid Skin Fibroblasts." *The International Journal of Biochemistry & Cell Biology* 34 (11): 1331–39. doi:10.1016/S1357-2725(02)00022-5.

Chen, Q M, K R Prowse, V C Tu, S Purdom, and M H Linskens. 2001. "Uncoupling the Senescent Phenotype from Telomere Shortening in Hydrogen Peroxide-Treated Fibroblasts." *Experimental Cell Research* 265 (2): 294–303. doi:10.1006/excr.2001.5182.

Chen, Qin M, Victoria C Tu, Jeffrey Catania, Maggi Burton, Olivier Toussaint, and Tarrah Dilley. 2000. "Involvement of Rb Family Proteins, Focal Adhesion Proteins and Protein Synthesis in Senescent Morphogenesis Induced by Hydrogen Peroxide." *Journal of Cell Science* 113 (Pt 2: 4087–97.

Chen, Wenqi, Jian Kang, Jiping Xia, Yanhua Li, Bo Yang, Bin Chen, Weiling Sun, et al. 2008. "p53-Related Apoptosis Resistance and Tumor Suppression Activity in UVB-Induced Premature Senescent Human Skin Fibroblasts." *International Journal of Molecular Medicine* 21 (5): 645–53. doi:10.3892/ijmm.21.5.645.

Chien, Yuchen, Claudio Scuoppo, Xiaowo Wang, Xueping Fang, Brian Balgley, Jessica E. Bolden, Prem Premsrirut, et al. 2011. "Control of the Senescence-Associated Secretory Phenotype by NF-κB Promotes Senescence and Enhances Chemosensitivity." *Genes and Development* 25 (20): 2125–36. doi:10.1101/gad.17276711.

Cho, Kyung A., Jin Ryu Sung, Sin Oh Yoon, Hyeun Park Ji, Weon Lee Jung, Hwang Phill Kim, Tae Kim Kyung, Soon Jang Ik, and Chul Park Sang. 2004. "Morphological Adjustment of Senescent Cells by Modulating Caveolin-1 Status." *Journal of Biological Chemistry* 279 (40): 42270–78. doi:10.1074/jbc.M402352200.

Chondrogianni, Niki, Fiona L L Stratford, Ioannis P. Trougakos, Bertrand Friguet, A. Jennifer Rivett, and Efstathios S. Gonos. 2003. "Central Role of the Proteasome in Senescence and Survival of Human Fibroblasts. Induction of a Senescence-like Phenotype upon Its Inhibition and Resistance to Stress upon Its Activation." *Journal of Biological Chemistry* 278 (30): 28026–37. doi:10.1074/jbc.M301048200.

Chung, J H, S H Youn, W S Koh, H C Eun, K H Cho, K C Park, and J I Youn. 1996. "Ultraviolet B Irradiation-Enhanced Interleukin (IL)-6 Production and mRNA Expression Are Mediated by IL-1 Alpha in Cultured Human Keratinocytes." *The Journal of Investigative Dermatology* 106 (4): 715–20. doi:10.1046/j.1523-1747.2002.01844.x.

Clydesdale, G. J., G. W. Dandie, and H. K. Muller. 2001. "Ultraviolet Light Induced Injury: Immunological and Inflammatory Effects." *Immunology and Cell Biology*. doi:10.1046/j.1440-1711.2001.01047.x.

Coppé, Jean-Philippe, Pierre-Yves Desprez, Ana Krtolica, and Judith Campisi. 2010. "The Senescence-Associated Secretory Phenotype: The Dark Side of Tumor Suppression." *Annual Review of Pathology* 5: 99–118. doi:10.1146/annurev-pathol-121808-102144.

Coppé, Jean-Philippe, Katalin Kauser, Judith Campisi, and Christian M Beauséjour. 2006. "Secretion of Vascular Endothelial Growth Factor by Primary Human Fibroblasts at Senescence." *The Journal of Biological Chemistry* 281 (40): 29568–74. doi:10.1074/jbc.M603307200.

Coppé, Jean-Philippe, Christopher K Patil, Francis Rodier, Yu Sun, Denise P Muñoz, Joshua Goldstein, Peter S Nelson, Pierre-Yves Desprez, and Judith Campisi. 2008. "Senescence-Associated Secretory Phenotypes Reveal Cell-Nonautonomous Functions of Oncogenic RAS and the p53 Tumor Suppressor." *PLoS Biology* 6 (12): e301. doi:10.1371/journal.pbio.0060301.

Courtois-Cox, S, S L Jones, and K Cichowski. 2008. "Many Roads Lead to Oncogene-Induced Senescence." *Oncogene* 27 (20): 2801–9. doi:10.1038/sj.onc.1210950.

Cristofalo, V J, C Volker, M K Francis, and M Tresini. 1998. "Age-Dependent Modifications of Gene Expression in Human Fibroblasts." *Critical Reviews in Eukaryotic Gene Expression* 8 (1): 43–80. doi:10.1615/critreveukargeneexpr.v8.i1.30.

D'Errico, Mariarosaria, Tiziana Lemma, Angelo Calcagnile, L. P D Santis, and Eugenia

Dogliotti. 2007. "Cell Type and DNA Damage Specific Response of Human Skin Cells to Environmental Agents." *Mutation Research - Fundamental and Molecular Mechanisms of Mutagenesis* 614 (1–2): 37–47. doi:10.1016/j.mrfmmm.2006.06.009.

Dahlmann, Burkhardt. 2007. "Role of Proteasomes in Disease." *BMC Biochemistry* 8 (Suppl 1): S3. doi:10.1186/1471-2091-8-S1-S3.

Dannenberg, J. H., A. Van Rossum, L. Schuijff, and H. Te Riele. 2000. "Ablation of the Retinoblastoma Gene Family Deregulates G1 Control Causing Immortalization and Increased Cell Turnover under Growth-Restricting Conditions." *Genes and Development* 14 (23): 3051–64. doi:10.1101/gad.847700.

Debacq-Chainiaux, Florence, Randa Ben Ameur, Emilie Bauwens, Elise Dumortier, Marie Toutfaire, and Olivier Toussaint. 2016. "Stress-Induced (Premature) Senescence." *Cellular Ageing and Replicative Senescence*.

Debacq-Chainiaux, Florence, Céline Borlon, Thierry Pascal, Véronique Royer, François Eliaers, Noëlle Ninane, Géraldine Carrard, et al. 2005. "Repeated Exposure of Human Skin Fibroblasts to UVB at Subcytotoxic Level Triggers Premature Senescence through the TGF-beta1 Signaling Pathway." *Journal of Cell Science* 118 (Pt 4): 743–58. doi:10.1242/jcs.01651.

Debacq-Chainiaux, Florence, Jorge D Erusalimsky, Judith Campisi, and Olivier Toussaint. 2009. "Protocols to Detect Senescence-Associated Beta-Galactosidase (SA-Betagal) Activity, a Biomarker of Senescent Cells in Culture and in Vivo." *Nature Protocols* 4 (12): 1798–1806. doi:10.1038/nprot.2009.191.

Deng, Yibin, Suzanne S. Chan, and Sandy Chang. 2008. "Telomere Dysfunction and Tumour Suppression: The Senescence Connection." *Nature Reviews. Cancer* 8 (6): 450–58. doi:10.1038/nrc2393.

Deruy, E, J Nassour, N Martin, C Vercamer, N Malaquin, J Bertout, F Chelli, a Pourtier, O Pluquet, and C Abbadie. 2014. "Level of Macroautophagy Drives Senescent Keratinocytes into Cell Death or Neoplastic Evasion." *Cell Death & Disease* 5 (12): e1577. doi:10.1038/cddis.2014.533.

Devalaraja, R M, L B Nanney, J Du, Q Qian, Y Yu, M N Devalaraja, and A Richmond. 2000. "Delayed Wound Healing in CXCR2 Knockout Mice." *The Journal of Investigative Dermatology* 115 (2): 234–44. doi:10.1046/j.1523-1747.2000.00034.x.

Dice, J. Fred. 2007. "Chaperone-Mediated Autophagy." *Autophagy*. doi:10.4161/auto.4144.

Dimri, G P, X Lee, G Basile, M Acosta, G Scott, C Roskelley, E E Medrano, M Linskens, I Rubelj, and O Pereira-Smith. 1995. "A Biomarker That Identifies Senescent Human Cells in Culture and in Aging Skin in Vivo." *Proceedings of the National Academy of Sciences of the United States of America* 92 (20): 9363–67. doi:DOI 10.1073/pnas.92.20.9363.

Dolan, David, Juan Troncoso, Susan M. Resnick, Barbara J. Crain, Alan B. Zonderman, and Richard J. O'Brien. 2010. "Age, Alzheimer's Disease and Dementia in the Baltimore Longitudinal Study of Ageing." *Brain* 133 (8): 2225–31. doi:10.1093/brain/awq141.

Druelle, Clémentine, Claire Drullion, Julie Deslé, Nathalie Martin, Laure Saas, Johanna Cormenier, Nicolas Malaquin, et al. 2016. "ATF6α Regulates Morphological Changes Associated with Senescence in Human Fibroblasts." *Oncotarget*. doi:10.18632/oncotarget.11505.

Duan, Weisong, Ruiyan Zhang, Yansu Guo, Yifang Jiang, Yanli Huang, Hong Jiang, and Chunyan Li. 2009. "Nrf2 Activity Is Lost in the Spinal Cord and Its Astrocytes of Aged Mice." *In Vitro Cellular & Developmental Biology. Animal* 45 (7): 388–97. doi:10.1007/s11626-009-9194-5.

Dumont, Patrick, Maggi Burton, Qin M. Chen, Efstathios S. Gonos, Christophe Frippiat, Jean Baptiste Mazarati, Fran??ois Eliaers, Jos?? Remacle, and Olivier Toussaint. 2000.

"Induction of Replicative Senescence Biomarkers by Sublethal Oxidative Stresses in Normal Human Fibroblast." *Free Radical Biology and Medicine* 28 (3): 361–73. doi:10.1016/S0891-5849(99)00249-X.

Dumont, Patrick, Florence Chainiaux, François Eliaers, Chariklia Petropoulou, José Remacle, Claudia Koch-Brandt, Efstathios S Gonos, and Olivier Toussaint. 2002. "Overexpression of Apolipoprotein J in Human Fibroblasts Protects against Cytotoxicity and Premature Senescence Induced by Ethanol and Tert-Butylhydroperoxide." *Cell Stress & Chaperones* 7 (1): 23–35. doi:10.1379/1466-1268(2002)007<0023:OOAJIH>2.0.CO;2.

Epel, Elissa S, Elizabeth H Blackburn, Jue Lin, Firdaus S Dhabhar, Nancy E Adler, Jason D Morrow, and Richard M Cawthon. 2004. "Accelerated Telomere Shortening in Response to Life Stress." *Proceedings of the National Academy of Sciences* 101 (49): 17312–15. doi:10.1073/pnas.0407162101.

Ewing, J. F., and M. D. Maines. 2006. "Regulation and Expression of Heme Oxygenase Enzymes in Aged-Rat Brain: Age Related Depression in HO-1 and HO-2 Expression and Altered Stress-Response." *Journal of Neural Transmission* 113 (4): 439–54. doi:10.1007/s00702-005-0408-z.

Faggioli, Francesca, Tao Wang, Jan Vijg, and Cristina Montagna. 2012. "Chromosome-Specific Accumulation of Aneuploidy in the Aging Mouse Brain." *Human Molecular Genetics* 21 (24): 5246–53. doi:10.1093/hmg/dds375.

Farage, M. A., K. W. Miller, P. Elsner, and H. I. Maibach. 2008. "Intrinsic and Extrinsic Factors in Skin Ageing: A Review." *International Journal of Cosmetic Science*. doi:10.1111/j.1468-2494.2007.00415.x.

Faragher, R G, I R Kill, J A Hunter, F M Pope, C Tannock, and S Shall. 1993. "The Gene Responsible for Werner Syndrome May Be a Cell Division 'counting' gene." *Proceedings of the National Academy of Sciences of the United States of America* 90 (24): 12030–34. doi:10.1073/pnas.90.24.12030.

Farrell, Andrew W., Gary M. Halliday, and James Guy Lyons. 2011. "Chromatin Structure Following UV-Induced DNA Damage-Repair or Death?" *International Journal of Molecular Sciences*. doi:10.3390/ijms12118063.

Fedarko, Neal S. 2011. "The Biology of Aging and Frailty." *Clinics in Geriatric Medicine*. doi:10.1016/j.cger.2010.08.006.

Finkel, T, and N J Holbrook. 2000. "Oxidants, Oxidative Stress and the Biology of Ageing." *Nature* 408 (6809): 239–47. doi:10.1038/35041687.

Fontana, L., L. Partridge, and V. D. Longo. 2010. "Extending Healthy Life Span--From Yeast to Humans." *Science* 328 (5976): 321–26. doi:10.1126/science.1172539.

Freund, Adam, Christopher K Patil, and Judith Campisi. 2011. "p38MAPK Is a Novel DNA Damage Response-Independent Regulator of the Senescence-Associated Secretory Phenotype." *The EMBO Journal* 30 (8): 1536–48. doi:10.1038/emboj.2011.69.

Frohlich, D a, M T McCabe, R S Arnold, and M L Day. 2008. "The Role of Nrf2 in Increased Reactive Oxygen Species and DNA Damage in Prostate Tumorigenesis." *Oncogene* 27 (31): 4353–62. doi:10.1038/onc.2008.79.

Fu, Zidong Donna, Iván L. Csanaky, and Curtis D. Klaassen. 2012. "Effects of Aging on mRNA Profiles for Drug-Metabolizing Enzymes and Transporters in Livers of Male and Female Mice." *Drug Metabolism and Disposition* 40 (6): 1216–25. doi:10.1124/dmd.111.044461.

Gallage, Suchira, and Jesús Gil. 2016. "Mitochondrial Dysfunction Meets Senescence." *Trends in Biochemical Sciences*. doi:10.1016/j.tibs.2016.01.005.

Gao, Sizhi Paul, Kevin G. Mark, Kenneth Leslie, William Pao, Noriko Motoi, William L. Gerald, William D. Travis, et al. 2007. "Mutations in the EGFR Kinase Domain Mediate STAT3 Activation via IL-6 Production in Human Lung Adenocarcinomas." *The Journal*

of Clinical Investigation 117 (12): 3846–56. doi:10.1172/JCI31871.
Garinis, George A., Gijsbertus T.J. van der Horst, Jan Vijg, and Jan H.J. Hoeijmakers. 2008. "DNA Damage and Ageing: New-Age Ideas for an Age-Old Problem." *Nature Cell Biology* 10 (11): 1241–47. doi:10.1038/ncb1108-1241.
GOLDSMITH, LOWELL A., STEPHEN I. KATZ, BARBARA A. GILCHREST, AMY S. PALLER, DAVID J. LEFFELL, and KLAUS WOLFF. 2012. "Fitzpatrick's Dermatology in General Medicine Eighth Edition." *McGraw-Hill* 150 (4): 22. doi:10.1017/CBO9781107415324.004.
Goldstein, S. 1990. "Replicative Senescence: The Human Fibroblast Comes of Age." *Science* 249 (4973): 1129–33. doi:10.1126/science.2204114.
Gonzalez, Jose M, Davinia Pla, Dolores Perez-Sala, and Vicente Andres. 2011. "A-Type Lamins and Hutchinson-Gilford Progeria Syndrome: Pathogenesis and Therapy." *Frontiers in Bioscience (Scholar Edition)* 3: 1133–46. doi:216 [pii].
Gosain, Ankush, and Luisa A. DiPietro. 2004. "Aging and Wound Healing." *World Journal of Surgery*. doi:10.1007/s00268-003-7397-6.
Gosselin, Karo, Emeric Deruy, Sébastien Martien, Chantal Vercamer, Fatima Bouali, Thibault Dujardin, Christian Slomianny, et al. 2009. "Senescent Keratinocytes Die by Autophagic Programmed Cell Death." *The American Journal of Pathology* 174 (2): 423–35. doi:10.2353/ajpath.2009.080332.
Gozzelino, Raffaella, Viktoria Jeney, and Miguel P Soares. 2010. "Mechanisms of Cell Protection by Heme Oxygenase-1." *Annual Review of Pharmacology and Toxicology* 50: 323–54. doi:10.1146/annurev.pharmtox.010909.105600.
Gredilla, Ricardo, Vilhelm a Bohr, and Tinna Stevnsner. 2010. "Mitochondrial DNA Repair and Association with Aging--an Update." *Experimental Gerontology* 45: 478–88. doi:10.1016/j.exger.2010.01.017.
Guo, S, and L A Dipietro. 2010. "Factors Affecting Wound Healing." *Journal of Dental Research* 89 (3): 219–29. doi:10.1177/0022034509359125.
Han, Shuo, and Anne Brunet. 2012. "Histone Methylation Makes Its Mark on Longevity." *Trends in Cell Biology*. doi:10.1016/j.tcb.2011.11.001.
Hanahan, D, and R A Weinberg. 2000. "The Hallmarks of Cancer." *Cell* 100 (1): 57–70. doi:10.1007/s00262-010-0968-0.
Hanahan, Douglas, and Robert A. Weinberg. 2011. "Hallmarks of Cancer: The next Generation." *Cell*. doi:10.1016/j.cell.2011.02.013.
Hanson, K M, and J D Simon. 1998. "Epidermal Trans-Urocanic Acid and the UV-A-Induced Photoaging of the Skin." *Proceedings of the National Academy of Sciences of the United States of America* 95 (18): 10576–78. doi:10.1073/pnas.95.18.10576.
Harman, Denham. 1972. "The Biologic Clock: The Mitochondria?" *Journal of the American Geriatrics Society* 20 (4): 145–47. doi:10.1111/j.1532-5415.1972.tb00787.x.
Hartl, F. Ulrich, Andreas Bracher, and Manajit Hayer-Hartl. 2011. "Molecular Chaperones in Protein Folding and Proteostasis." *Nature* 475 (7356): 324–32. doi:10.1038/nature10317.
Hayflick, L. 1965. "The Limited in Vitro Lifetime of Human Diploid Cell Strains." *Experimental Cell Research* 37 (3): 614–36. doi:10.1016/0014-4827(65)90211-9.
Hayflick, L., and P.S. Moorhead. 1961. "The Serial Cultivation of Human Diploid Cell Strains." *Experimental Cell Research* 25 (3): 585–621. doi:10.1016/0014-4827(61)90192-6.
Hiraku, Yusuke, Kimiko Ito, Kazutaka Hirakawa, and Shosuke Kawanishi. 2007. "Photosensitized DNA Damage and Its Protection via a Novel Mechanism." *Photochemistry and Photobiology* 83 (1): 205–12. doi:10.1562/2006-03-09-IR-840.
Hoare, Matthew, Tapas Das, and Graeme Alexander. 2010. "Ageing, Telomeres, Senescence, and Liver Injury." *Journal of Hepatology*. doi:10.1016/j.jhep.2010.06.009.

Holliday, R. 1995. "Understanding Ageing." In *Developmental and Cell Biology Series*, Cambridge, 207. New York.

Hussein, Mahmoud R. 2005. "Ultraviolet Radiation and Skin Cancer: Molecular Mechanisms." *Journal of Cutaneous Pathology*. doi:10.1111/j.0303-6987.2005.00281.x.

Itahana, K., Y. Zou, Y. Itahana, J.-L. Martinez, C. Beausejour, J. J. L. Jacobs, M. van Lohuizen, V. Band, J. Campisi, and G. P. Dimri. 2003. "Control of the Replicative Life Span of Human Fibroblasts by p16 and the Polycomb Protein Bmi-1." *Molecular and Cellular Biology* 23 (1): 389–401. doi:10.1128/MCB.23.1.389-401.2003.

Jacobs, Jacqueline J.L., and Titia De Lange. 2004. "Significant Role for p16INK4a in p53-Independent Telomere-Directed Senescence." *Current Biology* 14 (24): 2302–8. doi:10.1016/j.cub.2004.12.025.

Janzen, V, R Forkert, H E Fleming, Y Saito, M T Waring, D M Dombkowski, T Cheng, R A DePinho, N E Sharpless, and D T Scadden. 2006. "Stem-Cell Ageing Modified by the Cyclin-Dependent Kinase Inhibitor p16INK4a." *Nature* 443 (7110): 421–26. doi:nature05159 [pii] 10.1038/nature05159.

Jones, Simon A., Jürgen Scheller, and Stefan Rose-John. 2011. "Therapeutic Strategies for the Clinical Blockade of IL-6/gp130 Signaling." *Journal of Clinical Investigation*. doi:10.1172/JCI57158.

Kang, M K, C Bibb, M a Baluda, O Rey, and N H Park. 2000. "In Vitro Replication and Differentiation of Normal Human Oral Keratinocytes." *Experimental Cell Research* 258: 288–97. doi:10.1006/excr.2000.4943.

Kanitakis, Jean. 2002. "Anatomy, Histology and Immunohistochemistry of Normal Human Skin." *European Journal of Dermatology* 12 (4): 390–401.

Kaul, Zeenia, Anthony J Cesare, Lily I Huschtscha, Axel A Neumann, and Roger R Reddel. 2011. "Five Dysfunctional Telomeres Predict Onset of Senescence in Human Cells." *EMBO Reports* 13 (1): 52–59. doi:10.1038/embor.2011.227.

Kawanishi, Shosuke, and Shinji Oikawa. 2004. "Mechanism of Telomere Shortening by Oxidative Stress." In *Annals of the New York Academy of Sciences*, 1019:278–84. doi:10.1196/annals.1297.047.

Kim, Jeong-Mi, Eun-Mi Noh, Kang-Beom Kwon, Bo-Mi Hwang, Jin-Ki Hwang, Yong-Ouk You, Min Seuk Kim, et al. 2013. *Dihydroavenanthramide D Prevents UV-Irradiated Generation of Reactive Oxygen Species and Expression of Matrix Metalloproteinase-1 and -3 in Human Dermal Fibroblasts. Experimental Dermatology*. doi:10.1111/exd.12243.

Kim, Jong???Ki ???K, Dinshaw Patel, and Byong???Seok ???S Choi. 1995. "CONTRASTING STRUCTURAL IMPACTS INDUCED BY Cis???syn CYCLOBUTANE DIMER AND (6???4) ADDUCT IN DNA DUPLEX DECAMERS: IMPLICATION IN MUTAGENESIS AND REPAIR ACTIVITY." *Photochemistry and Photobiology* 62 (1): 44–50. doi:10.1111/j.1751-1097.1995.tb05236.x.

Koh, Jae Sook, Hoon Kang, Sung Woo Choi, and Hyung Ok Kim. 2002. "Cigarette Smoking Associated with Premature Facial Wrinkling: Image Analysis of Facial Skin Replicas." In *International Journal of Dermatology*, 41:21–27. doi:10.1046/j.1365-4362.2002.01352.x.

Krizhanovsky, Valery, Monica Yon, Ross A. Dickins, Stephen Hearn, Janelle Simon, Cornelius Miething, Herman Yee, Lars Zender, and Scott W. Lowe. 2008. "Senescence of Activated Stellate Cells Limits Liver Fibrosis." *Cell* 134 (4): 657–67. doi:10.1016/j.cell.2008.06.049.

Kuilman, Thomas, Chrysiis Michaloglou, Liesbeth C W Vredeveld, Sirith Douma, Remco van Doorn, Christophe J. Desmet, Lucien A. Aarden, Wolter J. Mooi, and Daniel S. Peeper. 2008. "Oncogene-Induced Senescence Relayed by an Interleukin-Dependent

Inflammatory Network." *Cell* 133 (6): 1019–31. doi:10.1016/j.cell.2008.03.039.
Kumazaki, T, M Kobayashi, and Y Mitsui. 1993. "Enhanced Expression of Fibronectin during in Vivo Cellular Aging of Human Vascular Endothelial Cells and Skin Fibroblasts." *Experimental Cell Research* 205 (2): 396–402. doi:10.1006/excr.1993.1103.
Kuningas, Maris, Karol Estrada, Yi Hsiang Hsu, Kannabiran Nandakumar, Andr?? G. Uitterlinden, Kathryn L. Lunetta, Cornelia M. van Duijn, et al. 2011. "Large Common Deletions Associate with Mortality at Old Age." *Human Molecular Genetics* 20 (21): 4290–96. doi:10.1093/hmg/ddr340.
Kurz, David J, Stephanie Decary, Ying Hong, and Jorge D Erusalimsky. 2000. "Senescence-Associated (Beta)-Galactosidase Reflects an Increase in Lysosomal Mass during Replicative Ageing of Human Endothelial Cells." *Journal of Cell Science* 113 (Pt 2 (20): 3613–22. http://www.ncbi.nlm.nih.gov/pubmed/11017877.
Laat, Wouter L. de, Nicolaas G. J. Jaspers, and Jan H. J. Hoeijmakers. 1999. "Molecular Mechanism of Nucleotide Excision Repair." *Genes & Development* 13 (7): 768–85. doi:10.1101/gad.13.7.768.
Lee, Bo Yun, Jung a Han, Jun Sub Im, Amelia Morrone, Kimberly Johung, Edward C Goodwin, Wim J Kleijer, Daniel DiMaio, and Eun Seong Hwang. 2006. "Senescence-Associated Beta-Galactosidase Is Lysosomal Beta-Galactosidase." *Aging Cell* 5 (2): 187–95. doi:10.1111/j.1474-9726.2006.00199.x.
Lewis, Davina A, Qiaofang Yi, Jeffrey B Travers, and Dan F Spandau. 2008. "UVB-Induced Senescence in Human Keratinocytes Requires a Functional Insulin-like Growth Factor-1 Receptor and p53." *Molecular Biology of the Cell* 19 (4): 1346–53. doi:10.1091/mbc.E07-10-1041.
Limoli, Charles L., Erich Giedzinski, William F. Morgan, Steven G. Swarts, George D D Jones, and William Hyun. 2003. "Persistent Oxidative Stress in Chromosomally Unstable Cells." *Cancer Research* 63 (12): 3107–11.
Liu, Baohua, Jianming Wang, Kui Ming Chan, Wai Mui Tjia, Wen Deng, Xinyuan Guan, Jian-dong Huang, et al. 2005. "Genomic Instability in Laminopathy-Based Premature Aging." *Nature Medicine* 11 (7): 780–85. doi:10.1038/nm1266.
Lodish, Berk A, and S L Zipursky. 2000. "Mutations : Types and Causes." In *Molecular Cell Biology 4th Edition*, Section 8.1 Mutations: Types and Causes.
López-Otín, Carlos, Maria A. Blasco, Linda Partridge, Manuel Serrano, and Guido Kroemer. 2013. "The Hallmarks of Aging." *Cell*. doi:10.1016/j.cell.2013.05.039.
López-otín, Carlos, Maria A Blasco, Linda Partridge, and Manuel Serrano. 2013. "Europe PMC Funders Group The Hallmarks of Aging" 153 (6): 1194–1217. doi:10.1016/j.cell.2013.05.039.The.
Lyer, Ravi R., Anna Pluciennik, Vickers Burdett, and Paul L. Modrich. 2006. "DNA Mismatch Repair: Functions and Mechanisms." *Chemical Reviews*. doi:10.1021/cr0404794.
Ma, Wenjian, Meinhard Wlaschek, Christina Hommel, Lars Alexander Schneider, and Karin Scharffetter-Kochanek. 2002. "Psoralen plus UVA (PUVA) Induced Premature Senescence as a Model for Stress-Induced Premature Senescence." In *Experimental Gerontology*, 37:1197–1201. doi:10.1016/S0531-5565(02)00143-2.
Maegawa, Shinji, George Hinkal, Hyun Soo Kim, Lanlan Shen, Li Zhang, Jiexin Zhang, Nianxiang Zhang, Shoudan Liang, Lawrence a Donehower, and Jean-Pierre J Issa. 2010. "Widespread and Tissue Specific Age-Related DNA Methylation Changes in Mice." *Genome Res* 20 (3): 332–40. doi:10.1101/gr.096826.109.
Mantovani, Alberto, Massimo Locati, Annunciata Vecchi, Silvano Sozzani, and Paola Allavena. 2001. "Decoy Receptors: A Strategy to Regulate Inflammatory Cytokines and

Chemokines." *Trends in Immunology*. doi:10.1016/S1471-4906(01)01941-X.
Mao, Zhiyong, Zhonghe Ke, Vera Gorbunova, and Andrei Seluanov. 2012. "Replicatively Senescent Cells Are Arrested in G1 and G2 Phases." *Aging* 4 (6): 431–35. doi:100467 [pii].
Matsumura, Yasuhiro, and Honnavara N. Ananthaswamy. 2004. "Toxic Effects of Ultraviolet Radiation on the Skin." *Toxicology and Applied Pharmacology*. doi:10.1016/j.taap.2003.08.019.
Maures, Travis J., Eric L. Greer, Anna G. Hauswirth, and Anne Brunet. 2011. "The H3K27 Demethylase UTX-1 Regulates C. Elegans Lifespan in a Germline-Independent, Insulin-Dependent Manner." *Aging Cell* 10 (6): 980–90. doi:10.1111/j.1474-9726.2011.00738.x.
McCord, Rachel Patton, Ashley Nazario-Toole, Haoyue Zhang, Peter S. Chines, Ye Zhan, Michael R. Erdos, Francis S. Collins, Job Dekker, and Kan Cao. 2013. "Correlated Alterations in Genome Organization, Histone Methylation, and DNA-Lamin A/C Interactions in Hutchinson-Gilford Progeria Syndrome." *Genome Research* 23 (2): 260–69. doi:10.1101/gr.138032.112.
Melnikova, Vladislava O, and Honnavara N Ananthaswamy. 2005. "Cellular and Molecular Events Leading to the Development of Skin Cancer." *Mutation Research* 571 (1–2): 91–106. doi:10.1016/j.mrfmmm.2004.11.015.
Molofsky, A V, S G Slutsky, N M Joseph, S He, R Pardal, J Krishnamurthy, N E Sharpless, and S J Morrison. 2006. "Increasing p16INK4a Expression Decreases Forebrain Progenitors and Neurogenesis during Ageing." *Nature* 443 (7110): 448–52. doi:nature05091 [pii] 10.1038/nature05091.
Morimoto, Richard I. 2008. "Proteotoxic Stress and Inducible Chaperone Networks in Neurodegenerative Disease and Aging." *Genes and Development*. doi:10.1101/gad.1657108.
Mouret, Stéphane, Caroline Baudouin, Marie Charveron, Alain Favier, Jean Cadet, and Thierry Douki. 2006. "Cyclobutane Pyrimidine Dimers Are Predominant DNA Lesions in Whole Human Skin Exposed to UVA Radiation." *Proceedings of the National Academy of Sciences of the United States of America* 103 (37): 13765–70. doi:10.1073/pnas.0604213103.
Mukherjee, A B, and S Thomas. 1997. "+'Aneuploidy in Skin Increases with age:' A Longitudinal Study of Human Age-Related Chromosomal Analysis in Skin Fibroblasts." *Exp Cell Res* 235 (1): 161–69.
Murano, S, R Thweatt, R J Shmookler Reis, R A Jones, E J Moerman, and S Goldstein. 1991. "Diverse Gene Sequences Are Overexpressed in Werner Syndrome Fibroblasts Undergoing Premature Replicative Senescence." *Molecular and Cellular Biology* 11 (8): 3905–14. doi:10.1128/MCB.11.8.3905.Updated.
Nardella, Caterina, John G Clohessy, Andrea Alimonti, and Pier Paolo Pandolfi. 2011. "Pro-Senescence Therapy for Cancer Treatment." *Nature Reviews Cancer* 11 (7): 503–11. doi:10.1038/nrc3057.
Narita, Masashi, Sabrina Nũnez, Edith Heard, Masako Narita, Athena W. Lin, Stephen A. Hearn, David L. Spector, Gregory J. Hannon, and Scott W. Lowe. 2003. "Rb-Mediated Heterochromatin Formation and Silencing of E2F Target Genes during Cellular Senescence." *Cell* 113 (6): 703–16. doi:10.1016/S0092-8674(03)00401-X.
Nguyen, Truyen, Paul Nioi, and Cecil B Pickett. 2009. "The Nrf2-Antioxidant Response Element Signaling Pathway and Its Activation by Oxidative Stress." *The Journal of Biological Chemistry* 284 (20): 13291–95. doi:10.1074/jbc.R900010200.
Nguyen, Truyen, Philip J Sherratt, and Cecil B Pickett. 2003. "Regulatory Mechanisms Controlling Gene Expression Mediated By the Antioxidant Response Element." *Annual Review of Pharmacology and Toxicology* 43 (2): 233–60.

doi:10.1146/annurev.pharmtox.43.100901.140229.
Nishio, Koji, Akira Inoue, Shanlou Qiao, Hiroshi Kondo, and Akio Mimura. 2001. "Senescence and Cytoskeleton: Overproduction of Vimentin Induces Senescent-like Morphology in Human Fibroblasts." *Histochemistry and Cell Biology* 116 (4): 321–27. doi:10.1007/s004180100325.
Oh, Juhyun, Yang David Lee, and Amy J Wagers. 2014. "Stem Cell Aging: Mechanisms, Regulators and Therapeutic Opportunities." *Nature Medicine* 20 (8): 870–80. doi:10.1038/nm.3651.
Pakyari, Mohammadreza, Ali Farrokhi, Mohsen Khosravi Maharlooei, and Aziz Ghahary. 2013. "Critical Role of Transforming Growth Factor Beta in Different Phases of Wound Healing." *Advances in Wound Care* 2 (5): 215–24. doi:10.1089/wound.2012.0406.
Passos, João F., Gabriele Saretzki, Shaheda Ahmed, Glyn Nelson, Torsten Richter, Heiko Peters, Ilka Wappler, et al. 2007. "Mitochondrial Dysfunction Accounts for the Stochastic Heterogeneity in Telomere-Dependent Senescence." *PLoS Biology* 5 (5): 1138–51. doi:10.1371/journal.pbio.0050110.
Patriarca, Stefania, Anna Lisa Furfaro, Luana Cosso, Elena Pesce Maineri, Emanuela Balbis, Cinzia Domenicotti, Mariapaola Nitti, et al. 2007. "Heme Oxygenase 1 Expression in Rat Liver during Ageing and Ethanol Intoxication." *Biogerontology* 8 (3): 365–72. doi:10.1007/s10522-006-9079-x.
Pattison, David I, and Michael J Davies. 2006. "Actions of Ultraviolet Light on Cellular Structures." *Exs*, no. 96: 131–57. doi:10.1007/3-7643-7378-4_6.
Picot, Cédric R., Martine Perichon, Jean Christophe Cintrat, Bertrand Friguet, and Isabelle Petropoulos. 2004. "The Peptide Methionine Sulfoxide Reductases, MsrA and MsrB (hCBS-1), Are Downregulated during Replicative Senescence of Human WI-38 Fibroblasts." *FEBS Letters* 558 (1–3): 74–78. doi:10.1016/S0014-5793(03)01530-8.
Polyak, K, Y Xia, J L Zweier, K W Kinzler, and B Vogelstein. 1997. "A Model for p53-Induced Apoptosis." *Nature* 389 (6648): 300–305. doi:10.1038/38525.
Proksch, Ehrhardt, Johanna M. Brandner, and Jens Michael Jensen. 2008. "The Skin: An Indispensable Barrier." *Experimental Dermatology* 17 (12): 1063–72. doi:10.1111/j.1600-0625.2008.00786.x.
Rastogi, Rajesh P., Richa, Ashok Kumar, Madhu B. Tyagi, and Rajeshwar P. Sinha. 2010. "Molecular Mechanisms of Ultraviolet Radiation-Induced DNA Damage and Repair." *Journal of Nucleic Acids* 2010: 1–32. doi:10.4061/2010/592980.
Ravanat, Jean-Luc, Thierry Douki, and Jean Cadet. 2001. "Direct and Indirect Effects of UV Radiation on DNA and Its Components." *Journal of Photochemistry and Photobiology B: Biology* 63 (1): 88–102. doi:10.1016/S1011-1344(01)00206-8.
Regoli, Francesco, and Maria Elisa Giuliani. 2014. "Oxidative Pathways of Chemical Toxicity and Oxidative Stress Biomarkers in Marine Organisms." *Marine Environmental Research* 93: 106–17. doi:10.1016/j.marenvres.2013.07.006.
Rera, Michael, Sepehr Bahadorani, Jaehyoung Cho, Christopher L. Koehler, Matthew Ulgherait, Jae H. Hur, William S. Ansari, Thomas Lo, D. Leanne Jones, and David W. Walker. 2011. "Modulation of Longevity and Tissue Homeostasis by the Drosophila PGC-1 Homolog." *Cell Metabolism* 14 (5): 623–34. doi:10.1016/j.cmet.2011.09.013.
Ressler, Sigrun, Jirina Bartkova, Harald Niederegger, Jiri Bartek, Karin Scharffetter-Kochanek, Pidder Jansen-Dürr, and Meinhard Wlaschek. 2006. "p16INK4A Is a Robust in Vivo Biomarker of Cellular Aging in Human Skin." *Aging Cell* 5 (5): 379–89. doi:10.1111/j.1474-9726.2006.00231.x.
Rheinwald, James G, William C Hahn, Matthew R Ramsey, Jenny Y Wu, Zongyou Guo, Hensin Tsao, Michele De Luca, Caterina Catricalà, and Kathleen M O'Toole. 2002. "A Two-Stage, p16(INK4A)- and p53-Dependent Keratinocyte Senescence Mechanism That

Limits Replicative Potential Independent of Telomere Status." *Molecular and Cellular Biology* 22 (14): 5157–72. doi:10.1128/MCB.22.14.5157-5172.2002.
Rodier, Francis, Jean-Philippe Coppé, Christopher K Patil, Wieteke A M Hoeijmakers, Denise P Muñoz, Saba R Raza, Adam Freund, Eric Campeau, Albert R Davalos, and Judith Campisi. 2009. "Persistent {DNA} Damage Signalling Triggers Senescence-Associated Inflammatory Cytokine Secretion." *Nat Cell Biol* 11 (8): 973–79. doi:10.1038/ncb1909.
Ross, David, Jadwiga K. Kepa, Shannon L. Winski, Howard D. Beall, Adil Anwar, and David Siegel. 2000. "NAD(P)H:quinone Oxidoreductase 1 (NQO1): Chemoprotection, Bioactivation, Gene Regulation and Genetic Polymorphisms." *Chemico-Biological Interactions* 129 (1–2): 77–97. doi:10.1016/S0009-2797(00)00199-X.
Sablina, Anna A, Andrei V Budanov, Galina V Ilyinskaya, S Larissa, Julia E Kravchenko, and Peter M Chumakov. 2005. "The Antioxidant Function of the p53 Tumor Suppressor." *Nat Med* 11 (12): 1306–13. doi:10.1038/nm1320.The.
Sage, Evelyne. 1993. "Distribution and Repair of Photolesions in Dna: Genetic Consequences and the Role of Sequence Context." *Photochemistry and Photobiology* 57 (1): 163–74. doi:10.1111/j.1751-1097.1993.tb02273.x.
Saitoh, Yasukazu, Aiko Morishita, Satomi Mito, Tsubasa Tsujiya, and Nobuhiko Miwa. 2013. "Senescence-Induced Increases in Intracellular Oxidative Stress and Enhancement of the Need for Ascorbic Acid in Human Fibroblasts." *Molecular and Cellular Biochemistry* 380 (1–2): 129–41. doi:10.1007/s11010-013-1666-y.
Salminen, Antero, Kai Kaarniranta, and Anu Kauppinen. 2012. "Inflammaging: Disturbed Interplay between Autophagy and Inflammasomes." *Aging* 4 (3): 166–75. doi:10.18632/aging.100444.
Sarg, Bettina, Elisavet Koutzamani, Wilfried Helliger, Ingemar Rundquist, and Herbert H. Lindner. 2002. "Postsynthetic Trimethylation of Histone H4 at Lysine 20 in Mammalian Tissues Is Associated with Aging." *Journal of Biological Chemistry* 277 (42): 39195–201. doi:10.1074/jbc.M205166200.
Schärer, Orlando D. 2013. "Nucleotide Excision Repair in Eukaryotes." *Cold Spring Harbor Perspectives in Biology*. doi:10.1101/cshperspect.a012609.
Serrano, Manuel, Athena W. Lin, Mila E. McCurrach, David Beach, and Scott W. Lowe. 1997. "Oncogenic Ras Provokes Premature Cell Senescence Associated with Accumulation of p53 and p16(INK4a)." *Cell* 88 (5): 593–602. doi:10.1016/S0092-8674(00)81902-9.
Shaw, Albert C., Samit Joshi, Hannah Greenwood, Alexander Panda, and Janet M. Lord. 2010. "Aging of the Innate Immune System." *Current Opinion in Immunology*. doi:10.1016/j.coi.2010.05.003.
Shay, J W, and W E Wright. 2000. "Hayflick, His Limit, and Cellular Ageing." *Nature Reviews. Molecular Cell Biology* 1 (October): 72–76. doi:10.1038/35036093.
Shay, Jerry W., and Woodring E. Wright. 2005. "Senescence and Immortalization: Role of Telomeres and Telomerase." *Carcinogenesis*. doi:10.1093/carcin/bgh296.
Sherr, Charles J., and Frank McCormick. 2002. "The RB and p53 Pathways in Cancer." *Cancer Cell*. doi:10.1016/S1535-6108(02)00102-2.
Simpson, R J, A Hammacher, D K Smith, J M Matthews, and L D Ward. 1997. "Interleukin-6: Structure-Function Relationships." *Protein Science : A Publication of the Protein Society* 6 (5): 929–55. doi:10.1002/pro.5560060501.
Sinha, Rajeshwar P., and Donat-P. Häder. 2002. "UV-Induced DNA Damage and Repair: A Review." *Photochemical & Photobiological Sciences* 1 (4): 225–36. doi:10.1039/b201230h.
Soroka, Yoram, Zeev Ma'or, Yael Leshem, Lilian Verochovsky, Rami Neuman,

François Menahem Brégégère, and Yoram Milner. 2008. "Aged Keratinocyte Phenotyping: Morphology, Biochemical Markers and Effects of Dead Sea Minerals." *Experimental Gerontology* 43 (10): 947–57. doi:10.1016/j.exger.2008.08.003.

Sottile, Jane. 2004. "Regulation of Angiogenesis by Extracellular Matrix." *Biochimica et Biophysica Acta - Reviews on Cancer*. doi:10.1016/j.bbcan.2003.07.002.

Stern, Robert S. 2007. "Psoralen and Ultraviolet a Light Therapy for Psoriasis." *The New England Journal of Medicine* 357 (7): 682–90. doi:10.1056/NEJMct072317.

Streuli, Charles. 1999. "Extracellular Matrix Remodelling and Cellular Differentiation." *Current Opinion in Cell Biology*. doi:10.1016/S0955-0674(99)00026-5.

Sulli, Gabriele, Raffaella Di Micco, and Fabrizio d'Adda di Fagagna. 2012. "Crosstalk between Chromatin State and DNA Damage Response in Cellular Senescence and Cancer." *Nature Reviews Cancer* 12 (10): 709–20. doi:10.1038/nrc3344.

Taguchi, Keiko, Hozumi Motohashi, and Masayuki Yamamoto. 2011. "Molecular Mechanisms of the Keap1-Nrf2 Pathway in Stress Response and Cancer Evolution." *Genes to Cells*. doi:10.1111/j.1365-2443.2010.01473.x.

Takubo, K, K Nakamura, N Izumiyama, E Furugori, M Sawabe, T Arai, Y Esaki, et al. 2000. "Telomere Shortening with Aging in Human Liver." *The Journals of Gerontology. Series A, Biological Sciences and Medical Sciences* 55 (11): B533-6. http://www.ncbi.nlm.nih.gov/pubmed/11078086.

Tortora, Gerard J., and Bryan Derrickson. 2014. *Principles of Anatomy & Physiology 14th Edition. Wiley.*

Toussaint, O., E. E. Medrano, and T. Von Zglinicki. 2000. "Cellular and Molecular Mechanisms of Stress-Induced Premature Senescence (SIPS) of Human Diploid Fibroblasts and Melanocytes." *Experimental Gerontology*. doi:10.1016/S0531-5565(00)00180-7.

Toutfaire, Marie, Emilie Bauwens, and Florence Debacq-Chainiaux. 2017. "The Impact of Cellular Senescence in Skin Ageing: A Notion of Mosaic and Therapeutic Strategies." *Biochemical Pharmacology*. Elsevier Inc. doi:10.1016/j.bcp.2017.04.011.

Ungvari, Zoltan, Lora Bailey-Downs, Danuta Sosnowska, Tripti Gautam, Peter Koncz, Gyorgy Losonczy, Praveen Ballabh, Rafael de Cabo, William E Sonntag, and Anna Csiszar. 2011. "Vascular Oxidative Stress in Aging: A Homeostatic Failure due to Dysregulation of NRF2-Mediated Antioxidant Response." *American Journal of Physiology. Heart and Circulatory Physiology* 301 (2): H363–72. doi:10.1152/ajpheart.01134.2010.

Venkatesan, R N, and C Price. 1998. "Telomerase Expression in Chickens: Constitutive Activity in Somatic Tissues and down-Regulation in Culture." *Proceedings of the National Academy of Sciences of the United States of America* 95 (25): 14763–68. doi:10.1073/pnas.95.25.14763.

Vermulst, Marc, Jason H Bielas, Gregory C Kujoth, Warren C Ladiges, Peter S Rabinovitch, Tomas A Prolla, and Lawrence A Loeb. 2007. "Mitochondrial Point Mutations Do Not Limit the Natural Lifespan of Mice." *Nat. Genet* 39 (4): 540–43. doi:10.1038/ng1988.

Wei, Shan, Wenyi Wei, and John M. Sedivy. 1999. "Expression of Catalytically Active Telomerase Does Not Prevent Premature Senescence Caused by Overexpression of Oncogenic Ha-Ras in Normal Human Fibroblasts." *Cancer Research* 59 (7): 1539–43.

Weiss, Robert S., Shuhei Matsuoka, Stephen J. Elledge, and Philip Leder. 2002. "Hus1 Acts Upstream of Chk1 in a Mammalian DNA Damage Response Pathway." *Current Biology* 12 (1): 73–77. doi:10.1016/S0960-9822(01)00626-1.

Werth, V P, X Shi, E Kalathil, and C Jaworsky. 1996. "Elastic Fiber-Associated Proteins of Skin in Development and Photoaging." *Photochemistry and Photobiology* 63 (3): 308–13. http://www.ncbi.nlm.nih.gov/pubmed/8881336.

West, Michael D., Olivia M. Pereira-Smith, and James R. Smith. 1989. "Replicative Senescence of Human Skin Fibroblasts Correlates with a Loss of Regulation and Overexpression of Collagenase Activity." *Experimental Cell Research* 184 (1): 138–47. doi:10.1016/0014-4827(89)90372-8.

Whitaker, Rachel, Shakeela Faulkner, Reika Miyokawa, Lucas Burhenn, Mark Henriksen, Jason G. Wood, and Stephen L. Helfand. 2013. "Increased Expression of Drosophila sir2 Extends Life Span in a Dosedependent Manner." *Aging* 5 (9): 682–91. doi:100599 [pii].

Wlaschek, Meinhard, Iliana Tantcheva-Poór, Lale Naderi, Wenjian Ma, Lars Alexander Schneider, Ziba Razi-Wolf, Jutta Schüller, and Karin Scharffetter-Kochanek. 2001. "Solar UV Irradiation and Dermal Photoaging." *Journal of Photochemistry and Photobiology B: Biology* 63 (1–3): 41–51. doi:10.1016/S1011-1344(01)00201-9.

Xue, Wen, Lars Zender, Cornelius Miething, Ross A Dickins, Eva Hernando, Valery Krizhanovsky, Carlos Cordon-Cardo, and Scott W Lowe. 2007. "Senescence and Tumour Clearance Is Triggered by p53 Restoration in Murine Liver Carcinomas." *Nature* 445 (7128): 656–60. doi:10.1038/nature05529.

Zglinicki, T. von, G. Saretzki, J. Ladhoff, F. d'Adda di Fagagna, and S.P. Jackson. 2005. "Human Cell Senescence as a DNA Damage Response." *Mechanisms of Ageing and Development* 126 (1): 111–17. doi:10.1016/j.mad.2004.09.034.

Zglinicki, T von, G Saretzki, J Ladhoff, F d'Adda di Fagagna, and S P Jackson. 2005. "Human Cell Senescence as a DNA Damage Response." *Mechanisms of Ageing and Development* 126 (1): 111–17. doi:10.1016/j.mad.2004.09.034.

Zhang, Guo, Juxue Li, Sudarshana Purkayastha, Yizhe Tang, Hai Zhang, Ye Yin, Bo Li, Gang Liu, and Dongsheng Cai. 2013. "Hypothalamic Programming of Systemic Ageing Involving IKK-B, NF-κB and GnRH." *Nature* 497 (7448): 211–16. doi:10.1038/nature12143.